Russian Chemical Reviews **78** (8) 683 – 715 (2009) © 2009 Russian Academy of Sciences and Turpion Ltd

DOI 10.1070/RC2009v078n08ABEH003758

Spectroscopy and structure of free radicals stabilized in cryogenic matrices

E G Baskir, E Ya Misochko, O M Nefedov

Contents

I.	Introduction	683
II.	Low-temperature matrix spectroscopy	684
III.	New methods of generating intermediates in matrices	686
IV.	Organic radicals containing unsaturated and aromatic fragments	687
V.	Nitrogen-containing radicals	691
VI.	Oxygen-containing radicals	693
VII.	Sulfur-containing radicals	704
VIII.	Radical structures containing metal atoms	705
IX.	Conclusion	710

Abstract. The results of spectroscopic (mainly vibrational IR spectroscopy and EPR spectroscopy) studies of radicals stabilized in solid inert-gas matrices are considered. Attention is focused on a comparison of experimental spectroscopic characteristics of radicals with those simulated by modern quantum chemical computation methods and on the use of these data for the elucidation of molecular and electronic structures of free radicals. The potential of new methods for radical generation in cryogenic matrices and the prospects for their application in spectroscopic studies are discussed. Data from the recent and earlier studies are compared. The bibliography includes 394 references.

I. Introduction

Studies on the mechanisms of reactions involving reactive intermediates is an important research problem of physical organic chemistry.[1–3] A conventional method of studying short-lived transient species is their freezing in inert-gas matrices at cryogenic temperatures. The use of inert gases as solid matrices for spectroscopic studies of radical species was pioneered by Pimentel and co-workers[4] and Norman and Porter[5] (1954). The exceptional versatility of the matrix isolation technique and the possibility of using standard instruments for the detection of species unstable under ambient conditions and the acquisition of their spectral characteristics make it possible to place this method among fundamental methods of studying reactive intermediates in chemistry and chemical physics. It is with the matrix isolation method that spectroscopic data could be obtained for the majority of the known free radicals. These data were analyzed in several reviews and monographs (*e.g.*, see Refs 1–3, 6–8).

Intrinsic spectroscopic characteristics of reactive intermediates permit their sufficiently easy identification in complex chemical processes, in the outer space, in biological systems and living organisms. Until recently, vibrational IR spectroscopy and EPR spectroscopy of isotopically substituted species with identical stoichiometric composition were virtually the only reliable methods of identification of new species and elucidation of their structures. The progress in computer engineering and the advances in quantum chemical computation methods opened up new prospects for solving these problems and introduced new fundamental modifications into the procedure of studying stabilized intermediates.

Since the 1990s, the accuracy of calculations of spectroscopic constants (vibration frequencies and HFC constants) by *ab initio* and density functional methods has reached a sufficiently high level (*e.g.*, see Refs 9–12) and the calculations themselves became accessible for a wide circle of scientists. The use of experimental spectroscopic data together with the results of theoretical calculations made it possible to simplify the procedure of spectra interpretation and enhance the reliability of identification of intermediates, which favoured the elucidation of their molecular structures and peculiarities of their electronic structures. The latter was especially important for intermediates of the free-radical type, because the configuration of open electron shells of these species determines their reactivity and the pathways of further transformations. This combined approach became a generally accepted method for studying

E G Baskir, E Ya Misochko, O M Nefedov N D Zelinsky Institute of Organic Chemistry, Russian Academy of Sciences, Leninsky prosp. 47, 119991 Moscow, Russian Federation. Fax (7-499) 137 53 28, tel. (7-499) 135 89 41, e-mail: bas@ioc.ac.ru (E G Baskir), tel. (499) 137 73 90, e-mail: nefedov@ioc.ac.ru (O M Nefedov), Institute of Problems of Chemical Physics, Russian Academy of Sciences, prosp. Akad. Semenova 1, 142432 Chernogolovka, Moscow Region, Russian Federation. Fax (7-496) 524 96 76, tel. (7-296) 522 82 80, e-mail: misochko@icp.ac.ru (E Ya Misochko)

Received 24 April 2009
Uspekhi Khimii **78** (8) 742 – 775 (2009); translated by T Ya Safonova

stabilized intermediates. It not only allowed elucidation of the structure of new more complicated polyatomic radical species, but also made it possible to revise† the structures of many radical species established earlier.

Despite the considerable progress in the development of methods of registration of the radical species and analysis of the acquired data, the mechanism and kinetics of formation of certain intermediates remain obscure. The following factors hamper the theoretical simulation and identification of such intermediates:

— formation of non-covalent bonds in radical–molecule complexes;

— considerable delocalization of the unpaired electron in radicals containing multiple bonds;

— spin–orbit coupling and relativistic effects in intermediates that are formed with involvement of heavy atoms;

— abundance of structural isomeric forms of the intermediates with similar enthalpies of formation;

— small differences in the energies of electronic states with different multiplicity.

The reliability of theoretical description of chemical bonds in such intermediates should be confirmed experimentally.

In the present review, attention is focused on the combined approach to the studies of the molecular and electronic structures of free-radical intermediates, involving the use of experimental spectral data and the results of quantum chemical calculations. Since the results of spectroscopic studies of carbene and nitrene intermediates have been summarized in several recently published reviews and monographs (*e.g.*, see Refs 1, 13–18), the information on these intermediates was not included in the present review.

II. Low-temperature matrix spectroscopy

1. Vibrational spectroscopy

IR absorption spectroscopy is the most widely used method of studying matrix-isolated species. The experimentally obtained sets of vibration frequencies represent dynamic characteristics of particular molecular structures. Moreover, the measured vibration frequencies and their changes upon isotopic substitutions allow one to judge on the presence of particular chemical bonds. The reliability of identification of an intermediate and determination of its molecular structure based on the analysis of experimental vibrational spectra depends on the fit of the experimental vibration frequencies with the frequencies obtained by quantum chemical calculations. The modern programme packages for quantum chemical calculations of spectral characteristics of molecules are adequately adapted to the experimental vibrational spectroscopy. They allow accurate simulation of harmonic vibration frequencies and integral intensities of transitions. However, for weakly bound molecular structures, the fit of experimental and simulated vibrational spectra could only be obtained with consideration of the anharmonicity effects. Several typical examples of the crucial effects of anharmonic phenomena on the identification of vibration frequencies were considered in recent publications.[19, 20]

† It should be noted that the development of quantum chemical methods was so rapid that calculations performed in the late 1990s now appear inadequate due to their poor correspondence to experimental data.

Solid argon and xenon matrices that provide spectral resolution $\Delta\nu/\nu \approx 10^{-4}-10^{-3}$ in matrix IR-spectroscopic studies are employed most often. Recently, it has been proposed to use solid hydrogen as the matrix substance for the determination of IR spectroscopic characteristics of stabilized intermediates and investigation of their reactions with H_2 molecules. The use of solid hydrogen has good perspectives as follows from ultrahigh spectral resolution $\Delta\nu/\nu < 10^{-6}$ attainable in such matrices.[21, 22] However, handling solid hydrogen requires special equipment due to the relatively high pressure of its saturated vapour even at 5 K. Recently, a special procedure has been elaborated for growing massive parahydrogen (pH_2) crystals, containing molecules of the intermediate under study as an admixture, to be used in the matrix IR spectroscopy.[23–26] The main attention was focused on the chemical transformations induced by the vibrational (IR) excitation of the admixture molecules and on the effect of excited vibration and rotation states of the admixture molecules on the rate of their reactions with hydrogen molecules. The results of these studies were summarized in reviews.[27, 28]

2. EPR Spectroscopy

The EPR method is widely used in different fields of physics, chemistry and biology for studying species with intrinsic magnetic moment, being one of the richest sources of information on free radicals in the doublet electronic state. The thus measured hyperfine coupling constants that characterize the distribution of spin density on different magnetic nuclei give information on the electronic structure of the radical intermediates. Hyperfine coupling in molecules in the $^2\Sigma$ electronic state includes the Fermi coupling and the electron–nucleus dipole–dipole coupling, which determine the isotropic (A_{iso}) and anisotropic (A_{dip}) components of the HFC tensor, respectively:

$$A_{izo} = \frac{8\pi}{3} g_e \beta_e g_n \beta_n |\psi(0)|^2 = \frac{A_\parallel + 2A_\perp}{3},$$

$$A_{dip} = g_e \beta_e g_n \beta_n \left\langle \frac{3\cos^2\theta - 1}{2r^3} \right\rangle = \frac{A_\parallel - A_\perp}{3},$$

where g_e and g_n are g-factors of the electron and the nucleus, respectively; β_e and β_n are the electronic and nuclear Bohr magnetons, respectively; $|\psi(0)|^2$ is the density of the spin wave function on the nucleus; r is the radius-vector that connects the electron and the nucleus; θ is the angle between the magnetic field direction and vector $\boldsymbol{r}$.

The isotropic coupling constant (A_{iso}) is proportional to the spin density on a magnetic atomic nucleus. Its value is determined by the spin population of spherical atomic *s*-orbitals. The constant of magnetic dipole–dipole coupling (A_{dip}) is determined by the spin population of non-spherical electron orbitals of p- and d-types. As a rule, the standard packages of programmes for quantum chemical calculations contain special options that allow the simulation of HFC constants of the species studied. By comparing theoretical and experimental data, it is possible to check the quality and reliability of quantum chemical calculations and also to analyze the spin density distribution on magnetic atoms of the radical intermediates and assess the spin population of different atomic orbitals.

EPR spectroscopy of matrix-isolated intermediates has at least two undeniable advantages over the EPR spectroscopy of intermediates in liquid solutions. These advantages

are associated with the longer lifetimes of matrix-isolated intermediates and the absence of their rotational mobility at cryogenic temperatures. The longer lifetimes allow one to use the standard EPR instrumentation for recording spectra, while the absence of rotational mobility makes it possible to acquire information on anisotropic parameters of HFC tensors and *g*-factors of the species under study, which cannot be recorded in liquid due to the fast molecular rotation.

Certain difficulties in the analysis of spectra and the determination of magnetic parameters of studied species were associated with the fact that EPR spectra recorded under conditions of low-temperature matrix isolation, *i.e.*, the so-called powder pattern spectra corresponded as a rule to a set of randomly oriented species. The appearance of computer programmes for simulating powder spectra based on exact solutions of magnetic spin Hamiltonians made this problem much easier. Moreover, the analysis of experimental spectra in combination with the computer simulation of EPR spectra corresponding to different positions of the sample with respect to the magnetic field strength vector makes it possible to obtain additional information on the orientation function of distribution for species exhibiting considerable anisotropy of HFC tensors and *g*-factor.[29–31] The highest spectral resolution in EPR spectra of matrix-isolated intermediates equal to $\sim 10^{-2}$ mT was attained in solid neon and parahydrogen. For radicals containing few atoms and stabilized in these matrices, the resolved hyperfine structure corresponding to the nonzero rotational quantum states of radical species could be obtained.[32–34]

The elucidation of anisotropic parameters of magnetic interactions was of particular importance for radical species with an unpaired electron localized preferentially on the outer non-spherical atomic p-orbitals. Such intermediates include, for example, fullerene radicals of the $C_{60}R$ type formed by the addition of a radical R (or an atom) to a double bond of the fullerene cluster. The isotropic HFC constants in these radicals are largely determined by the effects of spin polarization of inner s-orbitals and contain only indirect information on the spin population of atoms. Until recently, the electronic structures of such intermediates were discussed based on isotropic HFC constants in liquid solutions.[35–38] Recently, the anisotropic EPR spectrum of the $C_{60}F$ radical in solid argon has been obtained as a result of the addition of a fluorine atom that could migrate in the solid matrix to the C_{60} molecule trapped in this matrix.[39,40]

The quantum chemical calculations[40] of the $C_{60}F$ radicals have shown that the density functional theory (DFT) method with correlational basic sets of the three-exponential type and polarization functions on the inner shells provides good agreement between the measured and calculated magnetic parameters (Table 1). The best description of the HFC tensor was attained in quantum chemical calculations by the B3LYP/L2′2′#5 and PBE0/L2′2′#5 methods, which produced similar results, namely, the calculations underrated the HFC isotropic part by only 5%–7% and overrated its anisotropic part by 12%–13%. The correspondence between the theoretical and experimental parameters demonstrated the sufficiently high accuracy of quantum chemical calculations. Figure 1 shows the distribution of spin density on C and F atoms of a $C_{60}F$ radical calculated by the PBE0/L2′2′#5 method. The computations demonstrated considerable delocalization of the unpaired electron preferentially localized on the outer p-orbitals of carbon and fluorine atoms.

Table 1. Calculated HFC constants on the fluorine atom (^{19}F) in a $C_{60}F$ radical.

Density functional method		A_{iso}/mT	A_{dip}/mT
functional	electron basis set		
PBE	L1	5.04	2.06
PBE	L11	4.86	2.11
PBE	L2′	5.30	2.11
PBE	L2′2′	5.76	2.13
PBE	L2′2′#5	5.90	2.13
PBE	L22	5.70	2.16
PBE	L33	5.98	2.18
PBE	L33#5	6.03	2.17
PBE0	L1	5.89	2.15
PBE0	L11	5.73	2.18
PBE0	L2′	6.20	2.16
PBE0	L2′2′	6.70	2.16
PBE0	L2′2′#5	6.86	2.17
PBE0	L33#5	6.99	2.21
B3LYP	L1	5.85	2.12
B3LYP	L11	5.70	2.16
B3LYP	L2′	6.22	2.17
B3LYP	L2′2′	6.79	2.17
B3LYP	L2′2′#5	6.94	2.18

Note. The experimental A_{iso} found by the EPR method in a *tert*-butylbenzene solution at 325 K was 7.30 mT;[36] the A_{iso} and A_{dip} values obtained in solid argon at 15 K were 7.21 and 1.85 mT, respectively.[40]

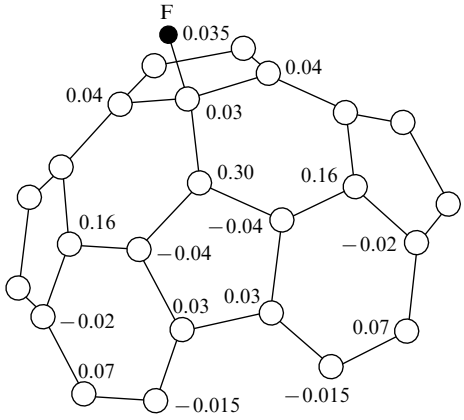


Figure 1. Spin density distribution over $C_{60}F$ radicals (according to the PBE0/L2′2′#5 calculations).[40]

The past decade witnessed the considerable growth of interest in radical-type compounds containing heavy atoms (first of all, metal atoms), which prompted the development of the corresponding methods for calculating HFC constants that would allow one to take proper account of different internal correlations, spin–orbit and relativistic effects. At present, several different theoretical approaches to the calculation of HFC constants are used (*e.g.*, see Refs 41–47) with the programme packages being constantly improved.

The analysis of anisotropic EPR spectra of the XeF radical in solid argon enriched with different isotopes of xenon and the comparison of the measured HFC constants with those calculated by quantum chemical methods made it possible to reveal the relativistic effects on the electronic structure of the $^2\Sigma$ ground state of this radical.[48] Table 2 shows the HFC parameters on magnetic nuclei of the ^{19}F and ^{129}Xe atoms. The constants of magnetic dipole–dipole coupling (A_{dip}) corresponded to the F(2p) atomic orbital occupied by 60% and the Xe(5p) orbital occupied by 40%, *i.e.*, the spin density was virtually uniformly distributed over the outer p-orbitals of atoms in the XeF radical. The measured characteristics of the XeF ground state were adequately described using quantum chemical methods that took into account relativistic effects in the electronic structure of radicals. These effects could be revealed by a considerable increase in the isotropic HFC component on the xenon atom (A_{iso}). The relativistic character of motion of heavy metal electrons gave rise to a considerable (more than twofold!) increase in the spin density on the Xe nucleus. It was also found that for the XeF radicals isolated in solid argon at 5 K, the parameters of HFC tensors and *g*-factor considerably differed from those of the same radicals generated by γ-irradiation on anisotropic molecular crystals XeF_2 and XeF_4 at 77 K.[49, 50]

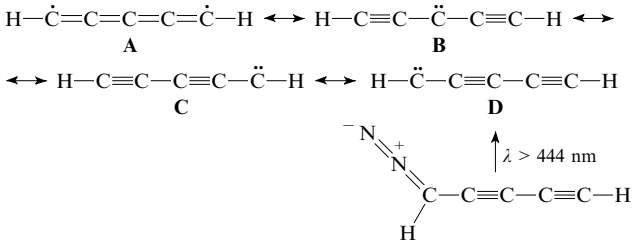
Table 2. HFC constants (MHz) of ^{129}Xe and ^{19}F atoms and the XeF radical calculated and measured in a solid argon matrix.[48]

Method	^{129}Xe				^{19}F			
	$A_\parallel$	$A_\perp$	A_{iso}	A_{dip}	$A_\parallel$	$A_\perp$	A_{iso}	A_{dip}
Results of calculations								
DFT (non-relativistic)			−581	−499			373	1040
DFT (relativistic)			−1420	−586			361	1045
Experimental data								
EPR	−2217	−969	−1385 (−1340)[a]	−416 (−485)[a]	2935	−814	435	1249

[a] Spin–orbit coupling is taken into account.

EPR spectroscopy served as the main tool in identification of high-spin ($S > 1/2$) organic radicals. In many publications, free-radical organic intermediates were studied in glassy organic matrices at 77 K. Recently, it has been shown that EPR spectra of such intermediates isolated in noble-gas matrices exhibited higher spectral resolution. Thus the original EPR spectra of high-spin nitrenopyridines in their septet ($S = 3$) [51, 52] and quintet ($S = 2$) [53, 54] electronic states stabilized in a solid argon matrix considerably differed from the spectra of these intermediates in solid organic matrices. The absence of non-uniform broadening of lines in the EPR spectra recorded in solid argon made it possible to reach higher resolution and thus measure the splitting tensor parameters in a non-zero field with higher precision.

An interesting example of the combined use of spectroscopic and computation methods was described.[55] A triplet intermediate with a linear hydrocarbon chain $H-C^{\bullet}=C=C=C=C^{\bullet}-H$ was generated for the first time by irradiation ($\lambda > 444$ nm) of 1-diazopentane-2,4-diyne in an Ar or N_2 matrix and characterized by IR and EPR spectroscopy.



The measured parameter of splitting in a non-zero field $|D|$ turned out to be equal to 0.6157 cm^{-1}, which is typical of carbene molecules with the axially symmetrical structure.[56] The experimental measurements together with the results of quantum chemical computations made it possible to conclude that the ground triplet electronic state of the intermediate HC_5H represents a hybrid combination of several resonance structures, where structure **B** is the main contributor. Recently,[57] the method of matrix IR spectroscopy together with DFT PBE/TZ2P quantum chemical computations have been used in detailed studies of yet another carbene of a similar structure with conjugated bonds, $(CH_3)_2C{=}CH\ddot{C}C{\equiv}CH$.

III. New methods of generating intermediates in matrices

The method of laser evaporation has been used in the past 20 years for vaporization of different elements and their incorporation into low-temperature matrices. In the initial stages of its development, a certain pessimistic prognoses were given in assessing the efficiency of this method due to the possibility that not only individual atoms, but also their numerous aggregates and clusters will be deposited in the matrix. Nonetheless, reliable evidence of the efficiency of laser evaporation in generating isolated atoms has recently been obtained, as confirmed by both their identification in low-temperature matrices and their further transformations in the course of annealing of the original condensate. The use of laser evaporation and vibrational spectroscopy in combination with the results of quantum chemical simulations made it possible to elucidate the molecular structures of unique reaction products of metal atoms with organic and inorganic compounds.

In recent years, the method of laser evaporation came into wide use in low-temperature stabilization and structural studies of nanosized particles (small clusters, aggregates, *etc.*). Thus the vibrational spectra of different carbon clusters C_n generated by laser evaporation of graphite and stabilized in solid argon were analyzed.[58–60] It was shown that the predominant compounds stabilized in solid argon represented a C_3 intermediate with the linear configuration. A procedure was developed for analyzing the IR spectra of linear and cyclic structures with the C_n composition for $n \leqslant 12$; moreover, the structure of singlet and triplet electronic states realized in two alternative C_4 structures,[61] namely, cumulene ($C{=}C{=}C{=}C$) and acetylene ($C{\equiv}C{-}C{\equiv}C$), was elucidated.

In the simultaneous laser evaporation of graphite with silicon, germanium or a metal, the reactive intermediate C_3 formed mixed compounds such as SiC_3Si, GeC_3Ge,[62, 63]

CrC_3,[64] TiC_3 (Ref. 65), *etc.*, stabilized in solid inert matrices.

Several promising methods of generation of highly reactive intermediates in cryogenic matrices were described in detail in recent reviews [66–69] and a monograph.[70] Thus the reviews [66,67] considered migration of active atoms (hydrogen, oxygen and fluorine) in cryogenic matrices of inert gases and described the possibility of using the translational mobility of these atoms for initiating the atom–molecule reactions directly in solid matrices aimed at the spectroscopic studies of radicals formed in these processes. Recently, the procedures of spectral studies of radical–molecule complexes incorporated into liquid helium nanodroplets have been developed. The advances in this research field were surveyed in a comprehensive review published in 2007.[68] The methods of low-temperature synthesis of species containing atoms and clusters of rare-earth and transition metals were discussed in a review [69] and a monograph.[70]

Among the new methods of preparation of stabilized intermediates, a method based on the use of the matrix substance as the chemically active reagent should be noted. The experiments carried out by Chertihin and Andrews [71] on the generation of various metal hydrides in solid hydrogen matrices can serve as a successful example of the use of chemically active matrices for generating reactive intermediates (see Section VIII). Yet another spectacular example of the usage of chemical activity of a solid matrix was the synthesis of new rare-gas compounds XRgH (X is an electronegative atom or a radical fragment; Rg = Xe, Kr, Ar).[72–74] The general method of synthesizing compounds HRgX included the dissociation of molecules HX (HF, HBr, H_2O, HCN, *etc.*) in a solid inert gas matrix followed by the formation of linear compounds HRgX (H–Ar–F, H–Xe–Br, H–Xe–OH, H–Kr–CN, *etc.*). The molecules HRgX were easily identified because the absorption bands in the IR spectrum corresponding to the Rg–H stretching modes have exclusively high intensities (the absorption coefficient of 10^3 km mol^{-1}) and are easily detected by IR spectroscopy.

Recently, the synthesis of the radicals HXeCC$^{\bullet}$ (Refs 75, 76) and HXeO$^{\bullet}$ (Ref. 77) and their IR spectroscopic identification were reported. Quantum chemical simulations [77] of the molecular and electronic structure of the HXeO$^{\bullet}$ radical demonstrated the preferentially ionic nature of the Xe–O bond with the partial transfer of the electron from the xenon atom to the oxygen atom (in the radical HXeO$^{\bullet}$, the charge on the xenon atom was +0.88 and the charge on the oxygen atom was −0.90). For the radical HXeCC$^{\bullet}$, quantum chemical calculations [75,76] also predicted the ionic nature of the Xe–C bond with the charges +0.89 on the xenon atom and −0.86 on the carbon atom and also the nonlinear structure for this radical with the XeCC angle equal to 123° (in contrast to the linear molecule HXeC≡CH [75,76,78]). According to calculations,[76] the length of the carbon–carbon bond in the HXeCC$^{\bullet}$ radical was 1.267 Å, *i.e.*, intermediate between the values typical of the double and the triple carbon–carbon bonds. The stretching mode ν_{CC} (1748 cm^{-1}) was closer to the stretching mode of the carbon–carbon double bond.

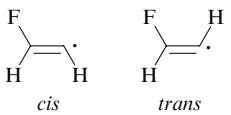
Preliminary experimental and theoretical magnetic-resonance parameters of the radical HXeCC$^{\bullet}$ were reported and the possibility of recording the EPR spectrum for this intermediate in solid xenon was discussed.[76] The main problem in studying the HXeCC$^{\bullet}$ radical by the EPR method was unreliable identification of its EPR spectrum against the background of spectra of other radical species formed in solid xenon–acetylene mixtures irradiated with accelerated electrons. A quantum chemical calculation of isotropic HFC constants predicted that the EPR spectrum of the HXeCC radical should include a doublet with splitting of 8.7 mT on the ^{129}Xe isotope with magnetic nucleus I = $^1/_2$. The EPR spectra of the HXeCC radicals contained a doublet with splitting of 13 mT. Based on the fact that the time variations of the doublet line intensity correlated with the changes in the intensity of the HXeCC lines in the IR spectrum, the doublet was assigned to the HXeCC radical.[76]

IV. Organic radicals containing unsaturated and aromatic fragments

In recent years, keen attention was drawn to organic radicals containing unsaturated and aromatic fragments. For certain previously detected species of this type, new studies were carried out on a higher level, which resulted in revision of the earlier results.

Information on the structure and the σ-nature of the simplest vinyl radical $CH_2{=}C^{\bullet}H$ was acquired from its EPR spectrum recorded for the first time upon the UV irradiation of HI and C_2H_2 molecules trapped in Ar and Ne matrices.[79–81] The IR spectrum of the vinyl radical generated [82] by UV photolysis (λ = 121.6 nm) of ethylene contained a band at 900 cm^{-1}, which was shifted to lower frequencies for isotopically substituted compounds, its deuterated and ^{13}C-analogues. The appearance of this band made it possible to infer the formation of the radical $CH_2{=}C^{\bullet}H$ in the reaction of excited Ne* atoms with C_2H_2 (see Ref. 83) and also upon annealing of the C_2H_2 photodecomposition products (λ = 193 or 250 nm) in a Xe matrix.[75,78] Later, [84] in the IR spectrum of the vinyl radicals generated by the photolysis of ethylene under the action of synchrotron radiation with λ = 120 nm in a neon matrix at 3 K, seven new bands were revealed at 3141.0, 2953.6, 2911.5, 1357.4, 677.1, 895.3 and 857.0 cm^{-1} and assigned to the ν_s(CH), $\nu_s(CH_2)$, $\nu_{as}(CH_2)$, $\delta(CH_2)$, δ(*cis*-HCCH), $w(CH_2)$ and w(CH) modes, respectively. This assignment was based on the fact that these bands shifted for isotopically substituted compounds, *viz.*, deuterated and ^{13}C-analogues, and also on the comparison of these frequencies with those calculated by the B3LYP and PW91PW91/aug-cc-pVTZ methods.

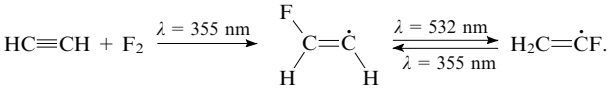
Fluorine atoms generated by F_2 photodecomposition (λ = 355 nm) reacted with acetylene in an argon matrix to afford the 2-fluorovinyl radical $CHF{=}C^{\bullet}H$. This radical was detected by the EPR [85] and IR spectroscopic techniques.[86] However, the close positions of vibrational lines in the absorption spectrum hampered the elucidation of the isomeric form of this radical for which *cis*- and *trans*-configurations are possible.[85,86]



cis *trans*

Later, this radical was studied by EPR and IR spectroscopy.[87] Based on the analysis of the EPR and IR spectra of the radical $CHF{=}C^{\bullet}H$ and its deuterated analogues and a comparison of experimental vibration frequencies with

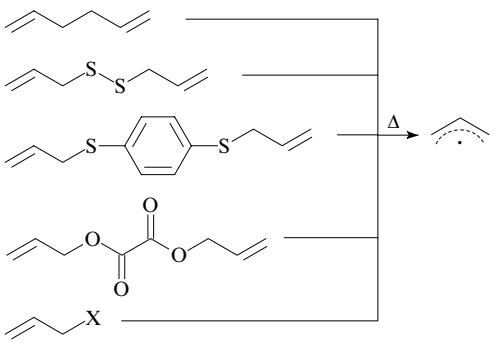
those calculated by the B3LYP/6-311++G(3df,2p) method, the bands observed in the IR spectrum were assigned to the *cis*-2-fluorovinyl radical rather than to the previously postulated[86] *trans* isomer. Pulsed laser photolysis of this radical in an Ar matrix at $\lambda = 532$ nm resulted in its partial isomerization to the radical $CH_2{=}C^{\bullet}F$ for which the EPR and IR absorption spectra were obtained for the first time.[87] Photolysis of the latter at 355 nm induced the reverse reaction:



It should be noted that the EPR spectroscopic data are more suitable for the reliable identification of different isomeric and structural forms of the radical $CHF{=}C^{\bullet}H$, because the HFC constants are extremely sensitive to the molecular structure variations. The observed HFC constants for *cis*-2-fluorovinyl radical ($a_F = 6.50$, $a_{\beta\text{-}H} = 3.86$, $a_{\alpha\text{-}H} = 0.25$ mT) and 1-fluorovinyl radical ($a_F = 13.71$, $a_{H\text{-}1} = 4.21$, $a_{H\text{-}2} = 1.16$ mT) substantially differed from one another and agreed well with the results of quantum chemical calculations. At the same time, the IR spectroscopic characteristics for these radicals differed insignificantly so that their correct interpretation could be carried out only due to the joint use of EPR and IR spectroscopy.[87]

The perfluorovinyl radical C_2F_3 generated by UV photolysis of C_2F_3I in an Ar matrix was first detected by the EPR method.[88] This radical is a σ-radical with a bent structure; nearly 70% of the unpaired electron density is localized on the α-carbon. The bands at 1780.4, 1282.4, 1216.9 and 900.0 cm^{-1} in the IR spectrum were assigned to this radical, which was synthesized in the gas phase by the decomposition of C_2F_3I, C_2F_3Br or C_2F_4 under the action of a pulsed electric discharge[89,90] and isolated in an Ar matrix, where the band at 1780.4 cm^{-1} was assigned to the stretching mode $\nu(C{=}C)$.[90]

The allyl radical generated by vacuum pyrolysis of different compounds was detected in an Ar matrix and comprehensively studied by IR spectroscopy first by Maltsev's research group [91–93] and later by the groups of Maier[94] and Oth.[95]



X = I, Cl, Br, $SiMe_3$.

The results obtained suggested a π-structure of the radical with considerably delocalized electron density, as confirmed by the data from an electron diffraction study.[96] However, some discrepancies in the band assignments are observed (Table 3).

In a study,[97] the interpretation of an IR spectrum of the oriented allyl radical‡ and its deuterated analogues was carried out with account of the absorption band polarization. Based on the comparison of experimental vibration frequencies of the allyl radicals frozen in an argon matrix and irradiated with polarized laser light ($\lambda = 351$ nm), with those calculated by the UB3LYP/6-311G(dp) method, a new assignment of absorption bands observed in the IR spectrum was accomplished. Several new bands were

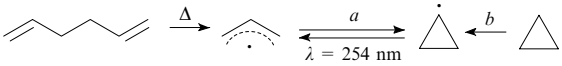
‡ In this study,[97] allyl radicals were generated by high-temperature thermolysis of $CH_2{=}CHCH_2I$, $CH_2{=}CHCH_2Br$, $(CH_2{=}CHCH_2S)_2$ and $(CH_2{=}CHCH_2)_2$ in a supersonic nozzle.

Table 3. Assignment of vibration frequencies of the Ar-matrix-isolated allyl radical and its deuterated analogues.

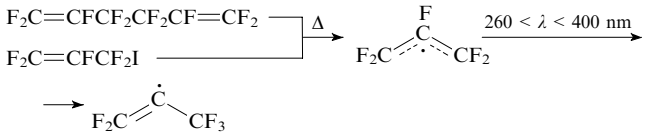
Symmetry type	Assignment	Observed frequencies /cm^{-1}						
		CH_2CHCH_2				CH_2CDCH_2 (see[97])	CD_2CDCD_2	
		from Ref. 94	from Refs 91–93	from Ref. 95	from Ref. 97		from Ref. 93	from Ref. 97
a_1	ν_1	3105	3107	3109	3109	3106		
	ν_2	3048	3051, 3040	3051	3052	3022	2285	2285
	ν_3	3016	3019	3019	3027	2268	2214	2215
	ν_4	1463	1463	1478	1478	1474	1018	1263
	ν_5	1403	1242,1182	1242	1242	1220		1018
	ν_6	1242	972.8	1183		1012		844
	ν_7	511						
b_1	ν_{10}	985	808.5	984	983	802		767
	ν_{11}	810	801.2	802	801	787	646	
	ν_{12}	802		511	510	511		
b_2	ν_{13}	3105	3107	3109	3107	3106		2372
	ν_{14}	3016	3019	3019	3020	3106	2209	2209
	ν_{15}	1477	1477	1464	1464	1452	1062	1387
	ν_{16}	1463	1389, 1317	1389	1390	1352	1007	1062
	ν_{17}	1389	1284	1284	1182	1010	1263	900
	ν_{18}	1285	983.2	810		845		689

revealed and certain earlier assignments [91–93] were revised with consideration of the vibrational symmetry.[97] For example, bands at 3109 (a_1) and 3107 cm^{-1} (b_2) were assigned to asymmetric stretching modes of the CH_2 group (ν_1 and ν_{13}) (see Table 3). A contradiction was eliminated associated with the assignment of bands at 1478 and 1464 cm^{-1} [in Ref. 97, they were assigned [97] to scissor symmetric modes of the CH_2 group (ν_4 and ν_{15}) of the a_1 and b_2 modes, respectively, whereas earlier [91–93] they were identified with the b_2 and a_1 modes] and the assignment of a band at 1242 cm^{-1} to the symmetric stretching mode of the carbon chain C–C–C of the a_1 mode was confirmed. The weak band at 1182 cm^{-1} (in place of the band at 1284 cm^{-1} suggested in Refs 91–93) was assigned to asymmetric mode (ν_{17}) of the b_2 mode. Taking into account the bathochromic shift of bands at 3027 and 983 cm^{-1} in the radical CH_2CHCH_2 to 2268 and 802 cm^{-1} for the monodeuterated isotopomer CH_2CDCH_2, these bands were assigned to the stretching mode of CH (ν_3) and the out-of-plane C–H bending mode (ν_{10}).

Photolysis of the allyl radical ($\lambda = 410$ nm) in solid argon at 18 K (conditions *a*) [95] or of cyclopropane in a xenon matrix containing Br_2 or I_2 at 10 K ($\lambda = 320$ nm, conditions *b*) afforded the cyclopropyl σ-radical with C_s symmetry.[98] Irradiation of this radical with $\lambda = 254$ nm led to the reverse isomerization.[98]

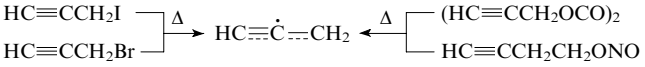


The perfluoroallyl radical C_3F_5 formed upon the pyrolysis of perfluorohexa-1,5-diene or 3-iodopentafluoroprop-1-ene in an argon matrix was characterized by IR spectroscopy.[99]



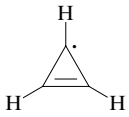
Five bands in the IR spectrum were assigned to this radical, of which the band at 1499.3 cm^{-1} was identified as an asymmetric stretching mode of the C–C–C skeleton.[99] This frequency proved to be intermediate between the frequencies characteristic of the double and the single bonds, which pointed to the noticeable delocalization of the electron density in this radical. In contrast to the allyl radical,[95] photolysis ($260 < \lambda < 400$ nm) of its perfluorinated counterpart afforded the perfluoroprop-2-enyl rather than the perfluorocyclopropyl radical.[100] The IR spectrum of the photolysis product of the perfluoroallyl radical in an Ar matrix revealed nine new absorption bands including a band of the C=C double bond stretching mode at 1785.4 cm^{-1}, which was assigned to the perfluoroprop-2-enyl radical based on a comparison of experimental frequencies with those calculated by the B3LYP/6-311G(d) method.[100]

In different periods, propargyl radical C_3H_3 was the subject of studies of several research groups.[20, 81, 101–104] The EPR spectrum of this radical recorded by Kasai [81] in 1972 pointed to its C_{2v} symmetry and delocalization of the unpaired electron density. The first IR spectrum of the propargyl radical recorded by Jacox and Milligan [102] contained three strong bands. Later, Korolev, Maltsev and Nefedov [103] observed twelve adsorption bands in the IR spectrum of this radical generated by vacuum pyrolysis of propargyl iodide $HC\equiv CCH_2I$ or dipropargyl oxalate $(HC\equiv CCH_2OCO)_2$, which allowed them to carry out force field calculations and infer the delocalization of the unpaired electron density in this radical.



In 2005, yet another attempt of the IR spectroscopic study of this radical generated in the gas phase by the pyrolysis of propargyl bromide or butynyl nitrate and stabilized in an argon matrix was undertaken.[20] The experimental § results together with quantum chemical calculations of the propargyl radical that took into account the anharmonicity of vibrations (CCSD(T)/ANO) made it possible to refine the assignments of the observed bands and their distribution over the symmetry types. Thus bands at 3308.5, 3028, 1935.4, 1440.4 and 1061.6 cm^{-1} were assigned to the a_1 mode, bands at 686.6 and 483.6 cm^{-1} were associated with the b_1 mode and bands at 1016.7 and 620 cm^{-1} were assigned to the b_2 mode. Bands at 1935.4 and 1061.6 cm^{-1} were attributed to stretching modes of multiple bonds in the $HC\equiv C$ and $C=CH_2$ fragments of the propagyl radical, respectively. The calculated structural parameters of this radical in the ground state X^2B_1 and the electron density distribution pointed to delocalization of the unpaired electron.

Another viewpoint on the identification of the band at 686.5 cm^{-1}, which was assigned [20] to propargyl radical, was advocated.[104] It was assumed that laser photolysis ($\lambda = 118.2$ nm) of methylacetylene afforded, in addition to the propargyl radical, the isomeric cyclopropenyl radical.



The band at 686.5 cm^{-1} was ascribed to the latter, which characterizes a mixed CH bending vibration (ν_{12}) with the $2\nu_{12}$ overtone at 1369.3 cm^{-1}. For both bands, insignificant batochromic shifts were observed on going from the cyclo-C_3H_3 radical to its deuterated analogues (cyclo-HCC•DCH, cyclo-DCC•HCH, cyclo-DCC•DCH, cyclo-DCC•HCD and cyclo-C_3D_3).[104] The obtained experimental data [104] were in good agreement with the results of calculations [105] of the cyclic structure mentioned. The data shown together with the asynchronous behaviour of these two bands (in contrast to other bands of the propargyl radical) in the matrix annealing and photolysis proved their correspondence to the isomeric species, *viz.*, the cyclo-C_3H_3 radical.

A silicon-containing analogue of the propargyl radical, $HC\equiv CSiH_2$ and its deuterated and ^{13}C isotopically substituted derivatives were synthesized by the vacuum UV photolysis ($\lambda = 122$ nm) of a mixture of silane and acetylene stabilized in an argon matrix at 10 K.[106]

$$SiH_4 + HC\equiv CH \xrightarrow{\lambda = 122\ nm} HC\equiv\dot{C}=SiH_2.$$

§ IR spectrum of the argon matrix-stabilized propargyl radical irradiated with polarized laser light with $\lambda = 248$ nm.

In the recorded IR spectrum,[106] bands at 2055.6 and 926.8 cm^{-1} corresponding to a sretching mode $\nu_3(a')$ of the C≡C bond and a bending mode $\nu_4(a')$ of the SiH_2 fragment, respectively, were ascribed to the $HC{\equiv}CSiH_2$ radical. These bands shifted in the spectra of isotopomers in good agreement with the results of calculations (B3LYP/cc-pVTS). According to calculations,[106] the $HC{\equiv}CSiH_2$ radical was nonplanar, in contrast to $HC{\equiv}CCH_2$.

The ethynyl radical $HC{\equiv}C^{\bullet}$ easily formed from acetylene under UV photolysis (λ = 122 nm)[107] or upon interaction of acetylene with excited Ar* atoms.[108] This fact explains the abundance of this radical in the interstellar space. Using the method of matrix EPR spectroscopy, it was shown[79,109] that the $HC{\equiv}C^{\bullet}$ radical in the ground electronic state $^2\Sigma^+$ has a linear structure.

The bands at 1848 and 3611 cm^{-1} detected[107] in the IR spectrum of the ethynyl radical were assigned to stretching modes of the C≡C (ν_3) and C−H (ν_1) bonds. However, in later studies,[108,110] based on the analysis of spectra of deuterated and ^{13}C isotopically substituted ethynyl radicals, this assignment was revised and the band at 3611 cm^{-1} was assigned to a compound mode ($\nu_1+\nu_2$ or $\nu_1+2\nu_2$). Furthermore, based on a new compound band ($\nu_2+\nu_3$) observed at 2104 cm^{-1}, the bending mode ν_2 (258 cm^{-1}) was determined.[110] In a recent IR spectroscopic study[111] of the photolysis (λ = 171 nm) product of acetylene in a Ne matrix at 3 K, a new band was detected at 3293.3 cm^{-1} and assigned to the stretching mode of the C−H bond (ν_1). In the deuterated radical, this band shifted to 2536.7 cm^{-1}. In the near IR region (4700–3500 cm^{-1}), several bands were revealed at 4133, 4020, 3805 and 3610 cm^{-1}, corresponding to the $A^2\Pi \leftarrow X^2\Sigma^+$ transitions. Electronic spectra of the photolysis products of acetylene demonstrated absorption in the vicinity of 195 nm, which corresponds to the ethynyl radical.[112] Additional information on the ground- and excited-state structure of the ethynyl radicals was obtained by comparing the matrix IR spectra of the unsubstituted $HC{\equiv}C$ radical and its deuterated and ^{13}C isotopically substituted analogues in the range of 700–12000 cm^{-1} (Ne matrix)[83,108] with the data of *ab initio* calculations.[113,114]

A silicon-containing analogue of the ethynyl radical, namely, $HC{\equiv}Si^{\bullet}$, was formed in the photolysis (λ = 122 nm) of a mixture of CH_4 and SiH_4 trapped in an argon matrix.[115]

$$CH_4 + SiH_4 \xrightarrow{\lambda = 122\ nm} HC{\equiv}Si^{\bullet}.$$

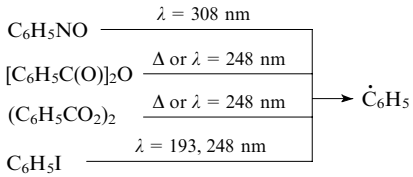
The IR spectrum of photolysis products contained a band at 1010.4 cm^{-1} assigned to a stretching mode ν_1(CSi) of the linear $HC{\equiv}Si^{\bullet}$ radical in the ground state $^2\Pi$.[115] This assignment agreed with the shift of this band to the low-frequency range for isotopically (D and ^{13}C) substituted analogues and was confirmed by the results of quantum chemical calculations at the CCSD(T)/6-31G(d,p) level.[115]

Polyacetylene radicals, namely, butadiynyl ($HC{\equiv}CC{\equiv}C^{\bullet}$) and hexatriynyl ($HC{\equiv}CC{\equiv}CC{\equiv}C^{\bullet}$), were formed as the vacuum ultraviolet photolysis products of diacetylene, buta-1,3-diene[116] and a mixture of buta-1,3-diene and acetylene[117] trapped in an Ar matrix at 10 K. For generating C_4H isotopomers, different deuterated and ^{13}C-substituted derivatives of diacetylene and buta-1,3-diene were used.[116] Detailed analysis of IR spectra of isotopically substituted molecules allowed reliable assignment of the bands corresponding to C−H and C≡C stretching modes. For the $HC{\equiv}CC{\equiv}C^{\bullet}$ radical, bands at 3307.4, 2083.9 and 2060.6 cm^{-1} were assigned to stretching modes ν_1(C−H), ν_2(C≡C) and ν_3(C≡C),¶ respectively,[116] whereas for the linear radical $HC{\equiv}CC{\equiv}CC{\equiv}C^{\bullet}$, the C≡C stretching mode was observed at 1953.4 cm^{-1} (Ref. 117).

An electronic absorption spectrum of ionization products of gaseous $Cl_2C{=}CClCCl{=}CCl_2$ has revealed recently[118] a chloro-substituted analogue of the butadiynyl radical, *i.e.*, the radical $ClC{\equiv}CC{\equiv}C^{\bullet}$. Cations $ClC{\equiv}CC{\equiv}C^{+}$, which were formed when a mixture of perchlorobuta-1,3-diene and helium was passed through a mass spectrometer with the ionization energy of 50–200 eV, were isolated using a quadrupole mass filter and stabilized in a neon matrix (6 K). Upon their co-condensation with Ne atoms, the majority of the $ClC{\equiv}CC{\equiv}C^{+}$ cations were neutralized to afford the $ClC{\equiv}CC{\equiv}C^{\bullet}$ radicals. In the electronic spectrum, absorption at 427 nm characterizing the $2^2\Pi \leftarrow X^2\Pi$ transition corresponded to the linear $ClC{\equiv}CC{\equiv}C^{\bullet}$ radical. Vibration frequencies of 1975, 459, 317 cm^{-1} were assigned to the $ClC{\equiv}CC{\equiv}C^{\bullet}$ radical in the excited state. They were associated with the C≡C (ν_1) stretching mode, the CCC (ν_4) bending mode and the C−Cl (ν_5) stretch, respectively. The ground-state radical was characterized by the frequency of 2022.1 cm^{-1} corresponding to the C≡C stretching mode (ν_1).

The method of matrix spectroscopy was successfully used in studying radicals containing aromatic fragments.

According to EPR data,[119] the phenyl radical, which in its ground electronic state X^2A_1 represents the simplest aromatic σ-radical, had C_{2v} symmetry. Further studies of the phenyl radical generated by photolysis or pyrolysis of benzoic anhydride or benzoyl peroxide and also by the photolysis of nitrobenzene or iodobenzene were carried out using the IR,[120,121] Raman[122] and electronic spectroscopic methods.[123]



For the C_6H_5 radical and its deuterated analogues (C_6D_5, *p*-C_6H_4D, *p*-C_6HD_4, *o*-C_6H_4D and *m*-C_6H_4D) generated from different precursors by photolysis with polarized light at different wavelengths, a full set of active IR spectral bands (24 bands) were detected.

A comparison of experimental absorption bands with those calculated (B3LYP/cc-pVDZ) as well as the different behaviour of the bands observed in the generation and the irradiation of the phenyl radical made it possible to reliably assign them to the corresponding normal vibrations. The most intense band at 706 cm^{-1} was assigned to the out-of-plane bend of C−H bonds. Certain inactive or very weak vibrations in the IR spectrum were observed in the Raman spectrum (a total of 27 bands).[122] Thus the highest intensity in the Raman spectrum corresponded to a band at 998 cm^{-1} that belonged to the ring breathing mode. The

¶ The frequencies ν_2 and ν_3 correspond to different C≡C bonds: ν_2 corresponds to the bond near the H atom and ν_3 corresponds to the C≡C bond remote from the H atom.

electron absorption spectrum contained three groups of bands corresponding to the transitions to three different electronic states, namely, $^2B_1$ (510.5 nm), $^2A_1$ (235.1 nm) and $^2B_2$ (211.5 nm).[123]

Hydrogen atoms generated by electron bombardment of benzene in a xenon matrix reacted with benzene when the matrix was annealed to 45 K to afford the cyclohexadienyl radical,[124] which gave rise to a strong doublet at 618/620 cm^{-1} and several weaker bands in the IR spectrum.

$$*C_6H_6 \longrightarrow {}^{\bullet}C_6H_5 + H^{\bullet},$$

$$C_6H_6 + H^{\bullet} \longrightarrow \text{cyclo-}{}^{\bullet}C_6H_7.$$

The EPR spectrum of this radical demonstrated a triplet of quartets, which corresponded to the strong hyperfine coupling of the unpaired electron with protons of the CH_2 group (a_{H_2} = 4.85 mT) and a weak coupling of the unpaired electron with hydrogen atoms of three CH groups (a_{H_2} = 1.05 mT) (splitting on protons of the rest two CH groups was weakly resolved and absent from the experimental spectrum). A comparison of IR and EPR spectroscopic data with the results of quantum chemical calculations (B3LYP/L22 and PBE0/L22) of the cyclo-C_6H_7 radical made it possible to assign the observed IR spectral bands to vibrations of the cyclohexadienyl radical with C_{2v} symmetry.

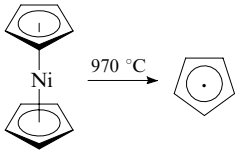
The benzyl radical $C_6H_5CH_2$, which, according to EPR spectroscopic data, was a planar π-radical,[125] was stabilized in inert gas matrices and characterized (in the ground and excited states) by different spectral methods. An UV spectrum of this radical[126] trapped in a Ne matrix contained bands at 454.4, 305.5 and 245 nm corresponding to the transitions between the 1^2B_2 ground state and the 1^2A_2, 2^2A_2 and 3^2B_2 excited states. The analysis of electronic spectral bands of the benzyl radical (C_7H_7) and its deuterated (C_7D_7) analogue, which were generated by the photolysis of toluene or toluene-d_8 in an Ar matrix,[127] made it possible to determine a set of vibration frequencies of these radicals. An IR spectrum of the benzyl radical was recorded when studying the vacuum pyrolysis products of benzyl bromide or 1,2-diphenylethane in an argon matrix.[128]

$$\left.\begin{matrix} C_6H_5CH_2Br \\ (C_6H_5CH_2)_2 \end{matrix}\right\} \xrightarrow[1000\ ^\circ C]{950\ ^\circ C} C_6H_5\dot{C}H_2$$

Based on the analysis of IR spectra of the benzyl radical and its deuterated analogues ($C_6H_5CD_2$ and $C_6D_5CH_2$) stabilized in an Ar matrix, fourteen observed bands were assigned.[128] The high frequency of the C–H bond stretch in the methylene fragment ($\nu_{as}(CH_2)$ = 3111 cm^{-1}) pointed to the sp^2-hybridization of the methylene carbon and the planar structure of the benzyl radical, which was consistent with the results of EPR studies.[125] A certain increase in the stretching vibration frequency for the *exo*-cyclic C–C bond (from 1215 to 1264 cm^{-1}) and the simultaneous decrease in the frequencies of C–C stretches in the benzene ring (from 1496 and 1467 cm^{-1} to 1469 and 1446 cm^{-1}) as compared with toluene were explained by the mutual effect of the radical centre and the benzene ring, being a consequence of electron density delocalization in the benzyl radical π-system. The analogous decrease in vibration frequencies of C–C bonds in the benzene ring (from 1657, 1525 and 1510 to 1597, 1501 and 1485 cm^{-1}) was observed earlier[129] in the perfluorobenzyl radical $C_6F_5CF_2$ generated by pyrolysis of perfluorobenzyl iodide or perfluorobibenzyl in Ar matrices.

$$\left.\begin{matrix} C_6F_5CF_2I \\ (C_6F_5CF_2)_2 \end{matrix}\right\} \xrightarrow[900\ ^\circ C]{750\ ^\circ C} C_6F_5\dot{C}F_2$$

The IR spectrum of the cyclopentadienyl radical synthesized by vacuum pyrolysis of bis(cyclopentadienyl)nickel in an argon matrix demonstrated three bands (3079, 1383 and 661 cm^{-1}) of the four bands possible for this highly symmetric species (D_{5h} symmetry), where the band at 1383 cm^{-1} was assigned[130] to the stretching mode of the C=C bond.



A comparison of this frequency with the frequencies of the C=C bond stretching modes in a cyclopentadienyl ligand of π-complexes and in the free (cyclo-C_5H_5)$^-$ anion[131] has shown that the vibration frequency of the C=C bond increased in the following sequence:

(cyclo-C_5H_5)$^{\bullet}$ (1383 cm^{-1}) < π-C_5H_5 (1410–1435 cm^{-1}) <

< (cyclo-C_5H_5)$^-$ (1455 cm^{-1}),

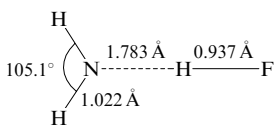
which was, most probably, due to the increase in the aromaticity of the cyclo-C_5H_5 moiety in this sequence.

V. Nitrogen-containing radicals

The simplest nitrogen-containing radical $H_2N^{\bullet}$, which by the way is the main photolysis product of the ammonia molecule, was among the first radicals detected by the matrix IR (Ref. 132) and EPR spectroscopy.[133] The reaction of fluorine atoms generated by the UV photolysis (λ = 337 nm) of F_2 in solid NH_3-containing argon afforded a complex with a hydrogen bond $H_2N^{\bullet}\cdots HF$. The existence of such a complex followed also from quantum chemical calculations (B3LYP/EPR-III).[134–136]

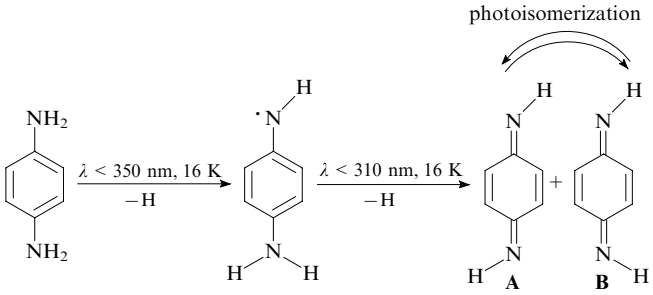
$$F + NH_3 \longrightarrow H_2\dot{N}\text{---}HF \longrightarrow H_2\dot{N} + HF.$$

The measured hyperfine coupling constants (a_N = 1.20, a_H = 2.40 and a_F = 0.70 mT) and the observed IR bands of the stretching and libration vibrations of the HF molecule (3267, 797, 791 cm^{-1}) in the $H_2N^{\bullet}\cdots HF$ complex agreed well with analogous parameters calculated using the density functional theory (B3LYP/EPR-III).[134] According to calculations,[135] such a complex has a planar structure with C_{2v} geometry and the H···N hydrogen bond energy equal to 51.5 kJ mol^{-1} (Ref. 134).



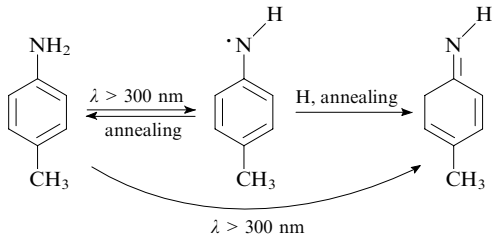
A study of photolysis (λ < 350 nm) products of 1,4-diaminobenzene in an argon matrix revealed[137] another nitrogen-containing species, *viz.*, 4-aminoanilino radical.

The IR spectrum contained 20 absorption bands belonging to this radical. Identification of these bands was carried out based on a comparison of the obtained IR-spectroscopic characteristics with those calculated by the B3LYP/6-31++G(d,p) method. The strongest band at 1614 cm^{-1} was assigned to the bending vibrations of the NH_2 group.

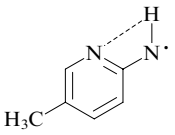


Shorter-wavelength irradiation of the argon-matrix-stabilized 4-aminoanilino radical ($\lambda < 310$ nm) led to the elimination of the second hydrogen atom to form cyclohexa-2,5-diene-1,4-diimine, which exists in two isomeric forms, **A** and **B**.

Yet another radical, 4-methylanilino radical, was detected in the photolysis of argon-matrix isolated 4-aminotoluene.[138] Nine IR absorption bands assigned to this radical disappeared when the matrix was annealed to the hydrogen diffusion temperature, which was accompanied by an increase in the intensity of bands corresponding to the original 4-aminotoluene and 4-methylcyclohexa-2,4-diene-1-imine.



The formation of the 5-methyl-2-pyridinamino radical was detected by IR spectroscopy[139] in the photolysis ($340 \geqslant \lambda \geqslant 300$ nm) of 2-amino-5-methylpyridine in an argon matrix. In the IR spectrum, this radical had 15 bands with absorption frequencies well consistent with those calculated by the B3LYP/6-31++G(d,p) quantum chemical method. According to results of calculations, a radical structure with the intramolecular hydrogen bond NH···N between the pyridine-ring nitrogen atom and the hydrogen atom in the radical centre was the most advantageous as regards the energy.

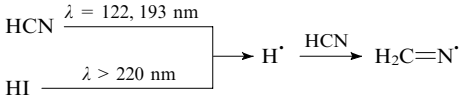


The band at 3417 cm^{-1} unobserved for the 4-amino- and 4-methylanilino radical was assigned to the N−H stretch of this radical.[137,138]

A simple diatomic nitrogen-containing σ-radical $N{\equiv}C^{\bullet}$ was first detected in 1962 by the EPR method[140] in the photolysis ($\lambda = 122$ nm) of hydrocyanic acid in an argon matrix at 4 K. Based on the electronic spectrum[141] of this radical, the stretching vibration $\nu(N{\equiv}C)$ frequency was calculated to be 2043 cm^{-1}. This value virtually coincided with the frequency of 2046 cm^{-1}found by IR spectroscopy.[142,143]

The possibility of formation of $N{\equiv}CC{\equiv}C^{\bullet}$ radicals upon the photolysis of cyanoacetylene was reported.[144] Recently,[145] such radicals with the linear structure were detected in the IR spectra of the photolysis products ($\lambda = 193$ nm) of cyanoacetylene in argon, krypton and xenon matrices. The IR spectra contained the following bands assigned to this radical: at 2303 and 2079 cm^{-1} (Ar), 2298 and 2076 cm^{-1} (Kr), 2280 and 2066 cm^{-1} (Xe).

The formation of nitrogen-centred radicals was observed in the reactions of highly reactive hydrogen or fluorine atoms with several simple nitrogen-containing molecules in the inert-gas matrices annealed to temperatures of hydrogen or fluorine diffusion. The methyleneimino radical $H_2C{=}N^{\bullet}$ was obtained in the reaction of HCN molecules with H atoms generated by photolysis of different precursors in inert-gas matrices. This radical was studied by EPR[146,147] and IR spectroscopic methods.[148,149]



According to EPR data,[146,147] the unpaired electron in the $H_2C{=}N^{\bullet}$ species was localized on the nitrogen π-orbital coplanar with the C−H bond and orthogonal to the C=N bond; thus, this radical had a planar structure. This conclusion was confirmed by the analysis of an anisotropic EPR spectrum of the radical containing a magnetic carbon isotope, ^{13}C. The planar structure of the $H_2C{=}N^{\bullet}$ radical was also confirmed by the results of IR spectroscopic studies.[148,149] The carbon–nitrogen bond ($\nu = 1725$ cm^{-1}) proved to be intermediate between the double and triple bonds.

Fluorine atoms generated by the photolysis of F_2 in argon matrices reacted with FCN and HCN molecules to produce the $F_2C{=}N^{\bullet}$ and $HFC{=}N^{\bullet}$ radicals.[150,151]

$$F + FCN \longrightarrow F_2C{=}N^{\bullet},$$
$$F + HCN \longrightarrow HFC{=}N^{\bullet}.$$

The structure of the $HFC{=}N^{\bullet}$ radical was studied by EPR and IR spectroscopic methods.[151] Quantum chemical calculations[151] [B3LYP/6-311++G(3df,2p)] confirmed the planar structure of the $H_2C{=}N^{\bullet}$, $F_2C{=}N^{\bullet}$ and $HFC{=}N^{\bullet}$ radicals. Table 4 summarizes the spectral and structural parameters of these isoelectronic radicals.

Based on the results of quantum chemical calculations[152–154] for the $H_2C{=}N^{\bullet}$, $F_2C{=}N^{\bullet}$ and $HFC{=}N^{\bullet}$ radicals, the existence of structural isomers with an unpaired electron localized on the carbon atom, the so-called σ-radicals $HN{=}C^{\bullet}H$, $FN{=}C^{\bullet}F$ and $HN{=}C^{\bullet}F$, respectively, were predicted. Until recently, the experimental data for such radicals were virtually absent. It was assumed[142,148] that the H* + HCN and F* + FCN reactions observed in solid argon can produce small amounts of $FN{=}C^{\bullet}F$ and $HN{=}C^{\bullet}H$ radicals in addition to the main products, namely, the $H_2C{=}N^{\bullet}$ and $F_2C{=}N^{\bullet}$ radicals.

However, in another study,[148] only one absorption band at 886 cm^{-1} could be assigned to the $HN{=}C^{\bullet}H$ radical and the band at 1053 cm^{-1} was assigned to the $FN{=}C^{\bullet}F$ radical. In a later study,[149] two IR bands, at 883 and

Table 4. Spectroscopic and structural parameters of isoelectronic radicals $H_2C{=}N^{\bullet}$, $F_2C{=}N^{\bullet}$ and $HFC{=}N^{\bullet}$ (according to Ref. 151).

Parameter	$H_2C{=}N^{\bullet}$		$F_2C{=}N^{\bullet}$		$HFC{=}N^{\bullet}$	
	experiment [a]	theory	experiment	theory	experiment	theory
a_N /mT	0.83	0.82	–	0.79	0.86	0.79
a_F /mT	–	–	–	4.84	10.87	11.15
a_H /mT	8.47	8.48			4.27	4.42
R_{CN} /Å	–	1.238	–	1.249	–	1.243
R_{CH} /Å	–	1.097	–	–	–	1.089
R_{CF} /Å	–	–	–	1.317	–	1.345
Angle HCN /deg	–	121.47	–	–	–	123.81
Angle FCN /deg	–	–	–	124.58	–	123.17
ν_{CN} /cm^{-1}	1725		1752		1673	1724

Note. Calculations were carried out by the B3LYP/6-311++G(3df,2p) method. [a] According to the data from Refs 147, 148.

1218 cm^{-1}, were assigned to the $HN{=}C^{\bullet}H$ radical generated by the photolysis of HCN (λ = 193 nm) in solid xenon or krypton. Recent EPR, IR and UV spectroscopic studies [151, 155–157] of reaction products of a fluorine atom with an HCN molecule in an argon matrix have shown that the fluorine atom that was originally capable of diffusion in the argon matrix at 25 K reacted with an HCN molecule to afford the $HFC{=}N^{\bullet}$ π-radical (**A**). The latter was transformed under UV radiation (λ = 355 nm) into a σ-radical $HN{=}C^{\bullet}F$ with *trans*-configuration.

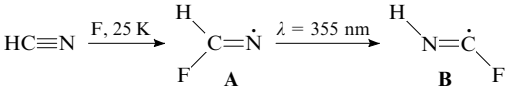


Table 5 shows the spectral parameters of the $HN{=}C^{\bullet}F$ radical and its deuterated analogue $DN{=}C^{\bullet}F$. It deserves mentioning that the frequencies of characteristic stretching vibrations of the $HN{=}C^{\bullet}F$ radical (ν_{CN} = 1700 cm^{-1} and ν_{CF} = 1172 cm^{-1}) weakly differed from those of its isomer

Table 5. Vibration frequencies and isotropic HFC constants of the *trans*-$HN{=}C^{\bullet}F$ and *trans*-$DN{=}C^{\bullet}F$ radicals in solid argon (data from Ref. 155).

Parameter	*trans*-$HN{=}C^{\bullet}F$		*trans*-$DN{=}C^{\bullet}F$	
	experiment	theory	experiment	theory
δ_{FCN} /cm^{-1}	595 (0.09)	600 (0.06)	–	547 (0.16)
δ_{HCN} (a'') /cm^{-1}	734 (0.30)	733 (0.28)	575 (0.22)	555 (0.16)
δ_{HCN} (a') /cm^{-1}	905 (1.0)	924 (1.0)	759 (0.64)	770 (0.50)
ν_{CF} /cm^{-1}	1172 (0.26)	1194 (0.29)	1142 (0.81)	1154 (0.50)
ν_{CN} /cm^{-1}	1700 (0.69)	1676 (0.80)	1701 (1.0)	1747 (1.0)
a_N /mT	0.19	0.21	–	–
a_F /mT	23.69	22.91	–	–
a_H /mT	1.90	2.18	–	–

Note. Calculations were carried out for free molecules by the B3LYP/6-311++G(3df,2p) method. In the parentheses, the intensity (rel. u.) is shown.

$HFC{=}N^{\bullet}$ (ν_{CN} = 1673 cm^{-1} and ν_{CF} = 1058 cm^{-1}). Larger deviations were observed in HFC parameters of these radicals (see Tables 4 and 5). The isotropic HFC constant on the fluorine atom (a_F) in σ-radical **B** more than doubled, while the other two HFC constants, a_N and a_H, decreased several times as compared with π-radical **A**.

UV Absorpion spectra of the $HFC{=}N^{\bullet}$ radical demonstrated bands at 488 and 355 nm corresponding to the $A^2A'' \leftarrow X^2A'$ and $B \leftarrow X$ transitions. Selective photoexcitation of π-radical **A** with the $A^2A'' \leftarrow X^2A'$ transition frequency led to the complete and irreversible conversion of this radical into σ-radical **B**. Based on kinetic studies and an analysis of absorption and fluorescence spectra of the $HFC{=}N^{\bullet}$ and $DFC{=}N^{\bullet}$ radicals, it was found that the transformation of radical **A** into radical **B** occurred in the electronically excited state A^2A'' due to the intermolecular tunnelling transfer of the hydrogen atom from the carbon atom to the nitrogen atom.

The $N{\equiv}CC^{\bullet}H_2$ radical generated by vacuum pyrolysis of iodoacetonitrile [3, 158] and stabilized in an Ar matrix at 12 K was detected by IR spectroscopy.

$$N{\equiv}CCH_2I \xrightarrow{950-1000\ ^{\circ}C} N{\equiv}\dot{C}{-}{-}CH_2 .$$

Seven absorption bands in the IR spectrum corresponded to this radical. Bands at 2087 and 1021 cm^{-1} were assigned to stretching vibrations of C≡N and C–C bonds, respectively; bands at 3142 (ν_{as}) and 3044 cm^{-1} (ν_s) were assigned to stretching vibrations of the CH_2 group. Based on the obtained spectroscopic data and the results of force-field simulations of the $N{\equiv}CC^{\bullet}H_2$ radical, which pointed to the weakening of the C≡N bond and the strengthening of the C–C and C–H bonds, it was concluded [158] that the electron density on this radical was considerably delocalized in the same manner as for the propargyl radical.[102]

VI. Oxygen-containing radicals

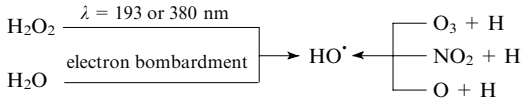
Strong interest in oxygen-containing radicals stems from their key role in the processes occurring in upper atmospheric layers.

1. Oxyradicals

The simplest oxygen-containing radical $HO^{\bullet}$ generated by passing an electric discharge through a mixture of hydrazine with water and isolated in an argon matrix was first detected in UV spectroscopic studies in 1958.[159] Later, the $HO^{\bullet}$ radical and its deuterated analogue stabilized in different matrices were studied in more detail by UV,[160, 161] laser [162] and IR [163–166] spectroscopy. Splitting of UV absorption bands was attributed to either the radical rotation in the matrix [161] or the effect of the matrix material.[161, 162] The magnetic circular dichroism (MCD) data obtained for the matrix-isolated $HO^{\bullet}$ radical [161] suggested that the $HO^{\bullet}$ radicals were randomly oriented in the Ar matrix and occupied five different positions in the host lattice (Ar matrix).

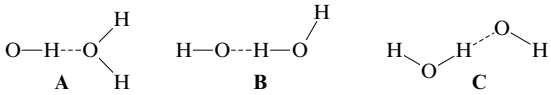
The IR spectrum of the electron bombardment products of H_2O isolated in an argon matrix revealed the band at 3548.9 cm^{-1}, which was assigned to the $HO^{\bullet}$ radical (see Ref. 165). The closely spaced bands were observed in the IR spectra of $HO^{\bullet}$ radicals generated in the reactions of hydrogen atoms with NO_2 or O_3 or O in the gas phase (the band

at 3548.2 cm^{-1}) [165] or by the photolysis of H_2O_2 in an Ar matrix (the band at 3554 cm^{-1}).[166]



Later studies [167–169] have shown that the HO• radical tended to form complexes with the matrix-trapped water molecules. Thus, the band observed [163] at 3452.3 cm^{-1}, which was shifted by 100 cm^{-1} with respect to the absorption band of the HO• species, belonged to its complex with a water molecule.

According to the calculations,[167, 169–171] the complex of the HO• radical with a water molecule could adopt different configurations in which the radical could act as either a donor (structure **A**) or an acceptor (structures **B**, **C**) of the hydrogen bond with respect to the water molecule.



Complex **A** possessed the highest stability. In the IR spectra of the HO•---H_2O complex and its deuterated analogue DO•---H_2O, the presence of three absorption bands in the stretching vibration ranges of the HO• and DO• radicals [3452.2, 3442.1 and 3428.0 cm^{-1} (HO•); 2542.9, 2536.4 and 2524.6 cm^{-1} (DO•)] was explained [169] by the different positions of complex **A** in the matrix.

The HO• radical could form complexes not only with water molecules, but also with CO_2, O_3 and CO molecules. The band at 3557 cm^{-1}, which was observed in the IR spectrum of photolysis products of H_2O molecules in a matrix of Ar and CO_2 in the ratio varying from 150 : 1 to 750 : 1,[172] shifted by only 8.8 cm^{-1} with respect to the stretching vibration band of the individual HO• radical. A more pronounced shift of this band to lower frequencies was observed for complexes of the HO• radical with O_3 molecules (by 12.6 cm^{-1}) and CO (by 21.8 cm^{-1}).[173]

The reaction of HO• radicals with alkenes afforded hydroxyalkyl radicals.[174–176] The 2-hydroxyethyl radical $HOCH_2C^{\bullet}H_2$ was discovered by matrix IR spectroscopy among the photolysis products of a C_2H_4 and H_2O_2 mixture (λ = 248 nm) in an Ar matrix (ratio $Ar : C_2H_4 : H_2O_2$ = 900 : 1 : 1).[174]

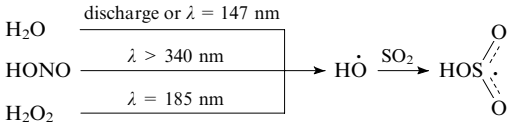
$$C_2H_4 + H_2O_2 \xrightarrow{\lambda = 248\ nm} C_2H_4 + H\dot{O} \longrightarrow HOCH_2\dot{C}H_2.$$

An analysis of the IR spectra of the hydroxyethyl radical and its ^{13}C-substituted analogue and a comparison of experimental absorption frequencies with those calculated by the MCSCF/DZP method made it possible to assign eight observed bands to the $HOCH_2C^{\bullet}H_2$ radical.[174] The absorption band at 3625.8 cm^{-1} was assigned to the O—H stretch.

The formation of more complex hydroxyalkyl radicals, namely, 2-hydroxy-1-methylethyl, 2-hydroxypropyl, 2-hydroxy-1-methylpropyl, 1-(hydroxymethyl)propyl, 2-hydroxybutyl, 2-hydroxy-1,1-dimethylethyl and 2-hydroxy-2-methylpropyl, was observed [175] in the reactions of more complex alkenes (propene, but-2-ene, but-1-ene and 2-methylpropene, respectively) with the HO• radical generated by photolysis of argon-matrix-isolated H_2O_2. The HO• radicals generated by photolysis (λ > 340 nm) of HONO in an Ar matrix reacted with 1,1-dichloroethylene to afford the 1,1-dichloro-2-hydroxyethyl radical,[176] which later reacted with NO• to form 2,2-dichloro-2-nitrosoethanol.

$$HONO \xrightarrow{\lambda > 340\ nm} H\dot{O} + \dot{N}O,$$
$$H_2C{=}CCl_2 \xrightarrow{HO^{\bullet}} CH_2(OH){-}\dot{C}Cl_2 \xrightarrow{\dot{N}O} CH_2(OH){-}CCl_2NO.$$

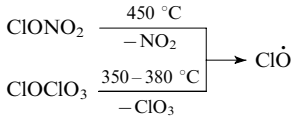
The HO• radical generated by photolysis of H_2O_2, H_2O or HONO in Ar or N_2 matrices [177–179] or high-voltage discharge of water vapour [180] reacted with SO_2 to afford the $HOS^{\bullet}O_2$ radical.



The shift of absorption bands in isotopically (^{18}O,^{34}S and D) substituted analogues of the $HOS^{\bullet}O_2$ radical made it possible to assign the bands at 3539.9, 1309.2, 1296.2, 1097.3 and 759.5 cm^{-1} to normal modes.[178, 180]

The fluoroxyl radical FO• was repeatedly observed [181–183] in inert matrices in the photolysis of F_2O. A complex of this radical with the oxygen molecule FO•---O_2, formed in an Ar matrix by the reaction of F atoms with ozone was detected [184] by the matrix IR spectroscopy. Absorption bands at 1522 and 968 cm^{-1} corresponding to the O—O and F—O vibrations in the complex turned out to be shifted to the low-frequency range as compared with the corresponding vibrations in individual O_2 and FO• molecules by 34 and 61 cm^{-1}, respectively. Irradiation (λ > 532 nm) of the FO•---O_2 complex isolated in an Ar matrix at 15 K led to the disappearance of an absorption band of this complex and the appearance of an absorption band of the matrix-isolated FO• radical.[183]

The ClO• radical generated by vacuum pyrolysis of $ClONO_2$ or $ClOClO_3$ in Ar, Kr, N_2, Ne or O_2 matrices was studied in detail by matrix IR spectroscopy.[185, 186]

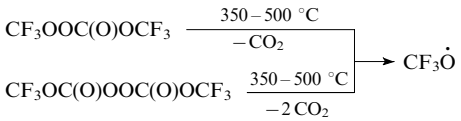


It was shown [185] that the position of absorption bands in the IR spectrum of the ClO• radical depends little on the matrix material. Thus the absorption band observed at 843.8 cm^{-1} in a Ne matrix was slightly shifted to the high-frequency range in the other matrices, namely, to 844.9 in Ar, 848.2 in N_2, 848.8 in Kr and 849.4 cm^{-1} in O_2. An additional weak band at 838.5 cm^{-1} in the IR spectrum of the ClO• radical in a Ne matrix, which was shifted to the low-frequency range as compared with the fundamental at 843.8 cm^{-1} of this radical in the ground state $X^2\Pi_{3/2}$, was assigned to the radical in the $X^2\Pi_{1/2}$ electronic state. Such assignment was made by taking into account the data from UV spectroscopy.[185] In the UV spectrum, the ClO• radical isolated in an Ne matrix absorbed in the range of 230–330 nm (the $A^2\Pi_{3/2} \leftarrow X^2\Pi_{3/2}$ transition with a small contribution of the $A^2\Pi_{1/2} \leftarrow X^2\Pi_{1/2}$ transition).[185, 186]

The simplest alkoxyl radical $CH_3O^{\bullet}$ was formed by photolysis ($\lambda = 320$ nm) of CH_3ONO in an Ar matrix or by laser excitation of the deposited reaction products of microwave discharge of CF_4 with CH_3OH diluted by Ar ($Ar:CF_4$ 50:1).[187] The $CH_3O^{\bullet}$ radical was detected by electronic spectroscopy. Among the progression of bands observed in the emission (310–420 nm) and absorption (273–322 nm) electronic spectra, the vibrational transitions corresponding to the ground (X^2E) and excited (A^2A_1) states of this radical were assessed. According to the IR spectroscopic data,[188,189] the $CH_3O^{\bullet}$ radical formed by either photolysis of Ar- or N_2-matrix-isolated methanol ($\lambda = 147$ nm and 122 nm)[188] or the reaction of CH_3OH with fluorine atoms or excited Ar atoms[189] represented a minor product, whereas the main product of these reactions was the isomeric hydroxymethyl radical $HOC^{\bullet}H_2$.

The far larger body of information was obtained in the IR-spectroscopic study of the perfluoromethoxyl radical $CF_3O^{\bullet}$. This radical formed by the photolysis ($240 < \lambda < 420$ nm) of a CF_3I-O_3 mixture isolated in an argon matrix was first detected in the IR spectrum[190] according to presence of the absorption band at 1223 cm^{-1}. The $CF_3O^{\bullet}$ radical was also found among the photolysis products ($\lambda = 254$ nm) of a CF_3I-O_2 mixture in an Ar matrix.[191]

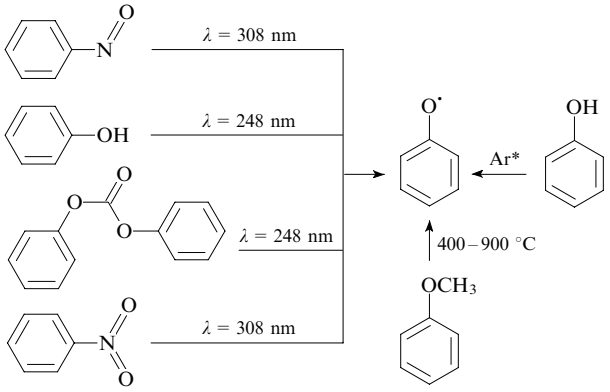
Recently,[192] a comprehensive IR and UV spectroscopic study of the $CF_3O^{\bullet}$ radical synthesized by the vacuum pyrolysis of peroxide compounds $CF_3OOC(O)OCF_3$ and $CF_3OC(O)OOC(O)OCF_3$ isolated in Ar or Ne matrices has been carried out.



Six absorption bands observed in the IR spectrum of pyrolysis products were assigned[192] to the $CF_3O^{\bullet}$ radical in the ground state X^2A' with C_s symmetry. A comparison of experimental absorption frequencies with those calculated by quantum chemical methods (B3LYP and BHLYP)[193] made it possible to attribute the bands at 1273 (in the Ne matrix) and 1260 cm^{-1} (in the Ar matrix) to the stretching vibration of the C–O bond (Table 6). In the UV absorption spectrum of the $CF_3O^{\bullet}$ radical, four progressions of bands corresponding to the electronic-vibrational transitions $A^2A_1 \leftarrow X^2E$ were revealed[192] in the range of 28517–32400 cm^{-1}. The observed UV spectrum was in good agreement with the fluorescence spectrum (LIF spectrum) of this radical in the gas phase according to which the $CF_3O^{\bullet}$ radical ground state was X^2E with C_{3v} symmetry.[194] Presumably,[192] the lower symmetry of the ground-state $CF_3O^{\bullet}$ radical stabilized in a solid matrix was associated with the strengthening of the Jahn–Teller effect due to the radical interaction with the matrix material.

The fluoroformyloxyl radical $FC(O)O^{\bullet}$ generated by quenching vacuum flash pyrolysis products (250 °C) of bis(fluoroformyl) peroxide in inert-gas matrices (N_2, Ne or Ar) was studied by IR and UV spectroscopy.[195] The assignment of six bands [1477.2, 975.1, 521.6 (a_1); 1113.6, 482.5 (b_1); 730.6 cm^{-1} (b_2)] observed in the IR spectrum of the $FC(O)O^{\bullet}$ radical to the ground state X^2B_2 with C_{2v} symmetry was made based on a comparison of these bands with those of isotopically (^{18}O and ^{13}C) substituted analogues and also with the bands calculated by the B3P86/3-21G density functional method.[195] From the UV spectrum of the $FC(O)O^{\bullet}$ radical stabilized in a Ne matrix, the absorption frequencies of this radical in the excited state B^2A_1 (1607, 1117, 839 and 611 cm^{-1}) were elucidated. The EPR spectroscopic data obtained recently[241] for the solid-argon isolated $FC(O)O^{\bullet}$ radical and the results of calculation of the spin density distribution (QCISD) in this radical confirmed the earlier conclusions that it has a planar structure and the unpaired electron is localized in electron orbitals of both oxygen atoms lying in the plane of this molecule. These results agreed well with the quantum chemical calculations,[242,243] which predicted the following structural parameters of the $FC(O)O^{\bullet}$ radical: $R(C-F) = 1.325$ Å, $R(C-O) = 1.167$ Å, bond angles $FCO = 127.8°$.

The phenoxyl radical $C_6H_5O^{\bullet}$ was first detected in an argon matrix in the course of co-condensation of excited argon atoms and phenol.[244]



The bathochromic shift of adsorption bands to 397.2 and 628.1 nm in the UV spectrum of the $C_6H_5O^{\bullet}$ radical as compared with phenol (210.5 and 270 nm) was explained by the ease of electron transitions in this radical. The most comprehensive study of the $C_6H_5O^{\bullet}$ radical and its isotopically labelled species $C_6D_5O^{\bullet}$ and $C_5H_5{}^{13}CO^{\bullet}$ was carried out by matrix IR (see Ref. 196) and matrix UV spectroscopy.[245] The IR spectra of the $C_6H_5O^{\bullet}$ radical and its isotopomers revealed almost the whole set of active bands. The analysis of spectra of isotopically substituted radicals and a comparison of experimental data with the results of quantum chemical calculations (B3LYP/cc-pVTZ) made it possible to reliably assign the observed bands to normal vibrations.[196]

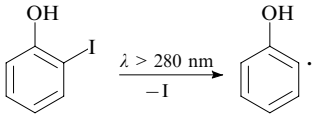
The band at 1481 cm^{-1} was assigned to the stretching vibration of the C–O bond in the $C_6H_5O^{\bullet}$ radical. In the spectra of isotopically substituted radicals $C_6D_5O^{\bullet}$ and $C_5H_5{}^{13}CO^{\bullet}$, this band shifted to the low-frequency range by 14 and 26 cm^{-1}, respectively. The considerably higher frequency of this vibration in the radical as compared with the C–O band in phenol (1255 cm^{-1}) pointed to the higher multiplicity of this bond due to the radical centre conjugation with the benzene ring π-system. The results acquired from electronic spectra and polarized IR spectra altogether allowed determination of the direction and symmetry of electron transitions for the low-lying excited electronic states of the phenoxyl radical.[245] The bands at 16 000 and 33 900 cm^{-1} were assigned to the $^2A_1$ state, the bands at 25 200 and 41 800 cm^{-1} were attributed to the $^2B_1$ state ($\pi-\pi^*$-transitions) and a weak band at 8900 cm^{-1} in the near IR range was assumed to correspond to the $^2B_2$ state ($n-\pi^*$-transition).

Table 6. Characteristic bands in the IR spectra of oxygen-containing radicals.

Radical	Matrix	ν(OO)	ν(CO)	ν(C=O)	Ref.	Radical	Matrix	ν(OO)	ν(CO)	ν(C=O)	Ref.
$CF_3O^{\bullet}$	Ar		1223		190	$HOO^{\bullet}$	Ar	1101.1			213
	Ar		1263		192		Ne	1100.3			214
	Ne		1270		192						
						$FOO^{\bullet}$	Ar	1490			184, 215,
$FC(O)O^{\bullet}$	Ar		1477.2,		195						216
			1113.6				Ar	1442.8,			217, 218
	Ne		1488.5,		195			1416.7			
			1097.7								
	N_2		1478.1,		195	$ClOO^{\bullet}$	Ne	1439.6			218, 219
			1116.5				Kr	1440.7,			218
								1412.1			
$C_6H_5O^{\bullet}$	Ar		1481		196						
2-(HO)$C_6H_4O^{\bullet}$	Ar		1457		197	$BrOO^{\bullet}$	Ar	1485			220 – 223
$HC^{\bullet}=O$	CO			1861	198	$O_3ClOOO^{\bullet}$	O_2	1525			185
	Ar			1863	199, 200	$FSO_2OOO^{\bullet}$	Ar	1540.6			224
	Xe			1858.4,	201		Ne	1543.8			224
				1856.6							
						$CH_3OO^{\bullet}$	Ar	1109	902		225, 226
$FC^{\bullet}=O$	CO			1855	202	$C_2H_5OO^{\bullet}$	Ar	1112	838		227
	Ar			1857	203	$CF_3OO^{\bullet}$	Ar	1093	869.2		191, 228
						$CF_3CHClOO^{\bullet}$	Ar	1102.1	972.7		229
$ClC^{\bullet}=O$	CO			1876.1	202	$Bu^{t}OO^{\bullet}$	Ar	1124	730		230
	Ar			1876.7	202,	$Pr^{i}OO^{\bullet}$	Ar	1101	789		231
					204 – 206	$CH_2=CHOO^{\bullet}$	Ar	1140.7	–		232
						$CH_2=CHCH_2OO^{\bullet}$	Ar	1128.6,	850.7,		208
$CH_3C^{\bullet}=O$	Ar			1875	207			1108.6	855.6		
						$C_6H_5OO^{\bullet}$	Ar	1122.9	793.9		233
$NH_2C^{\bullet}=O$	Xe			1794.2,	201	*cis*-$HC(O)OO^{\bullet}$	Ar	–	957.3	1821.5	234
				1796.6,		$HC(O)OO^{\bullet}\cdots HO_2$	O_2	–	1089.9	1790	235, 236
				1806.5,		*trans*-$FC(O)OO^{\bullet}$	Ar	1084.8	895.7	1919.2	228
				1811.8		*cis*-$FC(O)OO^{\bullet}$	Ar	1071.9	863.6	1904.5	228
						trans-$ClC(O)OO^{\bullet}$	Ar	1072	925	1886	237
$CH_2=CHC^{\bullet}=O$	Ar			1823.1	208	*cis*-$ClC(O)OO^{\bullet}$	Ar	1106	952	1824	237
trans-$CF_3OC^{\bullet}=O$	CO			1857	209	*trans*,*trans*-$CH_3C(O)OO^{\bullet}$	Ar	1094	731	1852	238
cis-$HOC^{\bullet}=O$	CO		1077	1833	210	*trans*,*cis*-$CH_3C(O)OO^{\bullet}$	Ar	1099	736	1842	238
						tans,*trans*,*trans*-	Ar	1087	936	1895	239, 240
trans-$HOC^{\bullet}=O$	Ar		1064.6	1843.6	211	$CF_3OC(O)OO^{\bullet}$					
	Ne		1050.4	1848	212	*trans*,*trans*,*cis*-	Ar	1087	955	1868	239, 240
						$CF_3OC(O)OO^{\bullet}$					

A complex formed by the phenoxyl radical with NO was observed [246] in an IR spectroscopic study of the photolysis products of nitrobenzene in an Ar matrix. It was established that the $C_6H_5O^{\bullet}$ radical was formed in the decomposition of an isomer of nitrobenzene, *i.e.*, phenyl nitrite. In the matrix IR spectrum of photolysis products ($250 < \lambda < 580$ nm) of nitrobenzene, sixteen bands were assumed to belong to a complex of the $C_6H_5O^{\bullet}$ radical with NO. A slight difference in the absorption frequencies of the $C_6H_5O^{\bullet}$ radical in its complex with NO (less than 2 cm^{-1}) from the earlier observed absorption frequencies of the free phenoxyl radical stabilized in an argon matrix [196] pointed to the weak interaction between the $C_6H_5O^{\bullet}$ radical and NO in this complex. The complexation process was reversible, namely, with the annealing of matrix, nitrite C_6H_5ONO was formed.

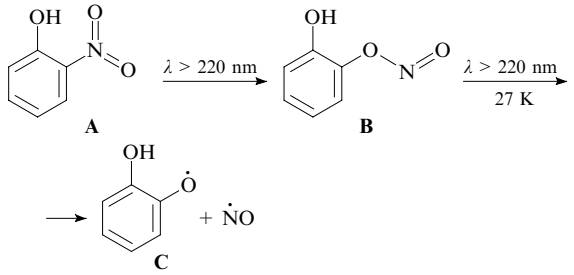
A phenoxyl radical isomer, namely, the 2-hydroxyphenyl radical, generated by photolysis ($\lambda > 280$ nm) of 2-iodophenol was detected by EPR [247] and IR spectroscopy.[248]



According to the DFT/B3LYP/6-31 + + G(d,p) calculations,[248] the 2-$HOC_6^{\cdot}H_4$ radical was 120 kJ mol^{-1} less stable than the $C_6H_5O^{\bullet}$ radical, which explained the easy isomerization of the 2-hydroxyphenyl radical to the phenoxyl radical in an attempt to obtain the former by pyrolysis of 2-iodophenol.[247] The IR spectrum of photolysis products of 2-iodophenol in an argon matrix [248] lacked eleven bands belonging to the 2-hydroxyphenyl radical. Based on the comparison of the observed frequencies with those calculated by quantum chemical methods,[248] these bands were assigned to a more stable conformer with the *syn* configuration.

An IR spectroscopic examination of photoisomerization ($\lambda > 220$ nm) products of 2-nitrophenol (**A**) to 2-hydroxy-

phenyl nitrite (**B**) revealed the presence of 2-hydroxyphenoxyl radicals 2-$HOC_6H_4O^{\bullet}$ (**C**) in the most stable *syn*-form.[197]



In the matrix IR spectrum, twelve bands belonging to the 2-$HOC_6H_4O^{\bullet}$ radical were observed. A band at 3336 cm^{-1} was assigned to the stretching vibration ν(OH). The lower frequency of the O–H bond vibration in radical **C** as compared with the O–H bond in phenol (3600 cm^{-1}) pointed to the presence of intramolecular interactions between the OH group and the oxygen atom with an unpaired electron. The presence of such interactions was confirmed by the results of quantum chemical calculations [B3LYP/6-31++G(d,p)],[197] which demonstrated that the O–H bond in the *syn*-conformer (0.983 Å) of this radical is much longer than in its *anti*-conformer (0.968 Å). Annealing of the matrix was accompanied by the reaction of radical **C** with the matrix-trapped $NO^{\bullet}$ radical to form 2-hydroxyphenyl nitrite (**B**).

2. Acyl radicals

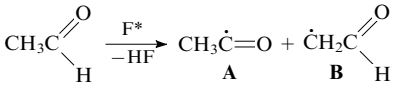
The formyl radical $HC^{\bullet}{=}O$ was first observed by matrix IR spectroscopy in the photolysis of HI in a CO matrix at 20 K.[198] Data on the isotope shift of absorption frequencies of this radical on going to its deuterated analogue made it possible to assign the bands observed at 1861 and 1090 cm^{-1} to stretching ν_2(C=O) and bending ν_3(HCO) vibrations, respectively, and also to calculate the force field of this molecule. Later,[199,200] the C–H stretching frequency (2488 cm^{-1}) was observed.

The $HC^{\bullet}{=}O$ radical was characterized by a higher frequency of C=O bond stretching vibration and a considerably lower frequency of C–H bond stretching vibration as compared with these bonds in formaldehyde. The obtained results agreed well with the EPR data,[249,250] which implied that this non-linear radical had the σ-structure with the HCO angle equal to 125°. The geometrical parameters for the formyl radical [R(C–H) = 1.148 Å, R(C–O) = 1.176 Å and the bond angle HCO = 123.3°] obtained by microwave spectroscopy in the gas phase[251] and also by numerous quantum chemical calculations[252,253] including those carried out by modern methods (CCSD[T]/CBS)[253] were close in values.

From the IR absorption spectra of this radical isolated in argon or CO matrices, the HCO bending frequencies (1375 cm^{-1}) and the C=O bond stretching vibrations (1035 cm^{-1}) in the electronically excited state were found. Spectral characteristics obtained from the matrix UV and IR spectra of the $HC^{\bullet}{=}O$ radical were later used for its identification in the UV photolysis products of the $H_2NC^{\bullet}{=}O$ radical in a Xe matrix.[201]

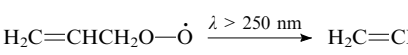
The matrix IR[202–206,254] and EPR[250] spectroscopic studies of halogen-substituted formyl radicals $XC^{\bullet}{=}O$ (X = F, Cl) revealed their non-linear structure. The stretching frequency of the C=O bond changed insignificantly on going from the $HC^{\bullet}{=}O$ radical to the $XC^{\bullet}{=}O$ radicals (X = F, Cl) (Table 6). Based on the spectroscopic data, the force field of $XC^{\bullet}{=}O$ radicals was calculated and the multiplicity of the C=O bond was assessed to be ~2.3.[254] Based on quantum chemical calculations (UHF, UMP2/TZ2P),[204] the ClCO angle was determined as 129.2°.

The acetyl radical $CH_3C^{\bullet}{=}O$ (**A**) was synthesized in the gas phase by a reaction of acetaldehyde vapour with excited fluorine atoms.[207]

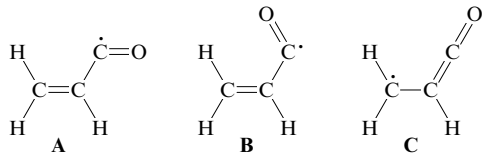


In the IR spectrum of the reaction products, two bands, namely, at 1842 and 1329 cm^{-1}, were assigned to radical **A.** In addition to radical **A**, its structural isomer, formylmethyl radical **B** was tentatively identified with the bands at 1542 and 1525 cm^{-1}. Such a structure of radical **B** agreed with the results of *ab initio* quantum chemical calculations[255] and the results of tunnelling laser IR spectroscopic studies of this radical in the gas phase.[256]

UV photolysis (λ > 250 nm) of the allylperoxyl radical stabilized in an argon matrix afforded the acryloyl radical $CH_2{=}CHC^{\bullet}{=}O$[208]



to which the bands at 1832.0, 1823.1, 1094.4, 975.3 and 870.7 cm^{-1} were assigned. According to HF/6-31G(d) calculations,[208] this radical can exist in the form of *trans*-(**A**) and *cis*-conformers (**B**), with the *trans*-configuration being more stable.



Bands at 1832.0 and 1823.1 cm^{-1} assigned to stretching vibrations of the C=O bond of the *cis*- and *trans*-conformers, respectively, were found to shift to 1797.3 and 1788.9 cm^{-1}, respectively, for isotopically (^{18}O) substituted species. These bands disappeared when the matrix was annealed to 35 K. The higher frequency of stretching vibration ν(C=O) as compared with the analogous vibration in acrolein indicated that the C=O bond in this radical was stronger. At the same time, the fact that this frequency is somewhat lower than the vibration frequencies of C=O bonds in formyl and acetyl radicals (see Table 6) was associated with the effect of the vinyl fragment.

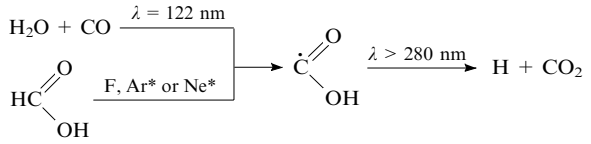
Quantum chemical calculations [B3LYP, MCSCF and QCISD with the 6-311G(d,p) basis set][257] predicted the existence of yet another stable conformer **C** with electron spin density concentrated on the terminal carbon atom. However, this species was not detected[208] among the photolysis products of the allylperoxyl radical, probably due to its further decomposition under experimental conditions to afford acetylene and carbon monoxide.

The vacuum ultraviolet photolysis (λ = 122 nm) of a CO, C_2H_2 and Ar mixture (1 : 1 : 150) and trapping the photolysis products in argon produced the propinoyl radical ($HC{\equiv}CC^{\bullet}{=}O$).[258]

The analysis of matrix IR spectra of the $HC{\equiv}CC^{\bullet}{=}O$ radical and its isotopically (D, ^{18}O and ^{13}C) substituted analogues and also of absorption frequencies calculated by the CISD/DZP methods[259] made it possible to reliably identify the fundamental vibration. The band at 2308.6 cm^{-1} was assigned to the antisymmetric stretching vibration of the CCCO fragment.

The obtained data made it possible to assume that this radical has a structure intermediate between the structures of acetylene ($HC{\equiv}CC^{\bullet}{=}O$) and cumulene ($O{=}C{=}C{=}C^{\bullet}H$) types. However, in later studies,[260, 261] a more stable acetylenic structure was assigned to this radical based on the rotational spectrum of the $HC{\equiv}CC^{\bullet}{=}O$ radical generated in the gas phase[228] and the results of quantum chemical calculations [QCISD/6-311G(d,p)].[261]

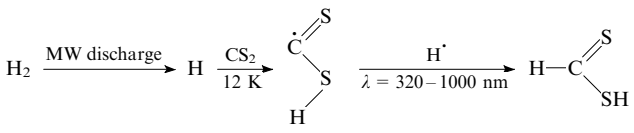
The hydroxycarbonyl radical $HOC^{\bullet}{=}O$ in the form of *trans*- and *cis*-conformers (depending on the positions of C=O and O−H bonds) was synthesized for the first time[210] by the photolysis (λ = 122 nm) of H_2O in a CO matrix. This radical in the *trans*-form was also formed when formic acid isolated in an Ar or Ne matrix reacted with F atoms located in the same matrix or with excited Ar* or Ne* atoms.[211, 212]



Analysis of the IR spectra of isotopically (D, ^{13}C and ^{18}O) substituted analogues of the $HOC^{\bullet}{=}O$ radical made it possible to assign the bands at 3602.9, 1843.6, 1064.6 cm^{-1} to the fundamental vibrations of the O−H, C=O and C−O bonds of the *trans*- rotamer.[211]

The high-level (CCSD(T)/6-31G(d)) quantum chemical analysis carried out later[262] confirmed the experimental[211] data. Upon UV photolysis (λ > 280 nm), the $HOC^{\bullet}{=}O$ radical decomposed to H and CO_2.[211] In the presence of matrix-isolated CO or HF molecules, the $HOC^{\bullet}{=}O$ radical could form complexes with them.[210, 211]

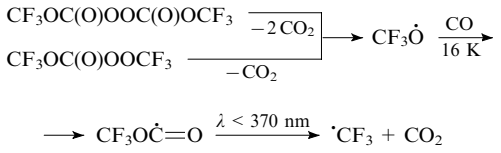
A thio analogue of the hydroxycarbonyl radical with *trans*-configuration of C=S and S−H bonds was formed in an Ar matrix in the co-condensation of carbon disulfide and hydrogen atoms[263] generated by the action of a microwave (MW) discharge on H_2. The low activation barrier to the reaction of CS_2 with the H atom (36 cal mol^{-1}) allowed the radical to be formed not only in the moment of condensation, but also at mild annealing of the Ar matrix (from 12 to 18 K).[263]



The assignment of five of IR spectral bands to the $HSC^{\bullet}{=}S$ radical was based on the analysis of spectra of its isotopically (D, ^{13}C, ^{34}S) substituted analogues and the data of quantum chemical calculations (HF/DZP). Absorption bands observed in the IR spectrum were assigned to this radical in the more stable *trans*-configuration. Bands at 2527, 1275 and 628 cm^{-1} were assigned to stretching vibrations of the S−H, C=S and C−S bonds, respectively. Photolysis (λ = 320 – 1000 nm) of the Ar-matrix isolated radical $HSC^{\bullet}{=}S$ led to a decrease in the intensity of bands corresponding to this radical and an increase in the intensity of bands belonging to dithioformic acid HSC(S)H.

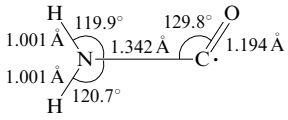
The trifluoromethoxycarbonyl radical $CF_3OC^{\bullet}{=}O$ was first detected by matrix IR spectroscopy in the flash pyrolysis products of perfluorinated peroxides $CF_3OC(O)OOC(O)OCF_3$ or $CF_3OC(O)OOCF_3$ quenched as a CO matrix (16 K).[209]

Irradiation of this matrix by UV light with λ < 370 nm led to dessociation of this radical into $CF_3^{\bullet}$ and CO_2.



From a comparison of experimental and simulated [B3LYP/6-311G(d,p)] spectra, it follows that the *trans*-conformer of this radical with C_s symmetry is more stable.

The formamide radical $H_2NC^{\bullet}{=}O$ was discovered when a xenon matrix containing the laser photolysis products (λ = 266 – 193 nm) of HN=C=O was annealed to 50 K.[201] According to the MP2/6-311++G(3df,3pd) quantum chemical calculation,[201] the following molecular structure conformed to the experimental vibrational spectrum:

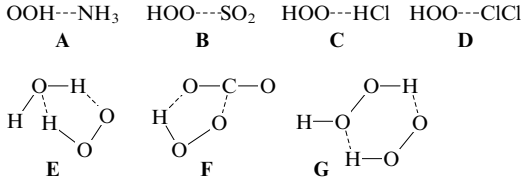


The quartet of bands (1794.2, 1796.6, 1806.5 and 1811.8 cm^{-1}) observed in the IR spectrum was assigned to the C=O stretching vibration of this radical and the absorption band at 3518.5 cm^{-1} was attributed to the stretching vibration of the N−H bond.

3. Peroxyl and trioxy radicals

The simplest peroxyl radical $HOO^{\bullet}$ was first observed by Milligan and Jacox[213] in a matrix IR spectrum of photolysis products (λ = 220 nm) of an $HI-O_2$ mixture (1 : 4) trapped in an argon matrix. Later, this radical has comprehensively been studied.[214, 264, 265]

Experimental studies of complexes formed by the $HOO^{\bullet}$ radical with certain stable molecules were carried out by Nelander *et al.*[266 – 270] In these complexes, the $HOO^{\bullet}$ radical acted as a donor of either a hydrogen bond or an unshared electron pair on the terminal oxygen atom. Thus in its complexes with NH_3 (Refs 266, 267), it acted as a hydrogen-bond donor (compound **A**), whereas in complexes with SO_2 (Ref. 269), HCl and Cl_2 (Ref. 266) it played the role of a donor of the lone electron pair (compounds **B**, **C** and **D**). In the reaction with H_2O,[266] CO_2 (Ref. 172) and HOOH (Ref. 270) molecules in an Ar matrix, the $HOO^{\bullet}$ radical formed cyclic complexes **E** – **G**. Here it simultaneously behaved as the hydrogen-bond donor and the donor of a lone electron pair.



The formation of complexes was evidenced by the shifts of the corresponding vibration frequencies in the IR spectra (Table 7).

Table 7. Absorption bands of the HOO• radical and its complexes observed in the IR spectrum (argon matrix).

Radical HOO• or its complex	Vibration frequencies /cm^{-1}				Ref.
	ν_1	ν_2	ν_3	$2\nu_2$	
HOO•	3413.0	1388.9	1100.8	—	264, 265
A	2654.2	1563.0	1126.8	—	266, 267
B	—	1455.8, 1458.2	—	—	269
C	3306.0	1425.2	1117.0	—	266
D	3335.0	1408.0	1110.6	—	266
E	3236.2	1479.3	1120.4	2875, 2858, 2833	266
F	3376.4, 3372.1	1415.6, 1410.1	1110.9, 1109.5	—	172
G	3208.0	1487.0, 1497.0	1121.0	—	270

The IR spectrum of FOO• radicals with absorption bands at 1490 and 584 cm^{-1} was recorded.[215] The radical was formed in the co-condensation of microwave discharge products of a NF_3-O_2 mixture in an argon matrix. In later studies, this radical was detected by IR spectroscopy as the basic photolysis product (λ = 355nm) of a mixture of F_2 and O_2 (Ref. 216) or of F_2 and O_3 (Ref. 184) in Ar matrices.

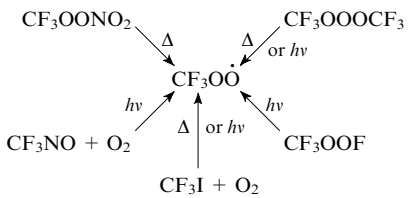
The chloroperoxyl radical ClOO• was first detected by matrix IR spectroscopy[271] as a photolysis product of Cl_2O in an N_2 matrix. Later, this radical has been prepared by the photolysis ($\lambda > 395$ nm) of either chlorine dioxide in Ar, Ne and Kr matrices[217–219] or Cl_2 in an O_2 matrix[217] and also by the reaction of microwave-discharge generated chlorine atoms with molecular oxygen in their co-condensation in an Ar matrix. In the IR spectrum, the vibration frequencies ν(O—O) at 1439–1442 cm^{-1} (depending on the matrix) corresponded to this radical. For the ClOO• radical and its isotopically (^{37}Cl and ^{18}O) substituted analogues, the whole set of fundamental frequencies were found and assigned, particularly, the Cl—O bond stretching vibration frequency in the far IR range was found to be 192.6 cm^{-1} (Ar matrix)[217] or 201.38 cm^{-1} (Ne matrix).[219] In an IR spectrum of the ClOO• radical generated by UV photolysis of OClO in Ar and Kr matrices, the presence of additional bands and the dependence of their intensity on the radiation energy was rationalized[218] by the different arrangement of the original OClO molecules and the ClOO• radicals formed with respect to the matrix lattice atoms.

The BrOO• radical was formed either in the co-deposition into an Ar matrix of oxygen molecules and bromine atoms generated by microwave discharge[220] of Br_2 and also by the photolysis (λ = 800–360 nm) of a Br_2-O_3 mixture in an Ar matrix.[221] In the IR spectrum, the ν(O—O) vibration frequency at 1485 cm^{-1} was identified with this radical. Photoisomerization of the BrOO• radical isolated in an Ar matrix to its more stable isomer OBrO was studied in detail.[222, 223]

$$Br_2 \xrightarrow{\text{MW discharge}} \dot{B}r \xrightarrow{O_2} BrO\dot{O} \underset{\lambda = 560\ nm}{\overset{\lambda = 275\ nm}{\rightleftharpoons}} OBrO.$$

A series of matrix IR spectroscopic studies[225, 227, 230, 231, 272] were devoted to alkylperoxyl radicals. Radicals ROO• were formed in the reaction of oxygen molecules with stable radicals (CH_3, C_2H_5, iso-C_3H_7 and *tert*-C_4H_9) generated by the pyrolysis of the corresponding diazoalkanes. Based on the spectral data for a series of isotopically (D, ^{13}C or ^{18}O) substituted radicals ROO•, the IR spectral bands were sufficiently reliably assigned to the relevant normal vibrations. Particularly, bands in the interval of 1092–1145 cm^{-1} were assigned to (O—O) stretching vibrations and bands in the range from 900 to 730 cm^{-1} were assigned to ν(C—O) vibrations. The latter shifted in the low-frequency range[230] on going from primary to tertiary alkyl fragments R (see Table 6). In later studies of alkylperoxyl radicals, these data were supplemented by the results of quantum chemical calculations. Thus the methylperoxyl radical[226] was studied using the modern experimental and theoretical methods; in particular, for the CH_3OO• radical, 10 of 12 possible bands could be observed in the IR spectrum. Based on the analysis of photooriented species, the polarization of vibrational spectrum bands was revealed and the latter were assigned to a certain symmetry type.

The trifluoromethylperoxyl radical CF_3OO• was obtained for the first time by the photolysis of the Ar-matrix-isolated CF_3OOF (λ = 300–400 nm) and CF_3OOOCF_3 ($\lambda < 300$ nm).[273] In addition, the CF_3OO• radical was formed by co-deposition of vacuum pyrolysis products of CF_3I and O_2 into an Ar matrix,[274] in the oxidation of $CF_2{=}CF_2$ (Ref. 275) and also in photolysis of CF_3I (λ = 254 nm)[191] or CF_3NO ($\lambda > 265$ nm)[276] in an O_2-doped Ar matrix. For the CF_3OO• radical prepared by vacuum flash pyrolysis of CF_3OONO_2 or CF_3OOOCF_3 and isolated in an Ar matrix, all vibrational bands were reliably assigned to normal modes of this radical,[228] based on the comparison of vibration frequencies observed for this radical and its isotopically ($CF_3{}^{18}O{}^{18}O$) substituted analogue with the frequencies calculated by the B3LYP/6-31(d) method. In particular, the bands at 1093.0, 869.2 and 447.6 cm^{-1} were assigned to ν(O—O), ν(C—O) and δ(COO), respectively. In the UV range, the band of the electron transition $2^2A'' \leftarrow X^2A''$ with the maximum at 207 nm was assigned to the CF_3OO• radical isolated in an Ne matrix.[228]



The 1-chloro-2,2,2-trifluoroethylperoxyl radical ($CF_3CHClOO$•) was prepared by co-condensation of oxygen and the vacuum pyrolysis products of $CF_3CHClBr$ in an argon matrix at 12 K.[229] Based on the comparison of the results of quantum chemical calculations [B3LYP/6-311G(d,p)] with the spectroscopic data for the $CF_3CHClOO$• radical and its ^{18}O-substituted analogue, all

thirteen bands observed in the IR spectrum were assigned to normal vibrations of the $CF_3CHClOO^{\bullet}$ radical.[229]

Bands at 1102.1 and 972.7 cm^{-1} were assigned to the O–O and C–O stretching vibrations, respectively. In the isotopically substituted radical, these bands shifted to 1044.7 and 954.1 cm^{-1}.

UV photolysis ($\lambda > 250$ nm) of this radical in an Ar matrix led to its dissociation into radicals $^{\bullet}CF_3$ and $ClC^{\bullet}=O$ and stable molecules FC(O)F, CO and HCl.

$$CF_3CHClBr \xrightarrow[-Br]{1000\ ^{\circ}C} CF_3\dot{C}HCl \longrightarrow$$

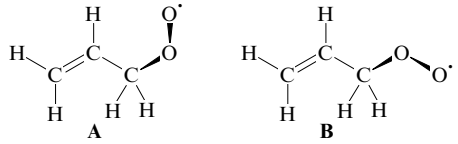
$$\xrightarrow[Ar]{O_2} CF_3CHCl\dot{O}O \xrightarrow[Ar,\ 12\ K]{\lambda > 250\ nm} \dot{C}F_3,\ Cl\dot{C}(O),\ FC(O)F,\ CO,\ HCl$$

$$\xrightarrow[-Cl]{} [CF_3\ddot{C}H] \longrightarrow F_2C{=}CHF$$

Annealing of an Ar matrix that contained oxygen and ethylene high-frequency discharge decomposition products afforded the vinylperoxyl radical $CH_2{=}CHOO^{\bullet}$.[232] Based on the comparison of experimental data obtained for several isotopically (D, ^{13}C and ^{18}O) substituted species with the results of quantum chemical calculations [UB3LYP/6-311++G(d,p)], the bands observed in the IR spectrum of the $CH_2{=}CHOO^{\bullet}$ radical were assigned to the normal vibrations of its *trans*-configuration relative to the C–O bond.

Bands at 1140.7 and 875.5 cm^{-1} were assigned to the ν(O–O) stretching vibration and the out-of-plane CH_2 wagging vibration, respectively. Upon the photolysis ($\lambda > 400$ nm) in an Ar matrix, the radical decomposed to form the $CH_2OH\cdots CO$ complex.

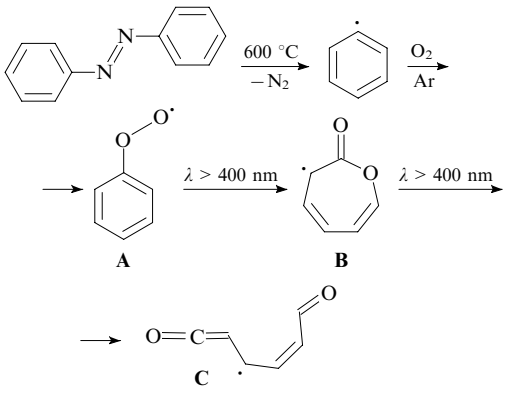
In the IR spectrum of the allylperoxyl radical $CH_2{=}CHCH_2OO^{\bullet}$ formed by co-condensing the allyl radical, generated by pyrolysis of hexa-1,5-diene, with O_2 molecules in an Ar matrix, 26 absorption bands were observed.[208]



A **B**

Calculations [UHF/6-31G(d)][208] made it possible to identify the observed bands with vibrations of two conformers **A** and **B** close in energy. Particular, the doublets at 1128.6, 1108.6 cm^{-1} and 855.6, 850.7 cm^{-1} were assigned to stretching vibrations of the peroxyl fragment in these conformers, namely, ν(OO) and ν(CO) vibrations, respectively. In the ^{18}O-substituted radical, these bands were observed at 1067.6, 1052.7 and 844.2, 837.9 cm^{-1}. Upon photolysis ($\lambda > 250$ nm), the allylperoxyl radical decomposed into CO, H_2O, C_2H_2, HO_2, the complexes CH_2O---HO and CH_2CHCHO---HO and also the acryloyl radical $CH_2{=}CHC^{\bullet}{=}O$ described above.

Recently, matrix IR spectroscopy made it possible to detect phenylperoxyl radicals $C_6H_5OO^{\bullet}$ when molecular oxygen and the phenyl radical generated by vacuum pyrolysis (650 °C) of diazobenzene were co-condensed in an Ar matrix.[233]



A **B** **C**

The IR spectrum of the $C_6H_5OO^{\bullet}$ radical demonstrated bands at 1122.9, 793.9 and 607.2 cm^{-1}, which were assigned to the peroxyl fragment vibrations ν(O–O), ν(C–O) and δ(CCO), respectively, based on the results of calculations (UB3LYP/cc-pVTZ) and the analysis of IR spectra of isotopically (D_5 and ^{18}O) substituted analogues. The UV spectrum of this radical demonstrated an absorption band with the maximum at 480 nm. Irradiation ($\lambda > 400$ nm) of the $C_6H_5OO^{\bullet}$ radical (**A**) afforded 2-oxepinoxyl radical **B** with a band at 1726.9 cm^{-1} in the IR spectrum corresponding to the stretching vibration ν(C=O) (for the isotopically substituted ^{18}O-analogue, this band shifted to 1696.2 cm^{-1}). Long-term irradiation ($\lambda > 400$ nm) converted radical **B** into a mixture of several conformers of radical **C** with absorption bands in the ranges of 2150–2050 and 1650–1600 cm^{-1}.

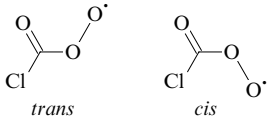
The formylperoxyl radical $HC(O)OO^{\bullet}$ and its complex with the $^{\bullet}O_2H$ radical were detected[234, 235] by IR spectroscopy. The $HC(O)OO^{\bullet}$ radical was produced by the photolysis ($270 < \lambda < 420$ nm) of formaldehyde in an oxygen matrix. In its IR spectrum, the two bands at 1790.2 and 1089.9 cm^{-1} were assigned to the stretching vibrations of the C=O and C–O bonds, respectively.

This radical also formed by a high-voltage discharge of CH_3OH/Ar and quenching the products in an oxygen-doped argon matrix.[236] The IR spectrum of the thus obtained radical revealed two absorption bands at 1821.5 and 957.3 cm^{-1}, which were assigned to stretching vibrations of the formylperoxyl radical with the *cis*-position of C–H and O–O bonds, based on the shift of these bands in the spectra of isotopically (^{18}O and ^{13}C) substituted analogues and their comparison with the calculated [B3LYP and MP2/6-311++G(d,p)] absorption bands.

The fluoroformylperoxyl radical $FC(O)OO^{\bullet}$ was prepared in the form of *cis*- and *trans*-rotamers by vacuum pyrolysis of $FC(O)OONO_2$ or FC(O)OOOC(O)F in an argon matrix. The IR spectrum of this radical demonstrated absorption bands typical of acylperoxyl radicals. Thus the band at 1919.2 cm^{-1} was assigned to the ν(C=O) vibration in the *trans*-rotamer and the band at 1904.5 cm^{-1} was identified with the *cis*-rotamer vibration. The UV absorption band with the maximum at 235 nm was assigned to the $FC(O)OO^{\bullet}$ radical stabilized in an Ne matrix.[228]

The chloroformylperoxyl radical $ClC(O)OO^{\bullet}$ generated by vacuum pyrolysis (250 °C) of $ClC(O)OONO_2$ in an Ar or Ne matrix or by photolysis ($\lambda > 305$ nm) of a $Cl_2 + CO + O_2$ (1 : 20 : 400) mixture in an O_2 matrix was studied by matrix IR spectroscopy.[237] The IR spectrum of the $ClC(O)OO^{\bullet}$

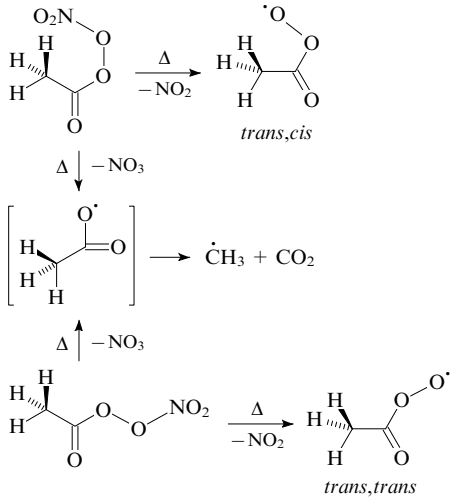
radical contained bands corresponding to two conformers of this radical in the ground state XA''. According to quantum chemical calculations [CCSD(T)/aug-cc-pVDZ] (Ref. 237) the *trams*-conformer was more stable ($\Delta E_{250\,^\circ C} = 1.5$ kJ mol^{-1}) and prevailed in the mixture of conformers, which was well consistent with the ratio of intensities of characteristic absorption bands of *trans*- and *cis*-conformers.



Thus the bands at 1886 and 1843 cm^{-1} were assigned to the stretching vibrations of C=O bonds in the *trans*- and *cis*-conformers isolated in an Ar matrix. The peroxyl fragment was characterized by bands at 1072 and 1093 cm^{-1} corresponding to ν(O–O) vibrations and also by bands at 925 and 952 cm^{-1}, corresponding to the ν(C–O) vibration. In the UV absorption spectrum, this radical was characterized by a wide band with the maximum at 230 nm. Photolysis ($\lambda = 255$ nm) of the Ar- or Ne-matrix-isolated ClC(O)OO$^\bullet$ radical led to a decrease in the intensities of all IR and UV bands and the simultaneous increase in the intensity of the IR bands corresponding to the CO_2 molecule; moreover, in the UV spectrum, characteristic absorption of the ClO$^\bullet$ radical appeared.

$$ClC(O)OO^\bullet \xrightarrow{\lambda = 255\ nm} CO_2 + ClO^\bullet.$$

Vacuum pyrolysis of $CH_3C(O)OONO_2$ produced the acetylperoxyl radical $CH_3C(O)OO^\bullet$ (Ref. 238). As follows from the IR spectroscopic studies, the acetylperoxyl radical frozen in an Ar or Ne matrix existed as the *trans*,*cis*- and *trans*,*trans*-rotamers [depending on the positions of bonds in the pentaatomic fragment H–CH$_2$–C(O)–O–O]. Bands at 1842 and 1852 cm^{-1} were assigned to the stretching vibrations of the C=O bond in the *trans*,*cis*- and *trans*,*trans*-rotamers, respectively. The higher intensity of a band corresponding to the *trans*,*cis*-rotamer pointed to the higher stability of this conformer. The obtained data agreed with the results of a quantum chemical calculations [B3LYP/6-311G(d,p)] according to which the energy difference between the *trans*,*trans*- and *trans*,*cis*-rotamers was 2.3 kJ mol^{-1}. According to calculations, the cleavage of the



N–O bond in peroxyacetyl nitrate was more advantageous as regards the energy than the scission of the O–O bond to form the thermally instable radical $CH_3C(O)O^\bullet$.

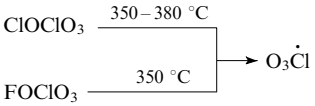
The trifluoromethoxycarbonylperoxyl radical $CF_3OC(O)OO^\bullet$ was prepared in a similar way as the acetylperoxyl radical, namely, by the pyrolysis of bis(fluoromethoxycarbonyl) trioxide $CF_3OC(O)OOOC(O)OCF_3$ or trifluoromethoxycarbonylperoxy nitrate $CF_3OC(O)OONO_2$ (Refs 239, 240). This radical also existed as two conformers, namely, *trans*,*trans*,*trans* and *trans*,*trans*,*cis* (the enthalpy of conversion of one conformer to another was 3.0 kJ mol^{-1}). The ν(C=O) stretching frequencies in these conformers considerably differed, being equal to 1895 and 1868 cm^{-1}, respectively. The analysis of absorption band intensities in the IR spectrum has shown that the concentration of the more stable *trans*,*trans*,*trans*-conformer decreased with the increase in the pyrolysis temperature. The UV spectrum of the $CF_3OC(O)OO^\bullet$ radical stabilized in an Ne matrix demonstrated absorption with the maximum at 240 nm corresponding to the $2^2A'' \leftarrow X^2A''$ transition. Under UV irradiation ($\lambda = 254$ nm), this radical decomposed to $CF_3OO^\bullet$ and CO_2.

$$CF_3OC(O)OO^\bullet \xrightarrow[-CO_2]{\lambda = 254\ nm} CF_3OO^\bullet \longrightarrow FC(O)F + FO^\bullet.$$

The $CF_3OO^\bullet$ radical that absorbed in the same range as $CF_3OC(O)OO^\bullet$ was in turn observed to decompose to FC(O)F and FO$^\bullet$.

Trioxyradicals were studied less comprehensively than peroxy radicals. The HOOO$^\bullet$ radical was originally produced by the matrix isolation method [277] according to which oxygen or ozone molecules together with the microwave-discharge-induced decomposition products of water or H_2 were condensed in an argon matrix. As follows from kinetic studies, the most probable ways of formation of the HOOO$^\bullet$ radicals were the reaction of an $^\bullet$OH radical with an oxygen molecule and the addition of oxygen atoms to a HOO$^\bullet$ radical. In the matrix IR spectrum, three bands (3361, 1233, 566 cm^{-1}) were assigned to the HOOO$^\bullet$ radical. Based on the shift of these bands for the isotopically substituted deuterio- and ^{18}O-analogues and a comparison of experimental frequencies with those calculated by quantum chemical methods, these bands were attributed to the *cis*-configuration of this radical.[278]

The $O_3Cl^\bullet$ radical prepared by vacuum pyrolysis of $ClOClO_3$ and $FOClO_3$ followed by isolation of pyrolysis products in different matrices (Ne, Ar, O_2) was thoroughly studied by IR spectroscopy.[185, 186]



The IR spectrum of the $O_3Cl^\bullet$ radical stabilized in an Ne matrix demonstrated seven bands of which four were assigned to stretching and bending vibrations of the $O_3Cl^\bullet$ radical ($\nu_{as} = 1081$, $\nu_s = 905$, $\delta_s = 567$ and $\delta_{as} = 476$ cm^{-1}) and the rest three were related to overtones. For the $O_3Cl^\bullet$ radicals as for the ClO$^\bullet$ radical, a slight shift of the IR bands in the high-frequency range was observed on going from an Ne matrix to those of Ar and O_2. Based on the comprehensive analysis of the IR spectra of the $O_3Cl^\bullet$ radical and

its isotopically substituted analogues (^{37}Cl, ^{18}O and ^{16}O in different combinations) and also on the results of force-field calculations, the structural parameters of the radical with C_{3v} symmetry [R(Cl—O) = 1.485 Å, angle OClO = 113.8°] were determined.[185] The found parameters agreed well with those calculated by the B3LYP/6-311+G(3df) quantum chemical method [R(Cl—O) = 1.452 Å, angle OClO = 114.2°][279] (Fig. 2 *a*).

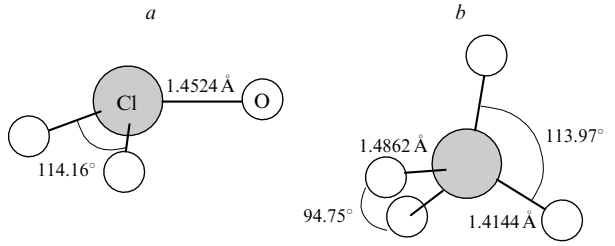


Figure 2. Structural parameters of $O_3Cl^{\bullet}$ (C_{3v}) (*a*) and $O_3ClO^{\bullet}$ (C_{2v}) radicals (*b*) calculated by the B3LYP/6-311+G(3df) method.[279]

In the UV and visible spectral regions, bands with maxima at 311.5 and 432.0 nm were related to the $O_3Cl^{\bullet}$ radical. From the fine structure of the UV bands, the vibration frequencies of the $O_3Cl^{\bullet}$ radical in the C^2E excited state were determined (794, 498, 280 cm^{-1}). Photolysis ($\lambda > 455$ nm) of the $O_3Cl^{\bullet}$ radical resulted in its decomposition to the $ClO^{\bullet}$---O_2 complex with the IR spectral bands at 839.5 and 1549.1 cm^{-1}. In this complex, the $ClO^{\bullet}$ radical was in the $^2\Pi_{1/2}$ state.[185] The insignificant shift of the IR spectral frequencies of the $ClO^{\bullet}$ radical observed in the formation of its complex with O_2 as compared with its complexation with the fluorine analogue $FO^{\bullet}$ (see above) pointed to the lability of this complex.[184]

The $O_3ClO^{\bullet}$ radical and its isotopically substituted ^{37}Cl- and ^{18}O-analogues stabilized in Ne, Ar and O_2 matrices were prepared by vacuum pyrolysis of dichlorine hexoxide Cl_2O_6.[185,280]

$$O_3Cl{-}O_3Cl \xrightarrow[-ClO_2]{240\ ^\circ C} O_3ClO^{\bullet} \begin{cases} \xrightarrow{O_2} O_3ClOOO^{\bullet} \\ \xrightarrow[-O_2]{\lambda = 495\ nm} OClO \end{cases}$$

The matrix IR spectrum of the $O_3ClO^{\bullet}$ radical demonstrated eight bands corresponding to fundamental vibrations and many overtones. Based on the experimental[185] and theoretical [B3LYP/6-311+G(3df)][279] data, the $O_3ClO^{\bullet}$ radical was deduced to have C_{2v} symmetry with two long (1.4862 Å) and two short (1.4144 Å) Cl—O bands (Fig. 2 *b*) with the angles of 94.75° and 113.97° between them. The band broadening observed in the IR spectrum could be associated with the Jahn–Teller effect and the presence of species with lower symmetry C_s. In contrast to $ClO^{\bullet}$ and $O_3Cl^{\bullet}$ radicals, the $O_3ClO^{\bullet}$ radical easily added oxygen to form the O_3ClO---O—O complex with the characteristic absorption band ν(O—O) = 1525 cm^{-1}. Irradiation of the $O_3ClO^{\bullet}$ radical with $\lambda > 495$ nm in an Ne matrix or with $\lambda > 395$ nm in an O_2 matrix led to its dissociation to O_2 and OClO.

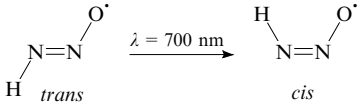
The trifluoromethyltrioxyl radical $CF_3OOO^{\bullet}$ was synthesized recently by condensing vacuum pyrolysis products of $CF_3OC(O)OOCF_3$ or $CF_3OC(O)OOC(O)OCF_3$ into an O_2 matrix.[281] It was concluded that the trioxyradical formed represented most likely the CF_3O---O—O complex with a very strong O—O bond (ν = 1500 cm^{-1}) and a weak F_3CO---O bond (ν = 219 cm^{-1}). Such a structure was hypothesized earlier[184] for the FO---O—O complex.

4. Formation of transient radicals in reactions involving NO and NO_2

The $F_2NO^{\bullet}$ radical was obtained for the first time in solid argon by stepwise addition of two fluorine atoms to the NO molecule and characterized by EPR and IR spectra.[282–284] The EPR spectrum contained 9 lines belonging to the $F_2NO^{\bullet}$ radical, which represented a triplet with the intensity ratio of 1:2:1 in which each line was in turn split into three lines with the intensity ratio of 1:1:1. This spectrum corresponded to a radical with the structure containing two equivalent fluorine atoms. A set of five bands with identical kinetic behaviour observed in the IR spectrum of the $F_2NO^{\bullet}$ radical was assigned to the relevant intramolecular vibrations. This was made based on the results of quantum chemical calculations carried out by the QCISD and QCISD(T) methods in the harmonic approximation.[284] Recently, the vibration frequencies of this radical were calculated by the CCSD(T)/VTZ and CCSD(T)/aVTZ methods with consideration of the anharmonicity of vibrations.[285] The band at 1573 cm^{-1} was assigned to the NO stretching vibration and the bands at 761 and 813 cm^{-1} were related to the symmetric and antisymmetric vibrations of NF_2. In addition to the presence of the $F_2NO^{\bullet}$ radical, the F---FNO complex with the same stoichiometry can exist, according to calculations; moreover, in the temperature range of 17–35 K, these compounds are interconvertible

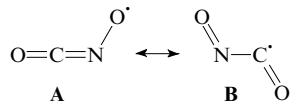
$$F{-}{-}{-}FNO \underset{k_-}{\overset{k_+}{\rightleftharpoons}} F_2NO^{\bullet}.$$

Nitrene NH formed in the photolysis (λ = 254 nm) of NH_3 in an Xe matrix reacted with the $NO^{\bullet}$ radical as the matrix was annealed to 40 K to afford the $HNNO^{\bullet}$ radical.[286] The matrix IR spectrum of this radical revealed three bands that belonged to *cis*- and *trans*-isomers. The more stable *trans*-isomer was transformed to the *cis*-form under irradiation with λ = 700 nm. A comparison of experimental and theoretical data for this radical and its isotopically substituted ^{15}N-analogue made it possible to assign the bands observed in the IR spectrum. The bands at 3254, 1628.9 and 1296.2 cm^{-1} were assigned to stretching vibrations of the N—H, N=N and N—O bonds, respectively, for the *trans*-isomer, and the bands at 3158, 1623.7 and 1273.4 cm^{-1} were assigned to the analogous vibrations for the *cis*-isomer.



The OCNO$^{\bullet}$ radical generated in the electron impact on the N_2+CO_2 matrix was detected by IR spectroscopy.[287]

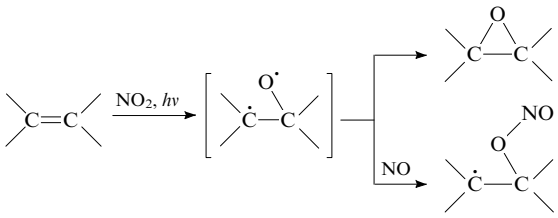
According to calculations,[288] the OCNO$^{\bullet}$ radical represents a hybrid combination of two resonance structures **A** and **B**.



A B

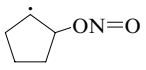
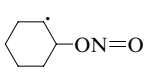
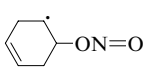
Thus, the C–N bond is intermediate between the single and double bonds, its length being equal to 1.283 Å. The band at 2113 cm^{-1} was assigned to the ν(C=O) stretching vibration of this radical; the shifts of this band in isotopically (^{15}N, ^{18}O, ^{13}C) substituted species were in good agreement with those calculated by the QCISD/6-31G(d) method.[287]

Nitrosooxyalkyl radicals formed in Ar or Kr matrices in the stepwise addition of photoexcited [λ = 555–650 nm (in Ar matrix) or λ = 350–450 nm (in Kr matrix)] NO_2 to alkenes, cycloalkenes, allene and 1,3-dienes was studied[289–300] (Table 8). It was assumed that a photoexcited oxygen atom formed in the NO_2 decomposition was primarily added to an alkene or diene molecule, which was followed by the NO addition to the resulting biradical.



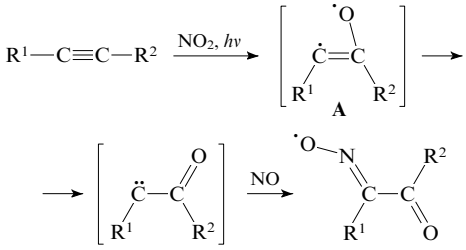
It deserves mention that depending on the nature of the alkene, the excitation light of different wavelengths (from 555 to 650 nm) (see Table 8) should be used for attaining the maximum concentration of a nitrosooxyalkyl radical, which may be due to both the structure of the alkene itself and the photochemical stability of the resulting biradicals and nitrooxyalkyl radicals. For substituted alkenes, different conformers were observed. All radicals demonstrated IR spectral bands in the vicinity of 1650 ± 20 cm^{-1} and 760 ± 30 cm^{-1} (see Table 8), which corresponded to the stretching vibrations of N=O and N–O bonds in the nitrosooxyl fragment. It is of note that the vibration frequencies of these bonds decreased with elongation of the carbon chain in alkenes (with the exception of nitrosooxy-*cis*-butyl radical).

Table 8. Spectral characteristics of nitrosooxyalkyl radicals stabilized in an Ar matrix.

Radical structure	λ/nm	ν/cm^{-1}		Ref.
		N=O	N–O	
$^{\bullet}CH_2CH_2ON{=}O$	574	1664	773	289
	575	1655	780	291
$CH_3C^{\bullet}HCH_2ON{=}O$	582	1650	770	292
trans-$CH_3C^{\bullet}HCH(CH_3)ON{=}O$	590	1645	755	293, 294
cis-$CH_3C^{\bullet}HCH(CH_3)ON{=}O$	590	1652	772	294
$(CH_3)_2C^{\bullet}CH_2ON{=}O$	620	1644	754	295
$(CH_3)_2C^{\bullet}C(CH_3)_2ON{=}O$	650	1634	744	296
trans-$CH_2{=}CHC^{\bullet}HCH_2ON{=}O$	582	1661	781	297
trans-$CH_2{=}C(CH_3)C^{\bullet}HCH_2ON{=}O$	582	1657	774	297
trans-$CH_2{=}C(CH_3)C^{\bullet}(CH_3)CH_2ON{=}O$	582	1657	775	297
$CH_2{=}C(ON{=}O)C^{\bullet}H_2$	580	1674	766	298
	590	1645	787, 750	299
	590	1655, 1644	769, 756	299
	574	1647	757	300

Iminoxyl radicals were formed in the reaction of carbenes with NO. The simplest iminoxyl radical was detected for the first time by matrix spectroscopy as the reaction product of methylene generated by ketene photodecomposition (λ = 355 or 380 nm) with an NO molecule in an argon matrix.[301]

Iminoxyl radicals containing carbonyl groups were formed similarly to nitrooxyalkyl radicals, namely, in the photochemical reaction of NO_2 with substituted alkynes (Table 9). The reaction mechanism assumed the transient formation of biradical **A** followed by its isomerization to carbonylcarbene. The latter reacted with NO to form the iminoxyl radical.[298, 302–305]



R^1, R^2 = H, CH_3, C_6H_5.

Absorption of acyliminoxyl radicals was characterized by the presence of IR bands of C=N bond stretching vibrations in the range of 1545–1591 cm^{-1}. For the simplest radical $CH_2{=}NO^{\bullet}$, this band appeared at 1664 cm^{-1}. A considerable shift of the ν(C=N) frequency for acetyliminoxyl radicals pointed to the electron density delocalization in such systems and the weakening of the C=N bond.[9]

Primary alkynes can, in principle, form iminoxyl radicals of both the aldehyde and ketone types. A comparison of experimental and calculated data has shown that the aldehyde form, *e.g.*, the formylmethyliminoxyl radical, is

Table 9. Spectral characteristics of iminoxyl radicals stabilized in an Ar matrix.

Radical structure	λ/nm	ν/cm^{-1}		Ref.
		C=O	C=N	
$H_2C{=}NO^{\bullet}$	380 or 355		1664	301
$HC(O)C(CH_3){=}NO^{\bullet}$	615	1714	1588	302
(see [a])		1721	1584	
		1716	1585	
		1708	1571	
$CH_3C(O)C(CH_3){=}NO^{\bullet}$	610	1717	1600 [b]	298
(see [a])		1711	1591	
		1707	1560, 1545	
$C_6H_5C(O)C(CH_3){=}NO^{\bullet}$	610	1715	1590	305

[a] Frequencies for different conformers are shown. [b] According to the data from Ref. 304.

more stable.[302] The formation of four different conformers (*trans*,*trans*, *cis*,*trans*, *trans*,*cis* and *cis*,*cis*) for acetylmethyliminoxyl radical was evidenced by the splitting of IR spectral bands in the range of characteristic vibrations ν(C=O) and ν(C=N).[298, 302–304] The benzoylmethyliminoxyl radical prepared by a procedure analogues to that of the acetylethyliminoxyl radical existed as the *trans*,*trans*-conformer,[305] which can be explained by the effect of its phenyl substituent.

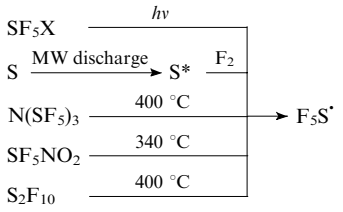
VII. Sulfur-containing radicals

The literature offers several examples of studies of sulfur-centred radicals by matrix spectroscopy.

Reliable identification of the simplest sulfur-containing radical HS$^{\bullet}$ generated by laser photolysis (λ = 193 nm) of H_2S in Ar, Kr, Xe or Ne matrices was carried out based on the UV and IR spectroscopic studies.[306, 307] In Ar matrices, the band at 2607 cm^{-1} was assigned to the HS$^{\bullet}$ radical and the band at 2563 cm^{-1} was assumed to correspond to its HS$^{\bullet}$---H_2S complex. On going to other rare-gas matrices, a small shift from these frequencies was observed. In an Kr matrix, in addition to the HS$^{\bullet}$---H_2S complex, the HS$^{\bullet}$---H_2O complex characterized by the band at 2556 cm^{-1} was also identified. In the luminescence spectrum, the band at 347.8 nm (in Ar matrix) and the doublet at 375 and 413 nm (in Kr matrix) were assigned to the $A^2\Sigma^+ \leftarrow X^2\Pi$ electron transition in the HS$^{\bullet}$ radical.

Laser photolysis (λ = 266 nm) of argon-matrix isolated S_2H_2 afforded the HSS$^{\bullet}$ radical (see Ref. 308). Based on the results of calculations [MP2 and CCSD(T) methods], the absorption bands at 2463, 2460 and 903 cm^{-1}, which disappeared on the matrix annealing, were assigned to the ν(SH) matrix-split stretching vibration and the δ_{as}(HSS) bending vibration, respectively.

The first matrix-spectroscopic study of the perfluorinated radical $F_5S^{\bullet}$ obtained in the photolysis (λ = 104.8, 106.7 nm) of sulfur halides with the general composition SF_5X (X = Cl, Br SF_5) was carried out by Smardzewski and Fox.[309] Later, this radical has been detected among the reaction products of sulfur atoms with fluorine.[310]

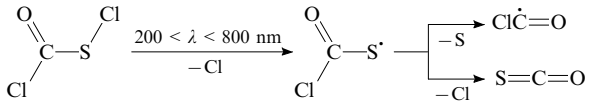


X = Cl, Br, SF_5.

A more comprehensive study of the Ar- or Ne-matrix isolated $F_5S^{\bullet}$ radical generated by vacuum pyrolysis of three independent precursors, namely, S_2F_{10}, SF_5NO_2 and $N(SF_5)_3$, revealed the following whole set of six IR-active bands: at 891.7, 817.8, 633.0, 553.4, 524.7, 387.2 cm^{-1}. The experimentally found absorption frequencies well agreed with those calculated by the B3LYP/6-311++G(3df,3pd) method for the radical with C_{4v} symmetry. These data were supplemented by the results of UV spectroscopy for the $F_5S^{\bullet}$ radical in an Ne matrix.

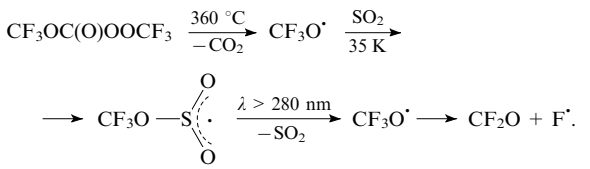
Condensation of the $F_5S^{\bullet}$ radical in an oxygen matrix[311] afforded the $SF_5OO^{\bullet}$ radical. In the IR spectrum, seven most intense bands belonged to this radical of which the band at 1135 cm^{-1} was assigned to the O–O stretching vibration of radical with C_s symmetry.

The ClC(O)S$^{\bullet}$radical was obtained by photolysis (λ = 200–800 nm) of chlorocarbonylsulfenyl chloride in an Ar or N_2 matrix and studied by IR spectroscopy.[312]



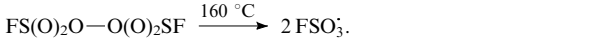
The IR spectrum of photolysis products revealed bands at 1774.9 and 913.5 cm^{-1} (Ar matrix) or at 1762.6 and 919 cm^{-1} (N_2 matrix), which were assigned to the ν(C=O) and ν_{as}(ClCS) vibrations of the ClC(O)S$^{\bullet}$ radical. This assignment was based on the comparison of experimentally found absorption frequencies with those calculated by different methods (HF, MP2 and B3LYP).[312] On the long-term photolysis, the ClC(O)S$^{\bullet}$ radical underwent further decomposition to form the ClC$^{\bullet}$(O) radical and the S=C=O molecule.

The $CF_3O^{\bullet}$ radical generated by vacuum pyrolysis of peroxide $CF_3OC(O)OOCF_3$ reacted with SO_2 under the conditions of Ar matrix annealing to 35 K to afford the trifluoromethoxysulfonyl radical[313] with the structure similar to that of the aforementioned[178, 180] hydroxysulfonyl radical $HOS^{\bullet}O_2$ (see Section VI.1).



The IR spectrum of pyrolysis products of the peroxide $CF_3OC(O)OOCF_3$ isolated in an SO_2-doped Ar matrix contained eleven bands, which were assigned to the $CF_3OS^{\bullet}O_2$ radical based of quantum chemical calculations [B3LYP/6-311++G(3df,3pd)]. All these frequencies were assigned to a conformer with C_1 symmetry, although the calculations predicted the possibility of existence of several conformers with similar energy and spectral characteristics. According to calculations, the $CF_3OS^{\bullet}O_2$ radical with C_1 symmetry had two short S=O bonds (1.44 Å) and one long S–O bond (1.686 Å) and was characterized by the unpaired electron delocalization over the SO_2 fragment (47 a.u. on the S atom and 22 a.u. on each of the oxygen atoms double bonded to the sulfur atom). Under UV irradiation (λ > 280 nm), the $CF_3OS^{\bullet}O_2$ radical dissociated into SO_2 and the $CF_3O^{\bullet}$ radical, followed by the transformation of the latter to FC(O)F with elimination of a fluorine atom.

The Ar- and Ne-matrix-stabilized fluorosulfate radical $FSO_3^{\bullet}$ synthesized by the pyrolysis of the dimer $(FSO_3)_2$ was studied in detail by EPR and IR spectroscopy.[314]



Earlier, attempts have been undertaken to elucidate the structure of this radical by matrix IR spectroscopy[315] and also by quantum chemical calculations.[316] However, certain difficulties encountered in the assignment of several bands in the IR spectrum of the $FSO_3^{\bullet}$ radical, which made the elucidation of the molecular structure of this radical impossible. A new interpretation to the results reported in

Ref. 315 has recently been given.[314] The careful study of the IR spectra of the $FSO_3^{\bullet}$ radical and its ^{18}O-isotopically substituted analogues in the middle and far spectral regions, allowed [314] reliable assignment of the bands at 1052.7, 832.5 and 531.0 cm^{-1} to the radical in the ground state $^2A_2$ with C_{3v} symmetry and the bands at 931.6, 426.2 and 161.6 cm^{-1} to this radical in the low-lying excited state ^2E. The results of anisotropic EPR also pointed to the high symmetry (C_{3v}) of the $FSO_3^{\bullet}$ radical in the ground electronic state characterized by the spin density distribution over the electron orbitals of three equivalent oxygen atoms [calculations [316] by the MP2(full)/6-311 + G(d) method predicted the low symmetry (C_s) of the radical and the presence of two short and one elongated S—O bonds].

Despite the equivalence of the oxygen atoms in the $FSO_3^{\bullet}$ radical, the latter easily reacted with oxygen molecules in a neon or argon matrix to form the complex $FS(O)_2O\text{---}O—O$.[224] Complexes of this type were characterized by the presence of an IR absorption band at 1543.5 (Ne) or 1540.6 cm^{-1} (Ar) corresponding to the $\nu(O—O)$ stretching vibration. According to calculations [UB3LYP/6-311 + G(3df)], [224] the $FS(O)_2O\text{---}O_2$ complex could exist as two isomers very close in energy and with either linear (**A**) or cyclic (**B**) structure (Fig. 3). Based on the analysis of the IR spectrum, six of seven absorption bands earlier identified with this complex were assigned to the more stable $FS(O)_2O\text{---}O_2$ complex with the linear structure **A**. In the UV spectrum, this complex was characterized by a wide absorption band at 450 nm.[224]

Decomposition of the peroxide $CF_3OS(O)_2O—O\text{-}S(O)_2OCF_3$ (at 90 °C) in vacuum produced the $CF_3OSO_3^{\bullet}$ radical, which was stabilized in an Ar or Ne matrix.[317]

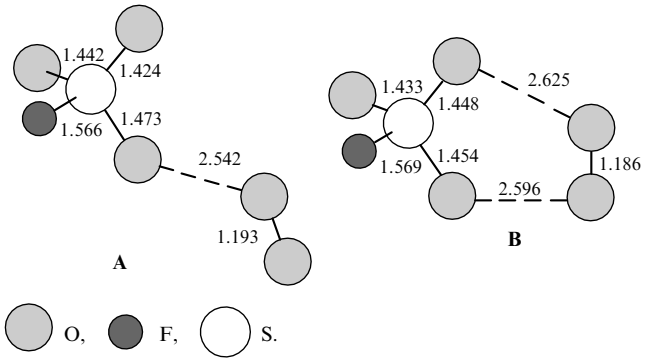
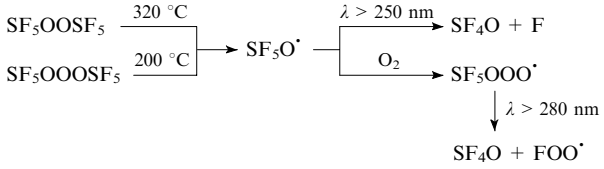


Figure 3. Linear (**A**) and cyclic (**B**) conformers of the $FS(O)_2O\text{---}OO$ complex (according to the UB3LYP/6-311 + G(3df) calculations).[224]

$$CF_3OS(O)_2O—OS(O)_2OCF_3 \xrightarrow{90\ ^\circ C} CF_3OSO_3^{\bullet}.$$

The matrix IR spectrum of decomposition products of this peroxide revealed nine new bands that disappeared upon photolysis. Based on the results of quantum chemical calculations [B3LYP/6-311 + G(3d,f)], these bands were assigned [317] to the $CF_3OSO_3^{\bullet}$ radical with C_1 symmetry and partial delocalization of free electron over the SO_3 fragment, the same as in the $FSO_3^{\bullet}$ radical discussed above.[314] The IR band at 1039 cm^{-1} was assigned to the $\nu_s(SO_3)$ stretching vibration.

In the IR spectrum of the $SF_5O^{\bullet}$ radical generated by vacuum pyrolysis of SF_5OOSF_5 or SF_5OOOSF_5 and stabilized in an Ne or Ar matrix, six bands were detected,[311] which were assigned to the radical with C_{2v} symmetry, based on quantum chemical calculations. Irradiation of the $SF_5O^{\bullet}$ radical with $\lambda > 250$ nm initiated its dissociation to SF_4O and a fluorine atom. The reaction of the $SF_5O^{\bullet}$ radical with oxygen molecules in an Ne or Ar matrix afforded the trioxyl radical $SF_5OOO^{\bullet}$.



In the IR spectrum, a band at 1513 cm^{-1} assigned to the $SF_5OOO^{\bullet}$ radical was identified with the stretching vibration of the terminal O—O group.[311] According to quantum chemical calculations,[311] the $SF_5OOO^{\bullet}$ radical represented a complex formed by the $SF_5O^{\bullet}$ radical with an O_2 molecule (C_1 symmetry). Despite the considerably long O—O bond (2.36 Å) between the SF_5O and O_2 fragments of this complex, which is typical of such trioxy radicals [*e.g.*, for $FOOO^{\bullet}$ (Ref. 184) or $CF_3OOO^{\bullet}$ (Ref. 281)], the terminal O_2 group in this complex exerted a pronounced effect on the position and intensity of IR bands corresponding to the SF_5O moiety in this complex as compared with the $SF_5O^{\bullet}$ free radical.[311] Photolysis ($\lambda > 280$ nm) of the $SF_5OOO^{\bullet}$ radical in an Ar or Ne matrix led to its dissociation to SF_4O and $FOO^{\bullet}$.

It should be noted that the reactions of sulfur-containing SF_5O_x radicals ($x = 0-3$) are very interesting in view of their important role in atmospheric processes.

The structure of the $^{\bullet}C(S)SH$ radical [263] was considered above in Section VI.2.

VIII. Radical structures containing metal atoms

In the recent decade, the method of laser ablation has successfully been used in the synthesis of free radicals containing metal atoms of different Groups of the Periodic Table and the elucidation of their structure. Studies on these radicals accomplished before 2001 were discussed in sufficient detail in several reviews.[7, 318, 319] These focused attention on the molecular structures with occupied electron shells. EPR studies of transient radicals containing metal atoms carried out by the end of the 1980s were summarized in the well-known monograph by Weltner.[320] In this Section, we consider the recent works mostly pertaining to the matrix EPR. Insofar as the spectral data obtained by this method contain information on the electronic structure of transient radicals (see Section II.2), attention is focused on the electronic structure of such type of intermediates.

Atoms of Group IIB metals (Zn, Cd, Hg) in the ground state have occupied electron shells (ns^2) and, correspondingly, the fundamental term ^1S. In the electron-excited state (^1P), atoms of Group IIB metals actively react with saturated hydrocarbons (CH_4, C_2H_6, C_3H_8) by inserting into the C—H bond to form H—M—R intermediates (R = CH_3, C_2H_5, C_3H_7; M = Zn, Cd, Hg), which decompose to the following two radicals: $HM^{\bullet}$ and $R^{\bullet}$ (Refs 321, 322). For example,

$$M(^1P) + CH_4 \longrightarrow H—M—CH_3 \longrightarrow HM^{\bullet} + H_3C^{\bullet}.$$

The existence of intermediates of the H−M−R type was postulated [321, 322] based on the analysis of the potential energy surface for the M + CH_4 reaction. Later, the H−M−CH_3 intermediates (M = Zn, Cd, Hg) were stabilized in solid argon.[323] For this purpose, metal vapour and CH_4 were co-condensed in argon. The intermediates $HMCH_3$ frozen in Ar matrices were studied by matrix IR spectroscopy. Analysis of the IR spectra and results of quantum chemical calculations [324] made it possible to conclude that the intermediates $HMCH_3$ had the C_{3v} configuration with the linear H−M−C fragment.

Knight *et al.*[325–328] carried out a detailed EPR study of zinc, cadmium and mercury hydrides (HM$^{\bullet}$) [325, 326] and also of the $CH_3M^{\bullet}$ radicals [327–329] stabilized in solid argon and neon matrices. Using different magnetic isotopes of these atoms, they have obtained reliable HFC constants (A_{iso} and A_{dip}) for these radicals and analyzed the spin population (ρ) of atomic orbitals *n*s and *n*p$_z$. Table 10 summarizes the data obtained for the HM$^{\bullet}$ and $CH_3M^{\bullet}$ radicals. For a comparison, this Table also shows the data for the CNM$^{\bullet}$ and FM$^{\bullet}$ radicals.[330, 331] For the HM$^{\bullet}$ and $CH_3M^{\bullet}$ radicals (M = Cd, Zn), good agreement between the experimental and simulated HFC constants (quantum chemical calculations by the HFSDCI, MRSDC and DFT methods) was achieved; on the other hand, for the HHg$^{\bullet}$ and $CH_3Hg^{\bullet}$ radicals, the calculated isotropic and dipolar HFC constants on the metal atom turned out to be considerably lower than those obtained experimentally.

Presumably,[326, 329] the reason for the high experimental HFC constants could be the relativistic effects that concern the outer electrons of heavy atoms (in this case, Hg). Indeed, calculations of the spin density based on experimentally found HFC constants for a radical and HFC constants of free atoms,

$$\rho(ns) = \frac{A_{izo}(\text{radical})}{A_{izo}(\text{atom})},$$

$$\rho(np_z) = \frac{A_{dip}(\text{radical})}{A_{dip}(\text{atom})},$$

carried of in the aforementioned studies [326, 329] produced an anomalously high spin density on the Hg atom (see Table 10). Hence, the total ($\Sigma\rho$) spin density (the sum of densities in electron orbitals of all atoms in a radical) for the HHg$^{\bullet}$ and $CH_3Hg^{\bullet}$ radicals proved to be much higher than unity. Although, for certain reasons, the thus calculated spin populations of electron orbitals were of limited accuracy (in the majority of cases, from 5% to 20%; for ^{13}C in the CH_3 fragment, 50% accuracy), the obtained data together with the results of quantum chemical calculations made it possible to characterize the chemical bonds formed by metal atoms with different radical groups.[326, 328, 329]

As follows from the results shown in Table 10, the unpaired electron in radicals under consideration was preferentially localized on the metal atom. The transfer of the spin density from a radical fragment to a metal atom was associated with the preferentially ionic nature of the R−M bond with a partial contribution of the covalent component. In the former case, a considerable decrease in the spin density on radical R and an increase in the s-nature of the spin density on the metal atom were observed. This was the most pronounced for the FM$^{\bullet}$ and CNM$^{\bullet}$ radicals, where the fluorine atom F and the CN group were characterized by high electron affinity. For fluorine-containing radicals of the FM$^{\bullet}$ type, less than 20% of the spin density remained on the outer 2p-orbital of the fluorine atom and decreased with the decrease in the ionization energy of the metal atom (Hg > Cd > Zn). These conclusions have recently been confirmed by quantum chemical calculations employing relativistic methods of the density functional theory [332, 333] and the results of an analysis of rotational spectra of the FZn radical (for the following five isotopes: ^{64}Zn, ^{66}Zn, ^{67}Zn, ^{68}Zn and ^{70}Zn) in the gas phase,[334] which have shown that the σ-orbital in the FZn$^{\bullet}$ radical included 4s(Zn) + 4p$_\sigma$(Zn) + 2s(F) + 2p$_\sigma$(F) atomic orbitals and was of the predominantly 4s(Zn) nature (∼80% – 90%). The rest atomic orbitals accounted for only 10% – 20% of the spin density. This confirms the predominantly ionic nature of the Zn−F bond with a partial covalent contribution made by the 4p(Zn)- and 2p(F)-orbitals that accounted for ∼10% of spin density each.

Among diatomic radicals of this type studied by the EPR method, the FBa$^{\bullet}$ (F^-Ba^+) radical had the bond of the most pronounced ionic nature. Its $A_{dip}(^{19}F)$ constant was only 2.8 MHz, which corresponded to the spin population of the fluorine atom 2p-orbital below 1%.[335]

A different electronic structure is typical of the HHg$^{\bullet}$ and $CH_3Hg^{\bullet}$ radicals. They exhibited low population of the metal atom s-orbital at the high spin densities on both the metal p-orbital and the radical fragments H and CH_3.

Table 10. Isotropic (A_{iso}/MHz) and dipolar (A_{dip}/MHz) HFC constants and spin populations (ρ) of the corresponding atomic electron orbitals in the HM$^{\bullet}$, $CH_3M^{\bullet}$, FM$^{\bullet}$ and CNM$^{\bullet}$ radicals.[325–331]

Radical	M				^{1}H		^{13}C				^{19}F		$\Sigma\rho$
	A_{iso}	ρ(*n*s)	A_{dip}	ρ(*n*p$_z$)	A_{iso}	ρ(1s)	A_{iso}	ρ(2s)	A_{dip}	ρ(2p$_z$)	A_{dip}	ρ(2p$_z$)	
H^{67}Zn	630	0.32	15	0.53	503	0.35							1.20
H^{111}Cd	3796	0.33	60	0.44	550	0.36							1.13
H^{199}Hg	6859	0.20	446	0.73	730	0.51							1.44
$CH_3{}^{67}$Zn	569	0.29	20	0.56	−14	−0.01	182	0.05	14	0.13			1.0
$CH_3{}^{111}$Cd	3471	0.26	17	0.45	−17	−0.01	195	0.05	17	0.16			0.89
$CH_3{}^{199}$Hg	4921	0.14	345	0.56	31	0.02	188	0.05	41	0.38			1.20
F^{67}Zn											177	0.10	
F^{111}Cd											202	0.11	
F^{199}Hg	22163	0.63	223	0.36							320	0.18	
CN^{199}Hg	15960	0.45	396	0.65									

Based on this, it was concluded [329] that the M–R bond in these radicals was preferentially covalent.

The Group IIIA metals (B, Al, Ga, In, Tl) have the $^2P_{1/2}$ doublet fundamental term with the ns^2p electronic configuration. Such electronic structure of the Group IIIA metal atoms allows them to form various hydrides, *e.g.*, monometallic hydrides such as H_nM ($n = 1-4$) or bimetallic hydrides such as H_nM_2. Earlier, only the simplest diatomic metal hydrides could be detected in the gas phase [336–338] or in matrices.[71, 339–341] Later, more complex compounds were synthesized in solid hydrogen matrices as a result of reaction of a metal hydride with the matrix substance.

An ingenious method of laser ablation of aluminium atoms and their co-deposition with molecular hydrogen in a low-temperature matrix was used by Andrews *et al.*[342–344] for synthesizing highly reactive hydrides such as H_nAl ($n = 1-3$) and H_mAl_2 ($m = 4-6$) identified by Fourier transform IR spectroscopy. The transient radicals such as $H_2M^{\bullet}$ and $H_5M_2^{\cdot}$ were found to play an important role in the formation of this type of compounds with closed electron shells.[345] Different aluminium hydrides were produced both during the co-deposition of hydrogen molecules with metal atoms on a substrate cooled to 3.5 K and under the action of UV irradiation or by the thermal diffusion of intermediates formed upon unfreezing of the H_2 matrix.

$$Al + H_2 \xrightarrow{3.5\ K} \begin{bmatrix} HAl \\ H_2\dot{A}l \\ H_3Al \end{bmatrix} \xrightarrow{3.5\ K,\ \lambda > 265\ nm} \begin{bmatrix} H_2\dot{A}l \\ H_3Al \end{bmatrix} \xrightarrow{5-6\ K} \begin{bmatrix} H_4Al_2 \\ H_6Al_2 \\ H_5\dot{A}l_2 \end{bmatrix}$$

The assignment of IR absorption bands to the corresponding aluminium hydrides was carried out based on the analysis of their behaviour in the course of photolysis and annealing of the hydrogen matrix and also based on their shift for deuterated species, which were synthesized by using HD and D_2 molecules in place of H_2. The resulting IR spectra were compared with the vibrational spectra of molecules calculated by quantum chemical methods. This made it possible to elucidate the main processes leading to formation of covalently bound molecules and free radicals.[344, 345] Particularly, it was shown that aluminium monohydride HAl was preferentially formed in the course of co-deposition of aluminium atoms and hydrogen molecules on a support cooled to 3.5 K; in addition, weak IR bands belonging to the $H_2Al^{\bullet}$ radical and the H_3Al molecule were observed. Subsequent photolysis of HAl, $H_2Al^{\bullet}$ and H_3Al resulted in a considerable increase in the amounts of $H_2Al^{\bullet}$ and H_3Al formed in the reaction of excited aluminium atoms or aluminium monohydride molecules [344] with a hydrogen molecule

$$Al^* + H_2 \longrightarrow H_2Al^{\bullet},$$

$$(HAl)^* + H_2 \longrightarrow H_3Al.$$

Warming of the matrix to 5–6 K led to the formation of unique bimetallic hydrides Al_2H_4 and Al_2H_6 and also of the $H_5Al_2^{\cdot}$ radical. According to certain data,[344] the formation of this type compounds proceeded as a result of translational diffusion of species in a solid hydrogen matrix during its annealing.

$$H_2Al^{\bullet} + H_2Al^{\bullet} \longrightarrow H_4Al_2,$$

$$H_2Al^{\bullet} + H_3Al \longrightarrow H_5Al_2^{\cdot},$$

$$H_3Al + H_3Al \longrightarrow H_6Al_2.$$

Quantum chemical calculations [B3LYP/6-311++G(d,p)] of $H_2Al^{\bullet}$ and $H_5Al_2^{\cdot}$ radicals were carried out and their IR spectra were studied.[345] The obtained data suggested that the $H_2Al^{\bullet}$ radical has a molecular structure with C_{2v} symmetry and the H–Al–H angle equal to 120°. Based on quantum chemical calculations, two stable structures **A** and **B** were proposed for the $H_5Al_2^{\cdot}$ radical (Fig. 4). Structure **A** with two bridging hydrogen atoms had C_s symmetry; it resulted from the removal of the terminal hydrogen atom from the Al_2H_6 molecule. Structure **B** with C_{2v} symmetry had one bridging hydrogen atom; it was formed upon elimination of one bridging hydrogen atom from the Al_2H_6 molecule. According to quantum chemical calculations, structural isomer **A** was ~6 kcal mol^{-1} more stable than isomer **B**.[345] A comparison of theoretical and experimental vibrational spectra has shown that the more stable structural isomer **A** was formed in experiments.

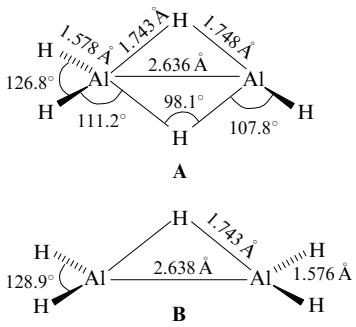


Figure 4. Structures of the $Al_2^{\cdot}H_5$ radical calculated by the B3LYP/6-311++G(d,p) method.[345]

EPR spectra of matrix-isolated $H_2B^{\bullet}$, $H_2Al^{\bullet}$, and $H_2Ga^{\bullet}$ radicals were studied by Knight *et al.*[346–348] The latter publication [348] contained results of quantum chemical calculations and the detailed analysis of the electronic structure of these intermediates. Table 11 summarizes the experimental magnetic parameters of these radicals. Estimates [348] of spin populations of hydrogen and metal atoms showed that the unpaired electron was preferentially localized on the p_z-orbital of metal atoms, namely, $\rho_{p_z}(B) = 0.8$, $\rho_{p_z}(Al) = 0.60$ and $\rho_{p_z}(Ga) = 0.68$. Populations of s-orbitals of B, Al and Ga atoms were 0.14, 0.21 and 0.17, respectively. The spin density on the hydrogen atom s-orbital did not exceed 10%.

The HFC constants and spin populations of the $H_2Ga^{\bullet}$ radical, calculated by the UHF method, agreed well with these parameters measured experimentally. The calculations

Table 11. HFC constants of $HM^{\bullet}R$ radicals (M = ^{11}B, ^{27}Al and ^{69}Ga; R = H, CH_3) measured in solid Ne.[346–348]

Radical	M		^1H	
	A_{dip}[tensor] /MHz	A_{iso} /MHz	A_{dip}[tensor] /MHz	A_{iso} /MHz
$H_2Ga^{\bullet}$	[−127, −167, 295]	2084	[−3, 2, 1]	179
$H_2Al^{\bullet}$	[−50, −48, 98]	834	[−5, 2, 2]	128
$H_2B^{\bullet}$		358		38
$HGa^{\bullet}CH_3$	[−129, −178, 306]	1999	[−9, 5, 4]	203
$HAl^{\bullet}CH_3$	[−49, −60, 108]	772	[−6, 2, 5]	152

pointed to a considerable charge transfer from metal to the hydrogen atom, as a result of which the charge on each hydrogen atom was −0.32.

Among hydrides of this group metals, mention should be made of the $H_4B^{\bullet}$ radical with a unique structure (Fig. 5). This radical was detected by EPR in the course of irradiation of $NaBH_4$.[349] Further *ab initio* studies [350–352] revealed its structure with C_{2v} symmetry. The recently recorded matrix EPR spectra of the $^{\bullet}BH_4$ radical in solid hydrogen [353] and IR spectra in solid neon [354] confirmed C_{2v} symmetry for this radical and the presence of two non-equivalent groups of H atoms located at different distances from the B atom.

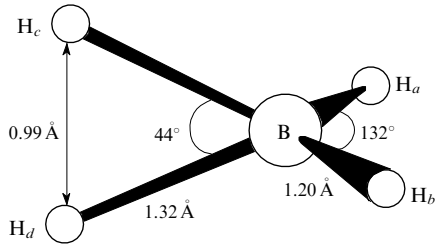


Figure 5. Equilibrium structure of the H_4B radical with C_{2v} symmetry calculated by the MCSCF method.[351]

Atoms of Group IIIA metals can insert into C−H bonds of methane to afford the transient radical $HMCH_3$.[348, 355, 356] Table 11 shows magnetic parameters of such radicals, which are close to the analogous parameters of $H_2M^{\bullet}$ radicals. The slight increase in the p_z-character of spin population on the metal atom in $HM^{\bullet}CH_3$ radicals and the higher spin density on the hydrogen atom as compared with $H_2M^{\bullet}$ radicals deserves mention. Photolysis of $HM^{\bullet}CH_3$ radicals with unfiltered light ($\lambda = 260-600$ nm) resulted in their dissiciation to form the simplest organometallic molecules CH_3M (M = Gd, In) stable in solid argon at $T < 30$ K.[356]

The unique trend of Al atoms towards insertion into different bonds was used for generation of different Al radical intermediates in inert matrices, namely, $HAl^{\bullet}OH$,[347, 357, 358] $HAl^{\bullet}NH_2$,[359, 360] $HAl^{\bullet}Cl$.[361, 362]

$$Al^{\bullet} + H_2O \longrightarrow HAl^{\bullet}OH,$$

$$Al^{\bullet} + NH_3 \longrightarrow HAl^{\bullet}NH_2,$$

$$Al^{\bullet} + HCl \longrightarrow HAl^{\bullet}Cl.$$

These compounds were characterized by EPR and IR spectroscopy. It was shown [362] that in the following sequence of Ar matrix-stabilized radicals: $HAl^{\bullet}H$, $HAl^{\bullet}Cl$ and $ClAl^{\bullet}Cl$, the spin population of the aluminium 3s-orbital progressively increased (0.21, 0.28 and 0.41), while the population of the 3p-orbital decreased (0.59, 0.50, 0.44), which pointed to higher ionic degree of the bond in compounds with chlorine atoms substituted for hydrogen atoms.

The first identification and IR spectral characterization of linear radical structures O−M−O ($^2\Pi_{1/2}$) formed upon insertion of boron,[363, 364] aluminium,[365–367] gallium and indium [368] were carried out using low-temperature matrices. In addition to linear structures, cyclic structures (^{2}A) with C_{2v} symmetry and the O−M−O angle of 35°–40° were detected.

$$M + O_2 \longrightarrow \begin{array}{c} O\!-\!O \\ \diagdown\ \diagup \\ M \end{array} \qquad (1)$$

M = Al, Ga, In.

Earlier, such cyclic structures were predicted based on quantum chemical calculations.[369] Apparently, the formation of cyclic structures stable at cryogenic temperatures has a very high activation barrier. Presumably,[368] this precedes the formation of linear O−M−O structures more energetically stable. However, the conversion of a cyclic MO_2 molecule into a linear OMO molecule proceeded with a substantial activation barrier.[370, 371] This conclusion has recently been confirmed by quantum chemical calculations [CCSD(T), MRMP2, MRCI].[372] According to these calculations, the cyclic structure of AlO_2 (^{2}A) was the intermediate product of gas-phase reaction (2).

$$Al + O_2 \longrightarrow OAl + O. \qquad (2)$$

Figure 6 shows the energy diagram of reaction (2). Apparently, this reaction is virtually exoergic, whereas reaction (1) is highly exothermic. The formation of the long-lived intermediate AlO_2 that averaged the reaction energy over the vibration-rotation degrees of freedom was confirmed in recent molecular beam experiments.[373]

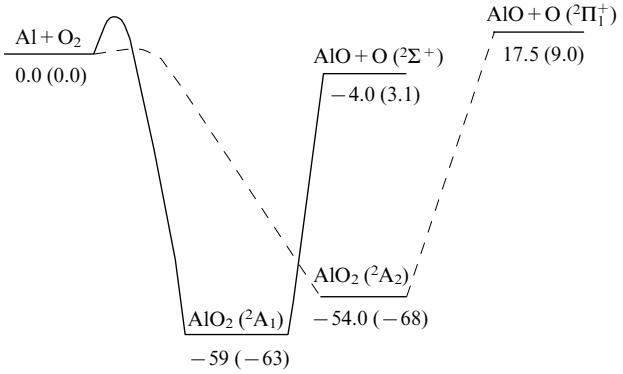


Figure 6. Diagram of the potential energy surface of the $Al + O_2 \rightarrow AlO + O$ reaction calculated by the MRMP2 and RCCSD(T) (values in parentheses) methods (according to the data from Ref. 372). Energies are expressed in kcal mol^{-1}.

The problem of theoretical description of the electronic structure of diatomic metal oxides OM (M = Al, Ga, In) concerns the correct consideration of contributions made by ionic states corresponding to the following two limiting cases: M^+O^- (unpaired electron is preferentially localized on the oxygen atom) and $M^{2+}O^{2-}$ (unpaired electron is preferentially localized on the metal atom). An attempt was undertaken [374] to solve this problem experimentally based on the analysis of EPR spectra of OM radicals (M = Al, Ga, In) in a neon matrix at 4 K. In this study, a magnetic isotope ^{17}O was used, in contrast to the previous EPR studies of the OB [375, 376] and OAl [377, 378] radicals. Highly resolved EPR spectra of OM radicals were determined,

Table 12. HFC constants of metal oxides (MHz) stabilized in solid neon (for a comparison, HFC constants of the corresponding radicals in the gas phase and HFC constants of free atoms are shown).[374, 376, 380]

Radical [a] or atom	M				O			
	A_{iso}	A_{dip}	$\rho(ns)$	$\rho(np_z)$	A_{iso}	A_{dip}	$\rho(2s)$	$\rho(2p_z)$
$^{17}O^{11}B$ (m)	1033	25	0.41	0.39	−19	−12	0.004	0.07
$^{17}O^{11}B$ (g)	1027.4	27.1						
$^{17}O^{27}Al$ (m)	766	52	0.20	0.63	−2	−50	0.0004	0.30
$^{17}O^{27}Al$ (g)	738.0	56.4						
$^{17}O^{69}Ga$ (m)	1483	127	0.12	0.62	−8	−77	0.002	0.46
$^{17}O^{115}In$ (m)	1368	180	0.07	0.63	−35	−131	0.007	0.78
$^{17}O^{45}Sc$ (m)	2018	24			−20.3	0.4		
$^{17}O^{80}Y$ (m)	−807.5	−9.5			−16.8	0.0		
$^{17}O^{139}La$ (m)	3751	29			~ (−10)	0.0		
Sc	2823							
Y	−1250	−18						
La	6007	67.7						
O	−5260	−168						

[a] Designations: (m) a radical in an Ne matrix, (g) a radical in the gas phase.

which made it possible to find the hyperfine structure parameters on both atoms of the diatomic radicals. Table 12 shows experimental HFC constants and spin populations of different atomic orbitals calculated based on these parameters. Although the calculated[374] HFC constants adequately agreed with their experimental values, considerable difficulties associated with the analysis of the spin density in these radicals were mentioned. The spin populations calculated from the experimental HFC constants of radicals and the corresponding constants of atoms (see Table 12) were tentative due to the possible internal correlations associated with the interaction of the oxygen valence orbitals with inner orbitals of the metal atom. The oxygen 2p-orbitals were less susceptible to this effect; hence, the resulting spin population of the oxygen 2p-orbitals should reflect more correctly the trend for the spin density redistribution in the sequence of monoxides of the Group IIIA metals (from ^{11}B to ^{115}In). It follows from the data in Table 12 that the population of the oxygen 2s-orbital was close to zero in all radicals, whereas the population of the oxygen 2p-orbital increased approximately tenfold on going from the light ^{11}B atom to the heavy ^{115}In atom. This suggests that the $O^{2-}M^{2+}$ state dominated in the BO radical and the $O^{-}M^{+}$ state prevailed in the OIn radical.

A similar result has recently been obtained in quantum chemical calculations[379] that took into account the spin–orbit and relativistic effects. Table 13 shows spin populations calculated for a series of diatomic radicals XM ($^2\Sigma$). It was noted[379] that calculations according to the Mulliken scheme (Mulliken population analysis) faced certain difficulties. Nonetheless, theoretical results correctly reflected the main trends in variations of spin population in the corresponding radical groups (depending on the nature of atoms X or M), observed in the matrix EPR spectra.

In the above study,[379] the HFC constants calculated by different methods were compared. The HFC constants in HgX radicals calculated with due allowance for the relativistic effects proved to be larger than the constants calculated without taking this into consideration. This was consistent with the data obtained earlier in Knight's laboratory.[326]

The EPR spectra of Group IIIB metals (Sc, Y, La) isolated in solid neon or argon and the results of quantum chemical calculations of these oxides were considered.[380] The EPR spectra of these radicals in contrast to EPR spectra of Group IIIA metal oxides demonstrated very low spin populations on the oxygen atom (see Table 13) and extremely high populations on *n*s-orbitals of metal atoms.

Table 13. Calculated spin populations of atomic electron orbitals of diatomic radicals of the XM type.[379]

Radical XM		Orbital [a]	M		X
X	M		$\rho(ns)$	$\rho(np_\sigma)$	ρ(orbital)
H	Zn	8σ	0.42	0.29	0.29 (1s)
H	Cd	11σ	0.42	0.27	0.32 (1s)
H	Hg	15σ	0.31	0.24	0.44 (1s)
H	Pd	10σ	0.35	0.38 [b]	0.26 (1s)
F	Zn	10σ	0.70	0.13	0.15 (2p)
F	Cd	13σ	0.69	0.11	0.19 (2p)
F	Hg	17σ	0.55	0.09	0.31 (2p)
Ag	Zn	17σ	0.19	0.15	0.66 (5s)
Ag	Cd	20σ	0.20	0.14	0.66 (5s)
Ag	Hg	24σ	0.11	0.11	0.79 (5s)
CN	Zn	12σ	0.56	0.25	0.18 (5σ)
CN	Cd	15σ	0.58	0.20	0.21 (5σ)
CN	Hg	19σ	0.45	0.19	0.32 (5σ)
O	B	5σ	0.62	0.28	0.05 ($2p_\sigma$)
O	Al	7σ	0.44	0.17	0.32 ($2p_\sigma$)
O	Ga	10σ	0.28	0.17	0.48 ($2p_\sigma$)
O	In	13σ	0.28	0.17	0.48 ($2p_\sigma$)
S	B	7σ	0.47	0.34	0.15 (np_σ)
O	Sc	9σ	0.84	0.07	0.08 ($2p_\sigma$)
O	Y	12σ	0.87	0.06	0.07 ($2p_\sigma$)
O	La	15σ	0.86	0.08	0.05 ($2p_\sigma$)
C	Rh	12σ	0.56	0.11 [b]	0.27 ($2p_\sigma$)

[a] A molecular orbital with unpaired electron. [b] The value for $\rho(4d_\sigma)$ is given.

The HFC constants on Group IIIB metals and oxygen calculated by quantum chemical methods well agreed with experimental constants. Analyzing the calculated charge and spin density distributions on M and X atoms, it was concluded[380] that the electronic structure of such oxides corresponds to the ionic structure with a covalent $O^- - M^+$ bond. Presumably,[380] the 'covalent' bond in the $O^-(^2P) - M^+(^3D)$ ion pair was formed due to interaction of the metal ion d_{z^2}-orbital with the oxygen ion $2p_z$-orbital.

The electronic structure of OV oxide ($^4\Sigma$) and OVO dioxide ($^2A_1$) was established by analyzing the matrix EPR[381,382] and IR spectra.[383,384] It was found that the spin density in the OV radical was completely localized on the metal atom, whereas in the OVO radical in the ground state $^2A_1$, a considerable part of the spin density was concentrated on electron orbitals of the oxygen atoms. For the OVO radical, the presence of a low-lying ($\sim$20 kcal mol^{-1}) excited twice degenerate electronic state $^2B_1$ formed as a result of strong spin–orbit coupling was noted.[382]

According to B3LYP/6-311+G* calculations,[384] the OVO radical ground state corresponds to $^2B_1$. These calculations[384] also predicted the existence of structural isomers of the OVO radical, namely, cyclic VO_2 and asymmetric OOV with much larger enthalpy of formation.

The molecular structure of certain paramagnetic metal complexes with polyfunctional aromatic ligands formed under the conditions of low-temperature co-condensation of metal and ligand vapour or upon their isolation in inert gas matrices was elucidated using IR and EPR spectroscopy. A detailed analysis of these studies was given in a review.[385] The synthesis of paramagnetic silver and copper biligand π-complexes by low-temperature co-condensation of metal vapour with alkylcyanobiphenyls was described.[386–389] HFC parameters of EPR spectra of these complexes pointed to the electron density transfer from the metal atom to the antibonding orbital of 4-pentyl-4′-cyanobiphenyl (5CB). The introduction of the third component, CCl_4, into this system led to the competitive interaction of metal atoms with CCl_4 and the 5CB ligand to afford several paramagnetic products, namely, a mixed-ligand σ-complex $Ag(5CB)CCl_4$ and the transient radical $Cl(Cl_3C)Ag$ formed in the reaction of silver chloride with the trichloromethyl radical.

Sergeev *et al.*[390–392] have found that the reaction of lanthanides (Eu, Sm) with 4-cyanobiphenyl (CB) afforded sandwich-type structures with antiparallel orientation of planar ligand molecules. Figure 7 shows the structure of europium complexes, namely, EuL_2 (**A**) and Eu_2L_2 (**B**). Quantum chemical calculations of such complexes have shown that complexes with high multiplicity have the lowest energy.[393,394] Thus the multiplicity of a monometallic complex EuL_2 was 10 and the multiplicity of a bimetallic

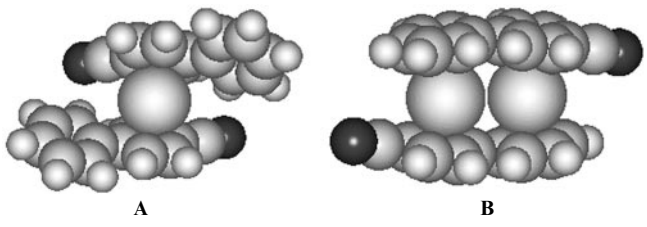


Figure 7. Structures of complexes $Eu(CB)_2$ (**A**) and $Eu_2(CB)_2$ (**B**).[392]

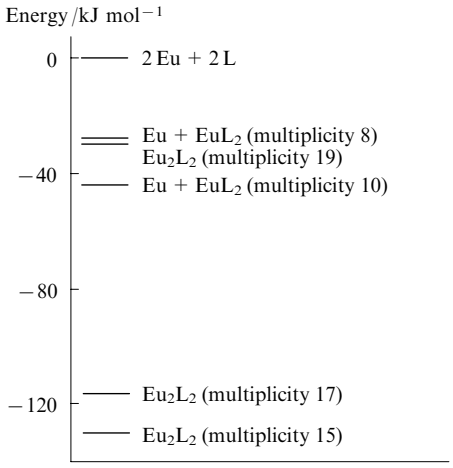


Figure 8. Correlation diagram of system total energy for electronic states of $Eu(CB)_2$ and $Eu_2(CB)_2$ complexes with different multiplicity.[394]

complex Eu_2L_2 was 15. These complexes considerably differed in the energy ($\sim$20–30 kcal mol^{-1}) between different spin states (Fig. 8).

IX. Conclusion

The material presented in this review points to considerable progress in the spectroscopic studies of matrix-isolated transient radicals. In addition to the perfection of conventional methods of generation and stabilization of transient radicals, new methods of their synthesis in cryogenic matrices have gained wide acceptance, *e.g.*, laser ablation, the use of mobile atoms, initiation of reactions with noble gas atoms and stabilization of radical–molecule complexes in helium nanodroplets.

Modernization of spectroscopic instrumentation and the methods of computer processing of EPR and IR absorption spectra and also the development of quantum chemical methods of calculating the structure and spectroscopic characteristics of chemical compounds were beneficial for the mutual enrichment of experimental and theoretical methods. On the one hand, the comparison of experimentally obtained spectroscopic characteristics with those calculated by various quantum chemical methods made it possible to reliably identify the spectra and characterize the structures of radical species. On the other hand, the experimental data served as a reliable test of the quality of calculations as regards the accuracy of predictions of molecular parameters and electronic structures of different types of intermediates.

The advances in the field of matrix spectroscopy were regularly discussed at international conferences, among which mention should be made of the Gordon Conferences on the Physics and Chemistry of Matrix-Isolated Species, International Conferences on the Low-Temperature Chemistry, International Conferences on Reactive Intermediates and Unusual Molecules, International Symposia on Free Radicals and also the All-Russian Schools-Conferences 'Highly Reactive Intermediates of Chemical Reactions'.

The recent studies of matrix-isolated intermediates carried out at the Institute of Problems of Chemical Physics of the Russian Academy of Sciences and the Institute of Organic Chemistry of the Russian Academy of Sciences

were financially supported by the Russian Foundation of Basic Research (Project Nos 01-03-33171, 01-03-33066, 04-03-32599 and 07-03-00768), the Grant of the President of the Russian Federation (NSh-6075.2006.3, NSh-3237.2008.3) and the Programme No. 1 of the Division of Chemistry and Material Sciences of the Russian Academy of Sciences.

References

1. *Reactive Intermediate Chemistry* (Eds R A Moss, M S Platz, M Jones Jr) (Hoboken, NJ: Wiley, 2004)
2. V A Korolev, O M Nefedov, in *Advances in Physical Organic Chemistry* Vol. 30. (Ed. D Bethell) (London: Academic Press, 1995) p 1
3. O M Nefedov *Izv. Akad. Nauk SSSR, Ser. Khim.* 2425 (1991) [a]
4. E Whitle, D A Dows, G C Pimentel *J. Chem. Phys.* **22** 1943 (1954)
5. I Norman, G Porter *Nature (London)* **174** 508 (1954)
6. V E Bondybey, A M Smith, J Agreiter *Chem. Rev.* **96** 2113 (1996)
7. M J Almond, K S Wiltshire *Annu. Rep. Prog. Chem., Sect. C* **97** 3 (2001)
8. M E Jacox *Chem. Soc. Rev.* **31** 108 (2002)
9. C W Murray, G J Laming, N C Handy, R D Amos *Chem. Phys. Lett.* **199** 551 (1992)
10. J Andzelm, E Wimmer *J. Chem. Phys.* **96** 1280 (1992)
11. V Barone, in *Recent Advances in Density Functional Methods* Pt. 1 (Ed. D P Chong) (Singapore: World Scientific, 1995) p. 287
12. P Scott, L Radom *J. Phys. Chem.* **100** 16502 (1996)
13. P S Zuev, O M Nefedov *Usp. Khim.* **58** 1091 (1989) [*Russ. Chem. Rev.* **58** 636 (1989)]
14. O M Nefedov, A I Ioffe, L G Menchikov *Khimiya Karbenov* (The Chemistry of Carbenes) (Moscow: Khimiya, 1990)
15. W Sander, in *Carbene Chemistry: From Fleeting Intermediates to Powerful Reagents* Ch. 1 (Ed. G Bertrand) (New York: Marcel Dekker, 2002) p. 1
16. M S Platz, in *Carbene Chemistry: From Fleeting Intermediates to Powerful Reagents* Ch. 2 (Ed. G Bertrand) (New York: Marcel Dekker, 2002) p. 27
17. W Sander, G Bucher, S Wierlacher *Chem. Rev.* **93** 1583 (1993)
18. N P Gritsan *Usp. Khim.* **76** 1218 (2007) [*Russ. Chem. Rev.* **76** 1139 (2007)]
19. M E Jacox *Acc. Chem. Res.* **37** 727 (2004)
20. E B Jochnowitz, X Zhang, M R Nimlos, M E Varner, J F Stanton, G B Ellison *J. Phys. Chem. A* **109** 3812 (2005)
21. T Oka *Annu. Rev. Phys. Chem.* **44** 299 (1993)
22. T Momose, T Shida *Bull. Chem. Soc. Jpn.* **71** 1 (1998)
23. S Tam, M E Fajardo *Rev. Sci. Instrum.* **70** 1926 (1999)
24. L Andrews, X Wang *Rev. Sci. Instrum.* **75** 3039 (2004)
25. Y-P Lee, Y-J Wu, R M Lees, L-H Xu, J T Hougen *Science* **311** 365 (2006)
26. J Ceponkus, B Nelander *J. Chem. Phys.* **124** 024504 (2006)
27. T Momose, M Fushitani, H Hoshina *Int. Rev. Phys. Chem.* **24** 533 (2005)
28. K Yoshioka, P L Raston, D T Anderson *Int. Rev. Phys. Chem.* **25** 469 (2006)
29. A Kh Vorob'ev, N A Chumakova *Izv. Akad. Nauk, Ser. Khim.* 2595 (2004) [a]
30. A Kh Vorob'ev, N A Chumakova *Izv. Akad. Nauk, Ser. Khim.* 190 (2005) [a]
31. A Kh Vorobiev, N A Chumakova *J. Magn. Reson.* **175** 146 (2005)
32. L B Knight Jr, G M King, J T Petty, M Matsushita, T Momose, T Shida *J. Chem. Phys.* **103** 3377 (1995)
33. T Kumada, J Kumagai, T Miyazaki *J. Chem. Phys.* **114** 10024 (2001)
34. E Popov, T Kiljunen, H Kunttu, J Eloranta *J. Chem. Phys.* **126** 134504 (2007)
35. J R Morton, K P Preston, P J Krusic, S A Hill, E Wasserman *J. Phys. Chem.* **96** 3576 (1992)
36. J R Morton, K F Preston, F Negri *Chem. Phys. Lett.* **221** 59 (1994)
37. R Borghi, L Lunazzi, G Placucci, P J Krusic, D A Dixon, N Matsuzawa, M Ata *J. Am. Chem. Soc.* **118** 7608 (1996)
38. B Tumanskii, O Kalina, in *Radical Reactions of Fullerenes and Their Derivates* (Dordrecht: Kluwer Academic, 2002)
39. E Ya Misochko, A V Akimov, V A Belov, D A Tyurin *Izv. Akad. Nauk, Ser. Khim.* 424 (2007) [a]
40. E Ya Misochko, A V Akimov, V A Belov, D A Tyurin, D N Laikov *J. Chem. Phys.* **127** 084301 (2007)
41. M Kaupp, M Bühl, V G Malkin *Calculation of NMR and EPR Parameters: Theory and Applications* (Weinheim: Wiley-VCH, 2004)
42. V Barone, V Crescenzi, R Improta *Quant. Struct.-Act. Relat.* **21** 105 (2002)
43. M Stein, E V Lenthe, E J Baerends, W Lubitz *J. Phys. Chem. A* **105** 416 (2001)
44. V Barone, P Cimino, E Stendardo *J. Chem. Theory Comput.* **4** 751 (2008)
45. C Remenyi, R Reviakine, A Arbuznikov, J Vaara, M Kaupp *J. Phys. Chem. A* **108** 5026 (2004)
46. D N Laikov, Yu A Ustyunyuk *Izv. Akad. Nauk, Ser. Khim.* 804 (2005) [a]
47. L Hermosilla, P Calle, J M García de la Vega, C Sieiro *J. Phys. Chem. A* **109** 1114 (2005)
48. E Ya Misochko, A V Akimov, I U Goldschleger, D A Tyurin, D N Laikov *J. Chem. Phys.* **122** 034503 (2005)
49. W E Falconer, J R Morton, A G Streng *J. Chem. Phys.* **41** 902 (1964)
50. R S Eachus, C R Symons *J. Chem. Soc. A* 304 (1971)
51. T Sato, A Narazaki, Y Kawaguchi, H Nino, G Bucher, D Grote, J J Wolff, H H Wenk, W Sander *J. Am. Chem. Soc.* **126** 7846 (2004)
52. E Ya Misochko, A V Akimov, S V Chapyshev *J. Chem. Phys.* **129** 174510 (2008)
53. E Ya Misochko, A V Akimov, V F Lavitskii, S V Chapyshev *Izv. Akad. Nauk, Ser. Khim.* 284 (2007) [a]
54. E Ya Misochko, A V Akimov, S V Chapyshev *J. Chem. Phys.* **128** 124504 (2008)
55. N P Bowling, R J Halter, J A Hodges, R A Seburg, P S Thomas, C S Simmons, J F Stanton, R J McMahon *J. Am. Chem. Soc.* **128** 3291 (2006)
56. R A Bernheim, R J Kempf, E F Reichenbecher *J. Magn. Reson.* **3** 5 (1970)
57. S E Boganov, V I Faustov, V D Gvozdev, K N Shavrin, M P Egorov, O M Nefedov *J. Am. Chem. Soc.* **131** 14688 (2009)
58. S L Wang, C M L Rittby, W R M Graham *J. Chem. Phys.* **107** 7025 (1997)
59. S L Wang, C M L Rittby, W R M Graham *J. Chem. Phys.* **107** 6032 (1997)
60. X D Ding, S L Wang, C M L Rittby, W R M Graham *J. Chem. Phys.* **112** 5113 (2000)
61. W Weltner Jr, R J Van Zee *Chem. Rev.* **89** 1713 (1989)
62. D L Robbins, C M L Rittby, W R M Graham *J. Chem. Phys.* **114** 3570 (2001)
63. D L Robbins, K-C Chen, C M L Rittby, W R M Graham *J. Chem. Phys.* **120** 4664 (2004)
64. S A Bates, C M L Rittby, W R M Graham *J. Chem. Phys.* **125** 074506 (2006)
65. R E Kinzer Jr , C M L Rittby, W R M Graham *J. Chem. Phys.* **125** 074513 (2006)
66. V A Apkarian, N Schwentner *Chem. Rev.* **99** 1481 (1999)
67. E Ya Misochko, A V Akimov, I U Goldshleger *Usp. Khim.* **72** 262 (2003) [*Russ. Chem. Rev.* **72** 233 (2003)]
68. J Kupper, J M Merritt *Int. Rev. Phys. Chem.* **26** 249 (2007)
69. G B Sergeev *Usp. Khim.* **70** 915 (2001) [*Russ. Chem. Rev.* **70** 809 (2001)]
70. A D Pomogailo, A S Rozenberg, I E Uflyand *Nanochastitsy Metallov v Polimerakh* (Nanoparticles of Metal in Polymers) (Moscow: Khimiya, 2000)
71. G V Chertihin, L Andrews *J. Phys. Chem.* **97** 10295 (1993)
72. J Lundell, L Khriachtchev, M Pettersson, M Risinen *Low Temp. Phys.* **26** 680 (2000)

73. L Khriachtchev, M Pettersson, N Runeberg, J Lundell, M Risinen *Nature (London)* **406** 874 (2000)
74. L Khriachtchev, M Pettersson, A Lignell, M Räsänen *J. Am. Chem. Soc.* **123** 8610 (2001)
75. L Khriachtchev, H Tanskanen, J Lundell, M Pettersson, H Kiljunen, M Räsänen *J. Am. Chem. Soc.* **125** 4696 (2003)
76. V I Fel'dman, F F Sukhov, A Yu Orlov, I V Tyul'pina, E A Logacheva, D A Tyurin *Izv. Akad. Nauk, Ser. Khim.* 1415 (2005) [a]
77. L Khriachtchev, M Pettersson, J Lundell, H Tanskanen, T Kiviniemi, N Runeb'erg, M Risinen *J. Am. Chem. Soc.* **125** 1454 (2003)
78. V I Feldman, F F Sukhov, A Yu Orlov, I V Tyulpina *J. Am. Chem. Soc.* **125** 4698 (2003)
79. E L Cochran, F J Adrian, V A Bowers *J. Chem. Phys.* **40** 213 (1964)
80. P H Kasai, E B Whipple *J. Am. Chem. Soc.* **89** 1033 (1967)
81. P H Kasai *J. Am. Chem. Soc.* **94** 5950 (1972)
82. R A Shepherd, T J Doyle, W R M Graham *J. Chem. Phys.* **89** 2738 (1988)
83. D Forney, M E Jacox, W E Thompson *J. Mol. Spectrosc.* **170** 178 (1995)
84. Y-J Wu, M-Y Lin, B-M Cheng, H-F Chen, Y-P Lee *J. Chem. Phys.* **128** 204509 (2008)
85. E L Cochran, F J Adrian, V A Bowers *J. Phys. Chem.* **74** 2083 (1970)
86. M E Jacox *Chem. Phys.* **53** 307 (1980)
87. I U Goldschleger, A V Akimov, E Ya Misochko, C A Wight *J. Mol. Spectrosc.* **205** 269 (2001)
88. P H Kasai *J. Phys. Chem.* **90** 5034 (1986)
89. B E Wurfel, A Thoma, V E Bondybey *Chem. Phys. Lett.* **198** 135 (1992)
90. A Thoma, B E Wurfel, R Schlachta, G M Lask, V E Bondybey *J. Phys. Chem.* **96** 7231 (1992)
91. A K Mal'tsev, V A Korolev, O M Nefedov *Izv. Akad. Nauk SSSR, Ser. Khim.* 2415 (1982) [a]
92. A K Mal'tsev, V A Korolev, N D Kagramanov, O M Nefedov *Izv. Akad. Nauk SSSR, Ser. Khim.* 1078 (1983) [a]
93. A K Mal'tsev, V A Korolev, O M Nefedov *Izv. Akad. Nauk SSSR, Ser. Khim.* 555 (1984) [a]
94. G Maier, H P Reisenauer, B Rohde, K Dehnicke *Chem. Ber.* **116** 732 (1983)
95. K Holtzhauer, C Cometta-Morini, J F M Oth *J. Phys. Org. Chem.* **3** 219 (1990)
96. E Vajda, J Tremmel, B Rozsondai, I Hargittai, A K Maltsev, N D Kagramanov, O M Nefedov *J. Am. Chem. Soc.* **108** 4352 (1986)
97. S Nandi, P A Arnold, B K Carpenter, M R Nimlos, D C Dayton, G B Ellison *J. Phys. Chem. A* **105** 7514 (2001)
98. G Maier, S Senger *Angew. Chem., Int. Ed. Engl.* **33** 558 (1994)
99. A K Mal'tsev, E G Baskir, N D Kagramanov, O M Nefedov *Izv. Akad. Nauk SSSR, Ser. Khim.* 555 (1986) [a]
100. E G Baskir, V A Korolev, O M Nevedov *Mendeleev Commun.* 125 (2000)
101. Y-W Wu, M-L Hwang, W-L Hsu, F-H Fang *J. Chin. Chem. Soc.* **45** 307 (1998)
102. M E Jacox, D E Milligan *Chem. Phys.* **4** 45 (1974)
103. V A Korolev, A K Mal'tsev, O M Nefedov *Izv. Akad. Nauk SSSR, Ser. Khim.* 1058 (1989) [a]
104. J W Huang, W R M Graham *J. Chem. Phys.* **93** 1583 (1990)
105. D M Chipman, K E Miller *J. Am. Chem. Soc.* **106** 6236 (1984)
106. D S Han, C M L Rittby, W R M Graham *J. Chem. Phys.* **109** 8355 (1998)
107. D E Milligan, M E Jacox, L Abouaf-Marguin *J. Chem. Phys.* **46** 4562 (1967)
108. M E Jacox, W B Olson *J. Chem. Phys.* **86** 3134 (1987)
109. M Jinguji, C A McDowell *J. Mol. Struct.* **130** 317 (1985)
110. R A Shepherd, W R M Graham *J. Chem. Phys.* **86** 2600 (1987)
111. Y-J Wu, B-M Cheng *Chem. Phys. Lett.* **461** 53 (2008)
112. K W Chang, W R M Graham *J. Chem. Phys.* **76** 5238 (1982)
113. R Tarroni, S Carter *J. Chem. Phys.* **119** 12878 (2003)
114. R Tarroni, S Carter *Mol. Phys.* **102** 2167 (2004)
115. D S Han, C M L Rittby, W R M Graham *J. Chem. Phys.* **108** 3504 (1998)
116. L N Shen, T J Doyle, W R M Graham *J. Chem. Phys.* **93** 1597 (1990)
117. T J Doyle, L N Shen, C M L Rittby, W R M Graham *J. Chem. Phys.* **95** 6224 (1991)
118. J van Wijngaarden, I Shnitko, A Batalov, P Kolek, J Fulara, J P Maier *J. Phys. Chem. A* **109** 5553 (2005)
119. P H Kasai, E Hedaya, E B Whipple *J. Am. Chem. Soc.* **91** 4364 (1969)
120. J G Radziszewski, M R Nimlos, P R Winter, G B Ellison *J. Am. Chem. Soc.* **118** 7400 (1996)
121. A V Friderichsen, J G Radziszewski, M R Nimlos, P R Winter, D C Dayton, D E David, G B Ellison *J. Am. Chem. Soc.* **123** 1977 (2001)
122. A Lapiński, J Spanget-Larsen, M Langgård, J Waluk, J G Radziszewski *J. Phys. Chem. A* **105** 10520 (2001)
123. J G Radziszewski *Chem. Phys. Lett.* **301** 565 (1999)
124. V I Feldman, F F Sukhov, E A Logacheva, A Yu Orlov, I V Tyulpina, D A Tyurin *Chem. Phys. Lett.* **437** 207 (2007)
125. P H Kasai, D McLeod Jr, H C McBay *J. Am. Chem. Soc.* **96** 6864 (1974)
126. C L Angell, E Hedaya, D McLeod Jr *J. Am. Chem. Soc.* **89** 4214 (1967)
127. J H Miller, L Andrews *J. Mol. Spectrosc.* **90** 20 (1981)
128. E G Baskir, A K Mal'tsev, V A Korolev, V N Khabashesku, O M Nefedov *Izv. Akad. Nauk, Ser Khim.* 1499 (1993) [a]
129. E G Baskir, V A Korolev, A K Mal'tsev, K Uisasi, I Tamash, O M Nefedov *Izv. Akad. Nauk SSSR, Ser Khim.* 818 (1989) [a]
130. V A Korolev, O M Nefedov *Izv. Akad. Nauk, Ser Khim.* 1497 (1993) [a]
131. V T Aleksanyan, B V Lokshin *Kolebatel'nye Spektry π-kompleksov Perekhodnykh Elementov. Stroenie i Khimicheskaya Svyaz' (Itogi Nauki i Tekhniki)* [Vibrational Spectra of π-Complexes of Transition Elements. Structure and Chemical Bond (Advances in Science and Engineering Series)] (Moscow: Izd. VINITI, 1976) Vol. 5
132. M Van Thiel, G C Pimentel *J. Chem. Phys.* **32** 133 (1960)
133. E L Cochran, F J Adrian, V A Bowers *J. Chem. Phys.* **51** 2759 (1969)
134. I U Goldschleger, A V Akimov, E Ya Misochko *J. Mol. Struct.* **519** 191 (2000)
135. E Ya Misochko, I U Goldschleger, A V Akimov, C A Wight *Low Temp. Phys.* **26** 727 (2000)
136. E Ya Misochko, I U Gol'dshleger, A V Akimov *Izv. Akad. Nauk, Ser. Khim.* 832 (2000) [a]
137. N Akai, S Kudoh, M Nakata *J. Phys. Chem. A* **107** 6725 (2003)
138. N Akai, H Yoshida, K Ohno, M Aida *Chem. Phys. Lett.* **403** 390 (2005)
139. N Akai, T Harada, K Shin-ya, K Ohno, M Aida *J. Phys. Chem. A* **110** 6016 (2006)
140. E L Cochran, F J Adrian, V A Bowers *J. Chem. Phys.* **36** 1938 (1962)
141. V E Bondybey *J. Chem. Phys.* **66** 995 (1977)
142. M E Jacox, D E Milligan *J. Chem. Phys.* **48** 4040 (1968)
143. D E Milligan, M E Jacox *J. Chem. Phys.* **47** 278 (1967)
144. R Kolos, J Waluk *J. Mol. Struct.* **408** 473 (1997)
145. L Khriachtchev, A Lignell, H Tanskanen, J Lundell, H Kiljunen, M Räsänen *J. Phys. Chem. A* **110** 11876 (2006)
146. F J Adrian, V F Bowers, E L Cochran *J. Chem. Phys.* **63** 919 (1975)
147. P H Kasai, L A Eriksson *Mol. Phys.* **96** 993 (1999)
148. M E Jacox *J. Phys. Chem.* **91** 6595 (1987)
149. M Pettersson, J Lundell, L Khriachtchev, M Räsänen *J. Chem. Phys.* **109** 618 (1998)
150. R D Hunt, L Andrews *Inorg. Chem.* **26** 3051 (1987)
151. I U Goldschleger, A V Akimov, E Ya Misochko, C A Wight *Mendeleev Commun.* 64 (2001)
152. R A Bair, T H Dunning Jr *J. Chem. Phys.* **82** 2280 (1985)
153. H Dupin, I Baraille, C Larrieu, A Dargelos *Chem. Phys.* **256** 7 (2000)

154. F Bernardi, F Cacace, G Occhiucci, A Ricci, I Rossi *J. Phys. Chem. A* **104** 5545 (2000)
155. E Ya Misochko, I U Goldschleger, A V Akimov, C A Wight *J. Am. Chem. Soc.* **123** 5156 (2001)
156. E Ya Misochko, A V Akimov, I U Goldschleger, C A Wight *J. Chem. Phys.* **116** 10318 (2002)
157. E Ya Misochko, A V Akimov, I U Goldschleger, C A Wight *J. Chem. Phys.* **116** 10307 (2002)
158. O M Nefedov *Pure Appl. Chem.* **63** 231 (1991)
159. G W Robinson, M McCarty Jr *J. Chem. Phys.* **28** 350 (1958)
160. D S Tinti *J. Chem. Phys.* **48** 1459 (1968)
161. V S Langford, B E Williamson *J. Phys. Chem. A* **101** 3119 (1997)
162. L E Brus, V E Bondybey *J. Chem. Phys.* **63** 786 (1975)
163. N Acquista, L J Schoen, D R Lide Jr *J. Chem. Phys.* **48** 1534 (1968)
164. S Suzer, L Andrews *J. Chem. Phys.* **88** 916 (1988)
165. B-M Cheng, Y-P Lee, J-F Ogilvie *Chem. Phys. Lett.* **151** 109 (1988)
166. L Khriachtchev, M Pettersson, S Touminen, M Räsänen *J. Chem. Phys.* **107** 7252 (1997)
167. A Engdahl, G Karlstrlm, B Nelander *J. Chem. Phys.* **118** 7797 (2003)
168. V S Langford, A J McKinley, T I Quickenden *J. Am. Chem. Soc.* **122** 12859 (2000)
169. P D Cooper, H G Kjaergaard, V S Langford, A J McKinley, T I Quickenden, D P Schofield *J. Am. Chem. Soc.* **125** 6048 (2003)
170. Y M Xie, H F Schaefer III *J. Chem. Phys.* **98** 8829 (1993)
171. B Wang, H Hou, Y Gu *Chem. Phys. Lett.* **303** 96 (1999)
172. T Svensson, B Nelander, G Karlström *Chem. Phys.* **265** 323 (2001)
173. A Engdahl, B Nelander *J. Chem. Phys.* **122** 126101 (2005)
174. Y P Kuo, G H Wann, Y P Lee *J. Chem. Phys.* **99** 3272 (1993)
175. E J Feltham, M J Almond, G Marston, K S Wiltshire, N Goldberg *Spectrochim. Acta, Part A* **56** 2589 (2000)
176. A Olbert-Majkut, Z Mielke *Phys. Chem. Chem. Phys.* **8** 4773 (2006)
177. S Hashimoto, G Inoue, H Akimoto *Chem. Phys. Lett.* **107** 198 (1984)
178. S Nagase, S Hashimoto, H Akimoto *J. Phys. Chem.* **92** 641 (1988)
179. M Wierzejewska, A Olbert-Majkut *J. Phys. Chem. A,* **107** 10944 (2003)
180. Y P Kuo, B M Cheng, Y P Lee *Chem. Phys. Lett.* **177** 195 (1991)
181. A Arkell *J. Phys. Chem.* **73** 3877 (1969)
182. L Andrews, J I Raymond *J. Chem. Phys.* **55** 3078 (1971)
183. L Andrews *J. Chem. Phys.* **57** 51 (1972)
184. E Ya Misochko, A V Akimov, C A Wight *J. Phys. Chem. A* **103** 7972 (1999)
185. R Kopitzky, H Grothe, H Willner *Chem. – Eur. J.* **8** 5601 (2002)
186. H Grothe, H Willner *Angew. Chem., Int. Ed. Engl.* **33** 1482 (1994)
187. S-Y Chiang, Y-C Hsu, Y -P Lee *J. Chem. Phys.* **90** 81 (1989)
188. M E Jacox, D E Milligan *J. Mol. Spectrosc.* **47** 148 (1973)
189. M E Jacox *Chem. Phys.* **59** 213 (1981)
190. L Andrews, M Hawkins, R Withnall *Inorg. Chem.* **24** 4234 (1985)
191. K C Clemitshaw, J R Sodeau *J. Phys. Chem.* **93** 3552 (1989)
192. G A Argüello, H Willner *J. Phys. Chem. A* **105** 3466 (2001)
193. R A Morris, T M Miller, J F Paulson, A A Viggiano, M T Feldmann, R A King, H F Schaefer III *J. Chem. Phys.* **110** 8436 (1999)
194. M-C Yang, J M Williamson, T A Miller *J. Mol. Spectrosc.* **186** 1 (1997)
195. G A Arguello, H Grother, M Kronberg, H Willner, H G Mack *J. Phys. Chem.* **99** 17525 (1995)
196. J Spanget-Larsen, M Gil, A Gorski, D M Blake, J Waluk, J G Radziszewski *J. Am. Chem. Soc.* **123** 11253 (2001)
197. M Nagaya, S Kudoh, M Nakata *Chem. Phys. Lett.* **432** 446 (2006)
198. G E Ewing, W E Thompson, G C Pimentel *J. Chem. Phys.* **32** 927 (1960)
199. D E Milligan, M E Jacox *J. Chem. Phys.* **41** 3032 (1964)
200. D E Milligan, M E Jacox *J. Chem. Phys.* **51** 277 (1969)
201. M Pettersson, L Khriachtchev, S Jolkkonen, M Räsänen *J. Phys. Chem.* **103** 9154 (1999)
202. D E Milligan, M E Jacox, A M Bass, J J Comeford, D E Mann *J. Chem. Phys.* **42** 3187 (1965)
203. M E Jacox *J. Mol. Spectrosc.* **80** 257 (1980)
204. H Schnöckel, R A Eberlein, H S Plitt *J. Chem. Phys.* **97** 4 (1992)
205. M E Jacox, D E Milligan *J. Chem. Phys.* **43** 866 (1965)
206. T D Fridgen, J M Parnis *J. Phys. Chem. A* **101** 5117 (1997)
207. M E Jacox *Chem. Phys.* **69** 407 (1982)
208. E G Baskir, O M Nefedov *Izv. Akad. Nauk, Ser. Khim.* 109 (1996) [a]
209. S vonAhsen, J Hufen, H Willner, J S Francisco *Chem. – Eur. J.* **6** 1189 (2002)
210. M E Jacox, D E Milligan *J. Chem. Phys.* **54** 927 (1971)
211. M E Jacox *J. Chem. Phys.* **88** 4598 (1988)
212. D Forney, M E Jacox *J. Chem. Phys.* **119** 10814 (2003)
213. D E Milligan, M E Jacox *J. Chem. Phys.* **38** 2627 (1963)
214. W E Thompson, M E Jacox *J. Chem. Phys.* **91** 3826 (1989)
215. M E Jacox *J. Mol. Spectrosc.* **84** 74 (1980)
216. E Ya Misochko, A V Akimov, C A Wight *Chem. Phys. Lett.* **274** 23 (1997)
217. K Johnsson, B A Engdahl, B Nelander *J. Phys. Chem.* **97** 9603 (1993)
218. L-H Lai, C-P Liu, Y-P Lee *J. Chem. Phys.* **109** 988 (1998)
219. H S P Muller, H Willner *J. Phys. Chem.* **97** 10589 (1993)
220. D E Tevault, R R Smardzewski *J. Am. Chem. Soc.* **100** 3955 (1978)
221. L Schriver-Mazzuoli, O Abdelaoui, C Lugez, A Schriver *Chem. Phys. Lett.* **214** 519 (1993)
222. G Maier, A Bothur *Z. Anorg. Allg. Chem.* **621** 743 (1995)
223. J Kölm, A Engdahl, O Schrems, B Nelander *Chem. Phys.* **214** 313 (1997)
224. H Beckers, P Garcia, H Willner, G A Arguello, C J Cobos, J S Francisco *Angew. Chem., Int. Ed.* **46** 3754 (2007)
225. P Ase, W Bock, A Snelson *J. Phys. Chem.* **90** 2099 (1986)
226. S Nandi, S J Blanksby, X Zhang, M R Nimlos, D C Dayton, G B Ellison *J. Phys. Chem. A* **106** 7547 (2002)
227. G Chettur, A Snelson *J. Phys. Chem.* **91** 3483 (1987)
228. S Sander, H Pernice, H Willner *Chem. – Eur. J.* **6** 3645 (2000)
229. E G Baskir, V A Korolev, J V Nefedov *J. Mol. Struct.* **480 – 481** 519 (1999)
230. G Chettur, A Snelson *J. Phys. Chem.* **91** 5873 **(**1987)
231. G Chettur, A Snelson *J. Phys. Chem.* **91** 913 (1987)
232. R J Yang, L Yu, X Jin, M Zhou, B K Carpenter *J. Chem. Phys.* **122** 014511 (2005)
233. A Mardyukov, W Sander *Chem. – Eur. J.* **15** 1462 (2009)
234. T-L Tso, M Diem, E K C Lee *Chem. Phys. Lett.* **91** 339 (1982)
235. T-L Tso, E K C Lee *J. Phys. Chem.* **88** 5475 (1984)
236. R Yang, L Yu, A Zeng, M Zhou *J. Phys. Chem. A* **108** 4228 (2004)
237. H Pernice, P Garcia, H Willner, J S Francisco, F P Mills, M Allen, Y L Yung *Proc. Natl. Acad. Sci. USA* **101** 14007 (2004)
238. S von Ahsen, H Willner, J S Francisco *J. Chem. Phys.* **121** 2048 (2004)
239. S von Ahsen, H Willner, J S Francisco *Chem. – Eur. J.* **8** 4675 (2002)
240. S von Ahsen, P Garcia, H Willner, G A Arguello *Inorg. Chem.* **44** 5713 (2005)
241. H Beckers, H Willner, D Grote, W Sander, J Geier *J. Chem. Phys.* **128** 224301 (2008)
242. W F Schneider, M M Maricq, J J Szente, J S Francisco *J. Chem. Phys.* **103** 6601 (1995)
243. J Breidung, W Thiel *J. Phys. Chem. A* **110** 1575 (2006)
244. D Pullin, L Andrews *J. Mol. Struct.* **95** 181 (1982)
245. J G Radziszewski, M Gil, A Gorski, J Spanget-Larsen, J Waluk, B J Mroz *J. Chem. Phys.* **115** 9733 (2001)
246. R Yang, X Jin, W Wang, K Fan, M Zhou *J. Phys. Chem. A* **109** 4261 (2005**)**
247. P H Kasai, D McLeod Jr *J. Am. Chem. Soc.* **96** 2338 (1974)
248. M Nagata, Y Futami, N Akai, S Kudoh, M Nakata *Chem. Phys. Lett.* **392** 259 (2004)

249. F J Adrian, E L Cochran, V A Bowers *J. Chem. Phys.* **36** 1661 (1962)
250. E L Cochran, F J Adrian, V A Bowers *J. Chem. Phys.* **44** 4626 (1966)
251. J F Ogilvie *Spectrochim. Acta, Part A* **3** 737 (1967)
252. T van Mourik, T H Dunning, K A Peterson Jr *J. Phys. Chem. A* **104** 2287 (2000)
253. A V Marenich, J E Boggs *J. Phys. Chem. A* **108** 5431 (2004)
254. J S Shirk, C Pimentel *J. Am. Chem. Soc.* **90** 3349 (1969)
255. L S Alconcel, H-J Deyerl, V Zengin, R E Continetti *J. Phys. Chem. A* **103** 9190 (1999)
256. Yu G Utkin, J-X Han, F Sun, H-B Chen, G Scott, R F Curl *J. Chem. Phys.* **118** 10470 (2003)
257. A L Cooksy *J. Phys. Chem. A* **102** 5093 (1998)
258. Q Jiang, W R M Graham *J. Chem. Phys.* **98** 9251 (1993)
259. Z A Tomašič, G E Scuseria *J. Phys. Chem.* **95** 6905 (1991)
260. A L Cooksy, J K G Watson, C A Gottlieb, P Thaddeus *J. Chem. Phys.* **101** 178 (1994)
261. A L Cooksy, F-M Tao, W Klemperer, P Thaddeus *J. Phys. Chem.* **99** 11095 (1995)
262. J S Francisco *J. Chem. Phys.* **107** 9039 (1997)
263. R B Bohn, G D Brabson, L Andrews *J. Phys. Chem.* **96** 1582 (1992)
264. D E Milligan, M E Jacox *J. Mol. Spectrosc.* **42** 495 (1972)
265. D W Smith, L Andrews *J. Chem. Phys.* **60** 81 (1974)
266. B Nelander *J. Phys. Chem. A* **101** 9092 (1997)
267. A Engdahl, B Nelander *Chem. Phys.* **249** 215 (1999)
268. T Svensson, B Nelander *Chem. Phys.* **262** 445 (2000)
269. T Svensson, B Nelander *Chem. Phys.* **286** 347 (2003)
270. A Engdahl, B Nelander *Phys. Chem. Chem. Phys.* **6** 730 (2004)
271. M M Rochkind, G C Pimentel *J. Chem. Phys.* **46** 4481 (1967)
272. B N Cyvin, S J Cyvin, A Snelson *Z. Anorg. Allg. Chem.* **542** 193 (1986)
273. R R Smardzewski, R A DeMarco, W B Fox *J. Chem. Phys.* **63** 1083 (1975)
274. R Butler, A Snelson *J. Phys. Chem.* **83** 3243 (1979)
275. L Liu, S R Davis *J. Phys. Chem.* **96** 9719 (1992)
276. K C Clemitshaw, J R Sodeau *J. Phys. Chem.* **91** 3650 (1987)
277. B Nelander, A Engdahl, T Svensson *Chem. Phys. Lett.* **332** 403 (2000)
278. T P W Jungkamp, J H Seinfeld *Chem. Phys. Lett.* **257** 15 (1996)
279. A Beltrán, J Andrés, S Noury, B Silvi *J. Phys. Chem. A* **103** 3078 (1999)
280. H Grothe, H Willner *Angew. Chem., Int. Ed. Engl.* **35** 768 (1996)
281. S von Ahsen, H Willner, J S Francisco *Angew. Chem., Int. Ed.* **42** 4690 (2003)
282. E Ya Misochko, A V Akimov, I U Goldshleger, C A Wight *Mendeleev Commun.* 181 (1998)
283. E Ya Misochko, A V Akimov, I U Goldshleger, C A Wight *J. Am. Chem. Soc.* **120** 11520 (1998)
284. E Ya Misochko, A V Akimov, I U Goldshleger, A I Boldyrev, C A Wight *J. Am. Chem. Soc.* **121** 405 (1999)
285. C Puzzarini, V Barone *J. Chem. Phys.* **129** 084306 (2008)
286. S L Laursen, A E Delia, K Mitchell *J. Phys. Chem. A* **104** 3681 (2000)
287. C S Jamieson, A M Mebel, R I Kaiser *Phys. Chem. Chem. Phys.* **7** 4089 (2005)
288. B D Benson, J S Francisco *Chem. Phys. Lett.* **233** 335 (1995)
289. M Nakata, K Shibuya, H Frei *J. Phys. Chem.* **94** 8168 (1990)
290. D J Fitzmaurice, H Frei *J. Phys. Chem.* **96** 10308 (1992)
291. J L Gossage, J A G Gomes, D L Cocke, K Y Li, C J Lin, R Tadmor, A Basu, S Bhat, S Tandel, P Jayabalu, H Balu *Appl. Spectrosc.* **58** 1236 (2004)
292. M Nakata, Y Somura, M Takayanagi, N Tanaka, K Shibuya, T Uchimaru, K Tanabe *J. Phys. Chem.* **100** 15815 (1996)
293. M Nakata, H Frei *J. Am. Chem. Soc.* **111** 5240 (1989)
294. M Nakata, H Frei *J. Phys. Chem.* **93** 7670 (1989)
295. M Nakata, H Frei *J. Chem. Soc. Jpn.* 1412 (1989)
296. M Nakata *Spectrochim. Acta, Part A* **50** 1455 (1994)
297. N Tanaka, Y Kajii, K Shibuya, M Nakata *J. Phys. Chem.* **97** 7048 (1993)
298. M Nakata, H Frei *J. Am. Chem. Soc.* **114** 1363 (1992)
299. D J Fitzmaurice, H Frei *J. Phys. Chem.* **95** 2652 (1991)
300. N Tanaka, M Nakata, K Shibuya *J. Photochem. Photobiol.* **106** 113 (1997)
301. M McCluskey, H Frei *J. Phys. Chem.* **97** 5204 (1993)
302. J A Harrison, H Frei *J. Phys. Chem.* **98** 12142 (1994)
303. J A Harrison, H Frei *J. Phys. Chem.* **98** 12152 (1994)
304. S Kudoh, T Uechi, M Takayanagi, M Nakata, H Frei *Chem. Phys. Lett.* **328** 283 (2000)
305. T Uechi, S Kudoh, M Takayanagi, M Nakata *J. Phys. Chem. A* **106** 3365 (2002)
306. E Isoniemi, M Pettersson, L Khriachtchev, J Lundell, M Risinen *J. Phys. Chem. A* **103** 679 (1999)
307. L Khriachtchev, M Pettersson, E Isoniemi, M Räsänen *J. Chem. Phys.* **108** 5747 (1998)
308. E Isoniemi, L Khriachtchev, M Pettersson, M Räsänen *Chem. Phys. Lett.* **311** 47 (1999)
309. R R Smardzewski, W B Fox *J. Chem. Phys.* **67** 2309 (1977)
310. P Hassanzadeh, L Andrews *J. Phys. Chem.* **96** 79 (1992)
311. M Kronberg, S von Ahsen, H Willner, J S Francisco *Angew. Chem., Int. Ed.* **44** 253 (2005)
312. R M Romano, C O D Védova, A J Downs *J. Phys. Chem. A* **108** 7179 (2004)
313. S von Ahsen, J S Francisco *Angew. Chem., Int. Ed.* **43** 3330 (2004)
314. H Beckers, H Willner, D Grote, W Sander *J. Chem. Phys.* **128** 084501 (2008)
315. E M Suzuki, J W Nibler, K A Oakes, D Eggers Jr *J. Mol. Spectrosc.* **58** 201 (1975)
316. S T Arnold, T M Miller, A A Viggiano *Int. J. Mass Spectrom.* **218** 207 (2002)
317. S von Ahsen, J S Francisco *J. Phys. Chem. A* **109** 9193 (2005)
318. M J Almond *Annu. Rep. Prog. Chem., Sect. C* **93** 3 (1997)
319. M J Almond, R H Orrin *Annu. Rep. Prog. Chem., Sect. C* **88** 3 (1991)
320. W Weltner Jr *Magnetic Atoms and Molecules* (Mineola, NY: Dover, 1989)
321. M-C Duval, B Soep, W H Breckenridge *J. Phys. Chem.* **95** 7145 (1991)
322. H Umemoto, S Tsunashima, H Ikeda, K Takano, K Kuwahara, K Sato, K Yokoyama, F Misaizu, K Fuke *J. Chem. Phys.* **101** 4803 (1994)
323. T M Greene, L Andrews, A J Downs *J. Am. Chem. Soc.* **117** 8180 (1995)
324. S Castillo, A Ramirez-Solis, D Diaz, E Poulain, O Novaro *Mol. Phys.* **81** 825 (1994)
325. L B Knight Jr, W Weltner Jr *J. Chem. Phys.* **55** 2061 (1971)
326. A C Stowe, L B Knight *Mol. Phys.* **100** 353 (2002)
327. E Karakyriakos, J R Davis, C J Wilson, S A Yates, A J McKinley, L B Knight Jr, R Babb, D J Tyler *J. Chem. Phys.* **110** 3398 (1999)
328. A J McKinley, E Karakyriakos, L B Knight Jr, R Babb, A Williams *J. Phys. Chem. A* **104** 3528 (2000)
329. E Karakyriakos, A J McKinley *J. Phys. Chem. A* **108** 4619 (2004)
330. L B Knight Jr, K C Lin *J. Chem. Phys.* **56** 6044 (1972)
331. L B Knight Jr, T A Fisher, M B Wise *J. Chem. Phys.* **74** 6009 (1981)
332. H M Quiney, P Belanzoni *Chem. Phys. Lett.* **353** 253 (2002)
333. I Malkin, O L Malkina, V G Malkin, M Kaupp *Chem. Phys. Lett.* **396** 268 (2004)
334. M A Flory, S K McLamarrah, L M Ziurys *J. Chem. Phys.* **125** 194304 (2006)
335. R D Urban, H Birk, P Polomsky, H Jones *J. Chem. Phys.* **94** 2523 (1991)
336. L B Knight Jr, W C Easley, W Weltner Jr *J. Chem. Phys.* **54** 322 (1971)
337. Y F Zhu, R Shehadeh, E R Grant *J. Chem. Phys.* **97** 883 (1992)
338. J M Campbell, M Dulick, D Klapstein, J B White, P F Bernath *J. Chem. Phys.* **99** 8379 (1993)
339. F A Kurth, R A Eberlein H Schnöckel, A J Downs, C R Pulham *J. Chem. Soc., Chem. Commun.* 1302 (1993)
340. Z L Xiao, R H Hauge, J L Margrave *Inorg. Chem.* **32** 642 (1993)

341. P Pullumbi, Y Bouteiller, L Manceron, C Mijoule *Chem. Phys.* **185** 25 (1994)
342. L Andrews, X Wang *Science* **299** 2049 (2003)
343. X Wang, L Andrews, S Tam, M E DeRose, M Fajardo *J. Am. Chem. Soc.* **125** 9218 (2003)
344. X Wang, L Andrews *J. Phys. Chem. A* **107** 11371 (2003)
345. L Andrews, X Wang *J. Phys. Chem. A* **108** 4202 (2004)
346. L B Knight Jr, M Winiski, P Miller, C A Arrington, D Feller *J. Chem. Phys.* **91** 4468 (1989)
347. L B Knight Jr, J R Woodward, T J Kirk, C A Arrington *J. Phys. Chem.* **97** 1304 (1993)
348. L B Knight Jr, J J Banisaukas III, R Babb, E R Davidson *J. Chem. Phys.* **105** 6607 (1996)
349. M C R Symons, T Chen, C Glidewell *J. Chem. Soc., Chem. Commun.* 326 (1983)
350. A I Boldyrev, J Simons *J. Chem. Phys.* **99** 4628 (1993)
351. R P Saxon *J. Phys. Chem.* **97** 9356 (1993)
352. H B Schlegel, A G Baboul, S J Harris *J. Phys. Chem.* **100** 9774 (1996)
353. R J Van Zee, A P Williams, W Weltner Jr *J. Chem. Phys.* **107** 4756 (1997)
354. L Andrews, X Wang *J. Am. Chem. Soc.* **124** 7280 (2002)
355. P Hassanzadeh, Y Hamachi, L Andrews *J. Phys. Chem.* **97** 6418 (1993)
356. H-J Himmel, A J Downs, T M Greene, L Andrews *Organometallics* **19** 1060 (2000)
357. R H Hauge, J W Kauffman, J L Margrave *J. Am. Chem. Soc.* **102** 6005 (1980)
358. L B Knight Jr, B Gregory, J Cleveland, C A Arrington *Chem. Phys. Lett.* **204** 168 (1993)
359. B Gaertner, H J Himmel *Inorg. Chem.* **41** 2496 (2002)
360. J A Howard, H A Joly, P P Edwards, R J Singer, D E Logan *J. Am. Chem. Soc.* **114** 474 (1992)
361. G A Olah, O Farooq, S M F Farnia, M R Bruce, F L Clouet, P R Morton, G K S Prakash, R C Stevens, R Bau, K Lammertsma, S Suzer, L Andrews *J. Am. Chem. Soc.* **110** 3231 (1988)
362. R Koppe, P H Kasai *J. Am. Chem. Soc.* **118** 135 (1996)
363. K Kawaguchi, E Hirota, C Yamanda *Mol. Phys.* **44** 509 (1981)
364. T R Burkholder, L Andrews *J. Chem. Phys.* **95** 8697 (1991)
365. L V Serebrennikov, S B Osin, A A Maltsev *J. Mol. Struct.* **81** 25 (1982)
366. I L Rozhanskii, G V Chertilikhin, L V Serebrennikov, V F Shevel'kov *Zh. Fiz. Khim.* **62** 2351 (1988) [b]
367. L Andrews, T R Burkholder, J T Yustein *J. Phys. Chem.* **96** 10182 (1992)
368. T R Burkholder, J T Yustein, L Andrews *J. Phys. Chem.* **96** 10189 (1992)
369. P L Cabot, F Illasa, J M Ricart, J Rubio *J. Phys. Chem.* **90** 30 (1986)
370. A V Nemukhin, J Almlof *J. Mol. Struct. (THEOCHEM)* **85** 101 (1992)
371. P Marshall, P B O'Connor, W Chan, P V Kristof, J D Goddard, in *Gas-Phase Metal Reactions* (Ed. A Fontijn) (Amsterdam: North-Holland, 1992)
372. M V Pak, M S Gordon *J. Chem. Phys.* **118** 4471 (2003)
373. K Honma *J. Chem. Phys.* **119** 3641 (2003)
374. L B Knight Jr, T J Kirk, J Herlong, J G Kaup, E R Davidson *J. Chem. Phys.* **107** 7011 (1997)
375. M Tanimoto, S Saita, E Hirota *J. Chem. Phys.* **84** 1210 (1986)
376. L B Knight Jr , J O Herlong, T J Kirk, C A Arrington *J. Chem. Phys.* **96** 5604 (1992)
377. L B Knight Jr, W Weltner Jr *J. Chem. Phys.* **55** 5066 (1971)
378. C Yamada, E A Cohen, M Fujitake, E Hirota *J. Chem. Phys.* **92** 2146 (1990)
379. P Belanzoni, E V Lenthe, E J Baerends *J. Chem. Phys.* **114** 4421 (2001)
380. L B Knight Jr, J G Kaup, B Petzoldt, R Ayyad, T K Ghanty, E R Davidson *J. Chem. Phys.* **110** 5658 (1999)
381. P H Kasai *J. Chem. Phys.* **49** 4979 (1968)
382. L B Knight Jr, R Babb, M Ray, T J Banisaukas III, L Russon, R S Dailey, E R Davidson *J. Chem. Phys.* **105** 10237 (1996)
383. L V Serebrennikov, A A Mal'tsev *Vestn. Mosk. Univ., Ser 2., Khim.* **21** 148 (1980) [c]
384. G V Chertihin, W D Bare, L Andrews *J. Phys. Chem. A* **101** 5090 (1997)
385. G B Sergeev *Nanokhimiya* (Nanochemistry) (Moscow: KDU, 2006)
386. T I Shabatina, E V Vovk, V A Timoshenko, Yu N Morosov, G B Sergeev *Colloids Surf., A* **198–200** 255 (2002)
387. T I Shabatina, V A Timoshenko, A A Belyaev, Yu N Morozov, G B Sergeev *Dokl. Akad. Nauk* **387** 219 (2002) [d]
388. T I Shabatina, Yu N Morosov, V A Timoshenko, G B Sergeev *Mol. Cryst. Liq. Cryst.* **440** 325 (2005)
389. V A Timoshenko, T I Shabatina, Yu N Morozov, G B Sergeev *Zh. Strukt. Khim.* **47** 146 (2006) [e]
390. T I Shabatina, A V Vlasov, E V Vovk, D J Stufkens, G B Sergeev *Spectrochim. Acta, Part A* **56** 2539 (2000)
391. T I Shabatina, A V Vlasov, E V Vovk, D J Stufkens, G B Sergeev *Mol. Cryst. Liq. Cryst.* **356** 149 (2002)
392. A V Vlasov, T I Shabatina, S V Konyukhov, A Yu Ermilov, A V Nemukhin, G B Sergeev *Zh. Strukt. Khim.* **45** 406 (2004) [c]
393. A V Vlasov, T I Shabatina, A Yu Ivanov, G G Sheina, A V Nemukhin, G B Sergeev *Mendeleev Commun.* 10 (2005)
394. T I Shabatina, A V Vlasov, S V Konyukhov, A Yu Ermilov, A V Nemukhin, G B Sergeev *Mol. Cryst. Liq. Cryst.* **440** 317 (2005)

[a] — *Russ. Chem. Bull., Int. Ed. (Engl. Transl.)*
[b] — *Russ. J. Phys. Chem. (Engl. Transl.)*
[c] — *Moscow Univ. Chem. Bull. (Engl. Transl.)*
[d] — *Dokl. Phys. Chem. (Engl. Transl.)*
[e] — *J. Struct. Chem. (Engl. Transl.)*